HELICAL MILLING: AN ENABLING TECHNOLOGY FOR MACHINING HOLES IN FULLY HARDENED AISI D2 TOOL STEEL

BY

RAVISHANKAR IYER,
B.Eng.

HELICAL MILLING: AN ENABLING TECHNOLOGY FOR MACHINING HOLES IN FULLY HARDENED AISI D2 TOOL STEEL

HELICAL MILLING: AN ENABLING TECHNOLOGY FOR MACHINING HOLES IN FULLY HARDENED AISI D2 TOOL STEEL

By

RAVISHANKAR IYER, B.ENG.

A Thesis
Submitted to the Faculty of Graduate Studies
in Partial Fulfillment of the Requirements
for the Degree of

Master of Applied Sciences

McMaster University

Master of Applied Sciences	McMaster University
Mechanical Engineering	Hamilton, Ontario, Canada

TITLE:	Helical Milling: An Enabling Technology for Machining Holes in Fully Hardened AISI D2 Tool Steel.
AUTHOR:	Ravishankar Iyer, B.Eng. University of Pune, India, 1998.
SUPERVISOR:	Dr. Philip Koshy, Ph.D.
NUMBER OF PAGES:	123 pages (i-xv, 1-108)

ABSTRACT

The machining of hardened steel is becoming widespread throughout the manufacturing industry owing to the benefits derived in the form of manufacturing flexibility, better product quality, and the prospect of dry machining. This coupled with developments in super hard cutting tool materials and machine tools, and better understanding of hard machining technology translates into significant economical benefits and faster turnaround times.

The majority of applications involving hardened steels comprising AISI D2 tool steel relates to the manufacturing of die and mold wherein the current trend of hard machining is restricted by the limitations imposed by hard drilling. Being the final operation in many manufacturing applications, it is imperative that the process of drilling be robust and reliable to enhance the value already added to the product. Problems associated with inherent deficiencies in the drilling process kinematics, combined with poor machinability of hardened D2 tool steels due to the presence of hard and abrasive carbide particles in its microstructure that lead to catastrophic drill failure, constitute the single major process chain bottleneck in realizing hard part manufacture.

The research work presented in this thesis focuses on the application of helical milling as an enabling technology for hole making in hardened AISI D2 tool steel in comparison to conventional drilling, which is not feasible at the current level of developments in drilling technology. Helical milling employs a rotating end mill of a diameter smaller than the hole, and traverses a helical path to generate a hole. The novel process derived by simple modification of tooling and process kinematics offers an excellent avenue to successful machining of precision holes in hardened D2 tool steel.

In order to compare the performance of helical milling against drilling, four types of conventional twist drills intended for drilling hardened steels were employed in the machining experiments while, end mills commonly used in the die and mold

industry, were chosen for helical milling. The processes were evaluated in terms of tool life, wear progression, wear mode, cutting forces and hole quality.

Accelerated wear followed by catastrophic fracture of the cutting edges at the periphery of the drill was observed to be the primary tool failure mode in conventional drilling as opposed to uniform progressive flank wear in helical milling. The innovative helical milling method is found to facilitate hole-making in hardened D2 tool steel with an order of magnitude improvement in tool life. The helical trajectory of the tool in helical milling facilitates material removal near and at the center of the hole by cutting rather than extrusion as seen in drilling, thereby reducing the excessive thrust forces that cause work material breakouts at the hole exit in conventional drilling.

Furthermore, chip evacuation in not problematic in helical milling considering that chips can be removed across the radial clearance between the tool and the hole as opposed to through the flute space in conventional drilling. This implies that an air blow could be employed to assist chip transport in helical milling facilitating dry machining, considering that in many drilling applications cutting fluid is merely used to flush the chips away from the cutting zone. The intermittent cutting action in helical milling further provides respite to the cutting edge from the imposed mechanical and thermal loads and offers exceptional chip control. The process represents an enabling technology with additional benefits of superior hole quality thus rendering the elimination of an additional reaming process.

ACKNOWLEDGMENTS

"The whole art of teaching is only the art of awakening the natural curiosity of young minds for the purpose of satisfying it afterwards."

Anatole France (1844 – 1924)

This is a perfect synopsis of the supervisory style of Dr. Philip Koshy, to whom I remain indebted in so many ways than I can state in this small space. An inspiring teacher and a highly dedicated researcher who believed in me and constantly encouraged me to realize my potentials and capabilities, I consider myself very fortunate to have known him as my guru, mentor and friend.

I would also like to express my sincere gratitude to "THAMBI", Dr. Eugene Ng, for his invaluable support, helpful critiques and discussions during the course of this work. It is a great pleasure and privilege to have gained a valuable friend in him. I have also had the distinguished opportunity to participate and interact with some of the most outstanding faculty members of MMRI during the past few years and thank them for making the association a very valuable and enriching experience.

The financial support extended in the form of scholarship from McMaster University, AUTO 21, Natural Sciences and Engineering Research Council (NSERC) and McMaster Manufacturing Research Institute (MMRI) is greatly acknowledged. Special acknowledgements are due to the Machining Systems Laboratory (MSL) team of Jim McClaren, Miky Dumitrescu and Warren Reynolds for their patience and helpfulness. I would like to express my gratitude to Dave Schick and Ron Lodewyks for their co-operation and support in times of need. The support extended in the form cutting tools, necessary for conducting some of the machining experiments in this research, from Brian Philips of Sandvik Coromant Canada is also highly acknowledged. The cooperation and support extended by Sylvia Ragis, Linlin Zhao, Betty Anne Bedell-Ryc, Janet Murphy and Florence Rosato is greatly appreciated.

I'm thankful to Maneesh Khanna, Sudheer Patil, Frederick Suresh, Andrew Weaver, Diaa Elkott, Jeremy Stenekes, Andy Simoneau and all my friends and colleagues at MMRI and the Mechanical Engineering department at McMaster University, for their friendship, support and willingness to help even though they were pressed for time themselves and for making my stay at McMaster very memorable.

I would also like to thank my parents for their love and support and my family, especially my uncle, Dr. Ramani Ramaseshan and aunt, Dr. Nithya Ramani for their support and guidance. I would not be at this place in life, if it were not for you both. The enthusiasm, encouragement and words of wisdom from my beloved eldest uncle, Mr. Krishnamurthy Narayan, have always inspired and motivated me and to whom I remain forever grateful. I would like to express my sincere gratitude towards my parents-in-law for their support and having faith in my abilities. Last but not the least, I would like to thank my dear wife Sheetal for her boundless love, unconditional support and enduring patience during the entire course of this work. None of this would have been possible without you all.

Hamilton, ON
February 2006 *Ravishankar Iyer*

Dedicated to my parents, Muralidharan and Chandra for their unwavering love, faith and encouragement throughout my life, without which I would not have been able to achieve my dreams.

CONTENTS

LIST OF TABLES

LIST OF FIGURES

LIST OF SYMBOLS

δ	Helix angle of the drill (^{0})
δ_o	Helix angle at the periphery of the drill (^{0})
2ρ	Point angle of the drill (^{0})
ρ	Half point angle of the drill (^{0})
θ	Clearance angle of the drill (^{0})
θ_o	Clearance angle at the periphery of the drill (^{0})
ξ	Wedge angle of the drill (^{0})
$2w$	Web thickness of the drill (mm)
w	Half web thickness of the drill (mm)
β	Web angle of the drill (^{0})
β_o	Web angle at the periphery of the drill (^{0})
r	Radial location along the cutting edge of the drill (mm)
D_H	Diameter of machined hole (mm)
$R_H = \frac{D_H}{2}$	Radius of machined hole (mm)
D_T	Diameter of cutting tool (mm)
$R_T = \frac{D_T}{2}$	Radius of cutting tool (mm)
D_{eff}	Effective tool diameter (mm)
$R_{eff} = \frac{D_{eff}}{2}$	Effective tool radius (mm)
a_o	Axial depth per 360^0 of circular tool travel (mm)
a_p	Axial depth of cut or Axial engagement (mm)
a_e	Radial depth of cut or Radial engagement (mm)
D_H/D_T	Bore to Tool ratio in Orbital drilling
V_B	Flank wear (mm)
K_B	Crater wear (mm)
K_T	Crater depth (mm)
V_f	Linear feed rate at tool center (mm/min)
V_{fc}	Circular feed rate at tool center (mm/min)

L	Lead of the helix in drills (mm)
L_H	Linear length of hole (mm)
L_E	Projection length of drill (mm)
L_O	Length of tool travel per 360^0 of circular tool travel (mm)
L_T	Total length of tool travel in helical milling (mm)
L_R	Ramping length per 360^0 of circular tool travel (mm)
N	Spindle speed (RPM)
f	Feed rate (mm/rev)
f_z	Feed per tooth (mm)
Z_n	Number of cutting edges (teeth) on the tool
b	Width of cut (mm)
$MRR\|_{CD}$	Metal removal rate in conventional drilling (mm^3/min)
$MRR\|_{HM}$	Metal removal rate in helical milling (mm^3/min)
V	Cutting speed (m/min)
V_{eff}	Effective cutting speed in ball end milling (m/min)
T	Machining time (min)
$T\|_{CD}$	Machining time in conventional drilling (min)
$T\|_{HM}$	Machining time in helical milling (min)
t	Uncut chip thickness (mm)
θ_R	Ramping angle in helical milling (^{0})
ϕ_R	Angle of rotation of the tool (^{0})
α_n	Normal rake angle in drilling (^{0})
ω	Angular velocity imparting helical motion to the drill chip (m/min)
ω_c	Angular velocity acting on the drill chip along drill axis (m/min)
ω_x	Angular velocity acting on the drill chip along X direction (m/min)
ω_z	Angular velocity acting on the drill chip along Z direction (m/min)
α_a	Axial rake angle in helical milling (^{0})
α_r	Radial rake angle in helical milling (^{0})

CHAPTER 1
INTRODUCTION

1.1 Research Problem and Motivation

This thesis presents an enabling technology called Helical Milling for machining of holes in hardened AISI D2 tool steel, the drilling of which is not feasible with the present state of conventional drilling technology.

Traditionally, hardened steel components are rough machined to their near net shape in the soft condition followed by heat treatment to the desired hardness and finishing by electrical discharge machining and grinding. Not only is this method time consuming, but is also labor and cost intensive. Hard machining on the other hand involves machining components to their final shape from hardened stock. The flexibility to manufacture complex workpiece geometries in a single set-up coupled with attaining surface finish and part accuracies comparable to that in grinding (Figure 1.1) are the main benefits of hard machining [1] [2]. In addition, hard machining is performed dry which eliminates cutting fluid costs and protects the environment.

Hence machining of steels in their hardened state is rapidly gaining importance as an economical method of producing high performance components. Technological innovations in machining technology facilitated by the development of ultra hard cutting tool materials such as ceramics, polycrystalline cubic boron nitride (PCBN) etc. coupled with a better understanding of the hard machining processes has proliferated the machining of ferrous alloys in their hardened state.

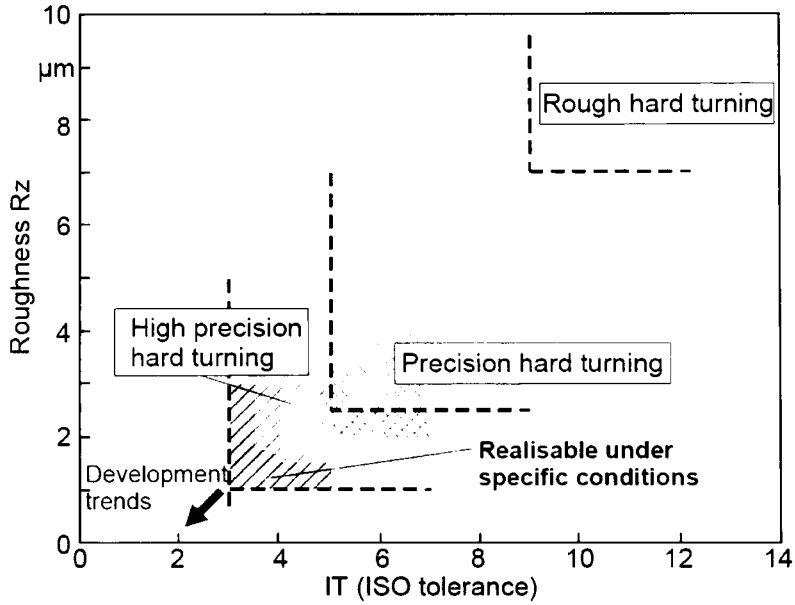

Figure 1.1: Surface finish and tolerance obtainable in hard turning [2].

AISI D2 tool steel in particular is being widely used in the manufacture of cold forming dies and molds owing to its exceptional hardenability and wear resistance. The alloying elements that increase the application potential of D2 are responsible for its poor machinability upon hardening. In its hardened state (> 60 HRC), D2 exhibits hard and abrasive chromium carbides in its matrix that seriously inhibit machinability. This thesis examines issues with drilling of this material, and proposes an alternative technology called helical milling for productive machining of precision holes in through hardened D2 tool steel.

Ever since its introduction in mid the 1800, drilling has been considered as one of the most indispensable metal cutting operations and has been a subject of research for over 140 years. Being the final operation in many machining applications, the process demands a high degree of reliability, robustness and productivity to enhance the value already added to the component. Not only have the drill materials and geometries evolved over time, but modern drills can boast of a wide range of complex point geometries and cutting edge designs, which greatly enhance their performance characteristics. Better understanding of drilling process mechanisms while machining different types of workpiece materials has not only led to the development of application-specific geometries but is also pushing the cutting parameter envelope for higher productivity gains [3].

Technical challenges related to drilling are quite unique in comparison to other machining processes with the cutting speed approaching zero in the vicinity of the drill center, inducing material removal by extrusion rather than cutting. This translates into high thrust forces limiting process productivity and proliferating work material breakouts at the hole exit. Despite advances in drilling technology, chip evacuation and effective heat dissipation are still difficult, especially for holes with high aspect ratios (L_H/D_T), where L_H is the length of the hole and D_T is the tool diameter. Besides, friction between the drill, chip and workpiece can be high enough to have a negative influence on the dimensional accuracy and surface finish of the machined hole by abetting tool wear and in the worst instance could culminate in catastrophic tool failure.

Problems in drilling are exacerbated in hard drilling, particularly in case of AISI D2 due to its poor machinability coupled with inherent deficiencies in the drilling process kinematics above and is seldom attempted. Difficulties associated with hard drilling of D2 dies and molds have serious implications in the die and mold industry

wherein the current trend is to manufacture components from hardened stock. Arai et. al. [4] investigated drilling of SKD 11 (Japanese equivalent of AISI D2) with respect to work hardness, and found drilling to be impractical as the hardness of the workpiece approaches 60 HRC. A comparative assessment of drilling of hardened AISI H13 and AISI D2 using carbide drills by Coldwell et. al. [5] illustrated drill life corresponding to the latter to be about 15 times lower.

The use of conventional carbide drills warrants the use of lower cutting speeds ($V \leq 10$ m/min) with copious amounts of cutting fluid to facilitate cooling and chip evacuation. At such low cutting speeds, adequate spindle power may not be available, considering that most die and mold making machines possess spindle speeds on the order of 20,000 rpm to facilitate high speed machining [6].

The design and manufacture of twist drills is long considered to be the strength of the individual drill manufacturers and are usually designed to satisfy a broad range of work material groups. A quick survey of product catalogues of cutting tool manufacturers for drilling indicates their product recommendations to be limited to material hardness less than 55 HRC. As these recommendations are not intended for hardened tool steels such as AISI D2, it is strongly advocated to reduce cutting speeds with increase in work material hardness thereby affecting productivity.

Since hard drilling of AISI D2 is not feasible, and as die and mold components invariably include hole features, it presents a significant process chain bottleneck precluding hard part manufacture. Although machinability of AISI D2 is poor in comparison to AISI H13, it can be successfully milled [7]. Hence the motivation in this research to adopt and develop helical milling technique for machining holes in through hardened (> 60 HRC) AISI D2 tool steel.

1.2 Helical Milling

Helical milling (Figure 1.2) is a hole making process wherein a rotating center cutting end mill traverses a helical course to generate the hole and is sometimes also referred to as circular milling [8] [9] or helical feed milling [10]. The advantages of this novel process over conventional drilling brought about by simple modifications of the tooling and process kinematics are manyfold [9]. On account of the process involving a secondary helical movement in addition to the primary cutting motion, material removal at the hole center does occur by cutting rather than by extrusion as in drilling, and could therefore be expected to relate to a significantly lower thrust force.

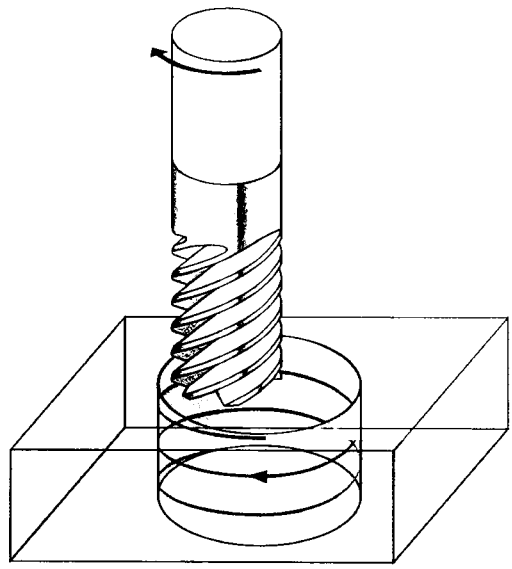

Figure 1.2: Helical milling process.

Since the tool diameter in helical milling is always smaller than the hole diameter, chip evacuation is not demanding as the chips can be conveyed through the clearance space between the tool and the workpiece. On account of this, helical milling is well suited for dry machining operations, in contrast to most drilling applications, where the primary function of the cutting fluid is transport of the chips through the

flute space.

Further, chip control is not an issue in helical milling on account of it being an interrupted cutting process, which also provides some respite for the cutting tool in terms of the nature of the imposed thermal load thereby controlling tool wear and propagation of sub-surface defects. The process is also highly flexible in that a single tool can be used to machine a range of hole diameters, hole geometries in helical milling are not limited to circular cross-sections, and it is feasible to machine blind holes with a flat face end mill.

With respect to the force system, tool deflection due to radial forces in helical milling could have an impact on the hole geometrical characteristics which is not the case in conventional drilling. In contrast to conventional drilling wherein the design of the tool cross-section is essentially a compromise between the tool stiffness and the flute space necessary for chip evacuation [11], the tooling used in helical milling can have a higher core diameter to counter tool deflection. If hole quality is the primary concern, then machining may well be accomplished in two passes, thereby eliminating hole finishing by reaming, leading to savings in tooling and production costs [8].

Information currently available on helical milling pertain to machining of carbon fibre reinforced composites [8] and aluminum [10]. The current research investigates the application helical milling process to hardened AISI D2 tool steel vis-*à*-vis conventional twist drilling.

1.3 Thesis Outline

This thesis comprises five chapters. Chapter 2 provides a basic understanding of the chip formation process in conventional drilling. An overview of properties of alloy steels is presented, with particular emphasis on AISI D2 highlighting some of the important properties of hardened D2 that inhibit its machining. An extensive

review of research literature on turning, milling and drilling of hardened AISI D2 tool steel is provided as an essential platform for understanding the research presented in this thesis.

Chapter 3 presents a detailed description of the experimental work undertaken in this research. The section identifies the experimental setup, work material and tooling descriptions employed and outlines the process strategies adopted for conducting machining experiments. The cutting parameters and test conditions used to verify the performance of the novel hole making process over conventional drilling is also presented.

The results obtained when hole making in AISI D2 using conventional drilling and helical milling processes are discussed in detail in Chapter 4. The performance of both the processes in terms of tool life, hole accuracy, surface finish and wear progression while machining holes in hardened steel are discussed in this section. The reasons for catastrophic failure of drilling tools under hard drilling of AISI D2 is investigated.

Chapter 5 presents the conclusions drawn from the current work. Although a successful attempt has been made to understand and apply the process of helical milling to machine holes in hardened steels, a lot more needs to be done in this area and this chapter provides some recommendations in this regard for possible future areas of research.

CHAPTER 2
BACKGROUND AND LITERATURE REVIEW

2.1 Introduction

The present chapter introduces the basic mechanics of the drilling process and outlines some of the important design features of the twist drill and their impact on drill performance. Following this, the influence of alloying elements on the mechanical properties of alloy steels with particular reference to AISI D2 is indicated. The chapter then delves on the concept of hard machining highlighting some of the key elements of the technology that are crucial for its successful implementation. The chapter finally presents a review of the existing work on the machining of hardened D2 tool steel ($55 - 62$ HRC) and emphasizes the difficulties associated with hard drilling of this material.

2.2 Overview of Drilling Mechanics

A twist drill is a complex end-cutting tool with two or more straight or helical flutes that are symmetrical about the drill axis and involve two cutting edges designed to produce identical chips. Depending upon the application requirement, the drill body may or may not facilitate passage of cutting fluid through it. Drills are usually classified according to the material of manufacture, flute length, number of flutes, point geometry and shank style [11] [12].

A twist drill comprises three distinct parts: the shank which is used to hold and drive the drill; the body, which consists of the helical or straight flutes that are used as a passage for cutting fluid and also chip evacuation; and the cutting elements, comprising the drill point, cutting edges and flanks as seen in Figure 2.1. The main cutting edges of the drill, also known as cutting lips produce chips similar to that in turning. Cutting occurs along the entire lip length (cutting edge length) and accounts for most of the torque and power consumption in drilling. The cutting lips are connected to the secondary cutting edge or chisel edge at the center of the drill, which removes material by extrusion and accounts for a significant portion of the thrust forces generated in drilling. The design of the chisel edge was originally adapted from the flat drill and is a very critical component in drill design as it not only affects the centering accuracy and buckling phenomenon of the drill, but also influences the axial thrust produced while drilling.

For the most part, the marginal edges, which form the periphery of the drill, serve the sole purpose of guiding the drill into the hole. They do not undertake any cutting action and hence have little impact on the performance of the drill and are usually ignored in most analyses [11] [13] [14].

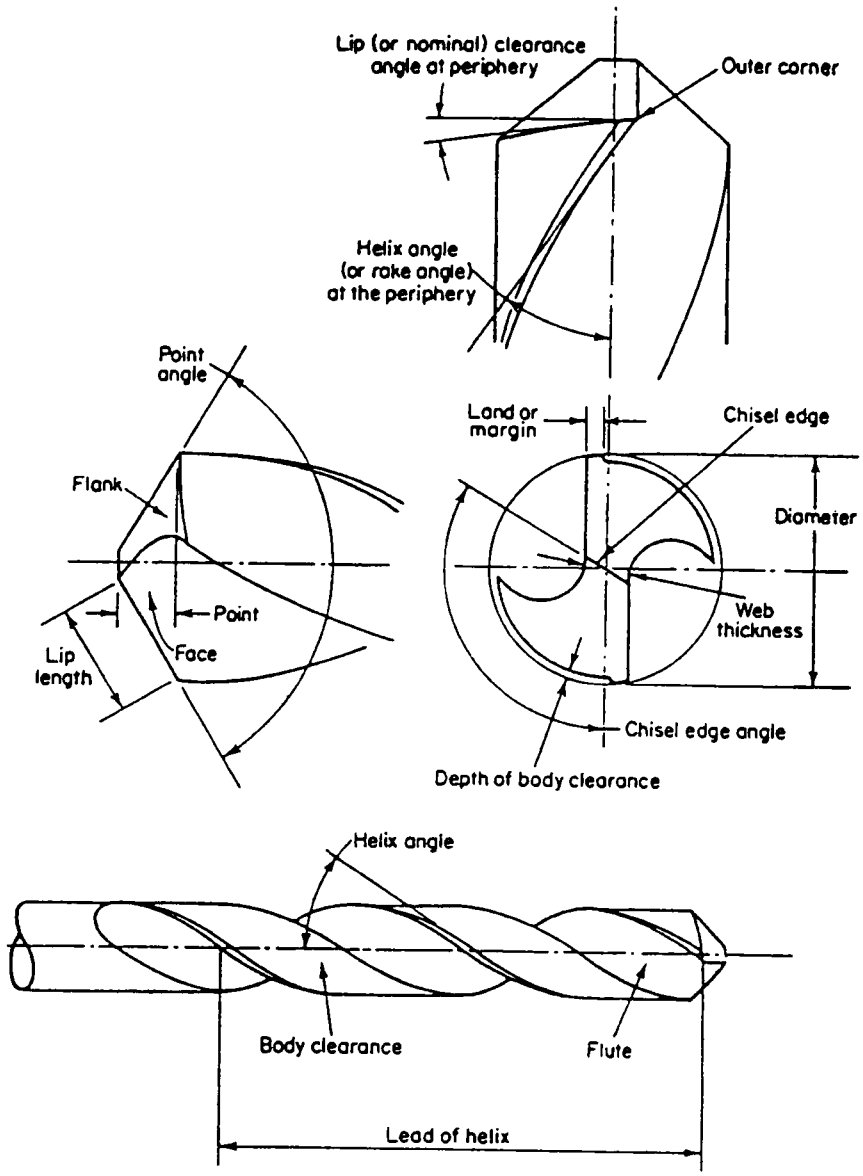

Figure 2.1: Twist drill nomenclature [14].

Given the basic understanding of the drill geometry, the complex process of drilling can be explained as follows [12] [15]:

- The drill is rotated about it own axis and is simultaneously fed axially into the material.

- ☞ At the center of the drill, the linear velocity is zero and the chisel edge is subjected to the feed velocity alone in the axial direction (Figure 2.2a) resembling deformation of a metal by indentation.

- ☞ This material is extruded towards the rotating cutting edges of the drill where a combination of rotational and feed velocities are active and the mode of machining is essentially oblique (Figure 2.2b).

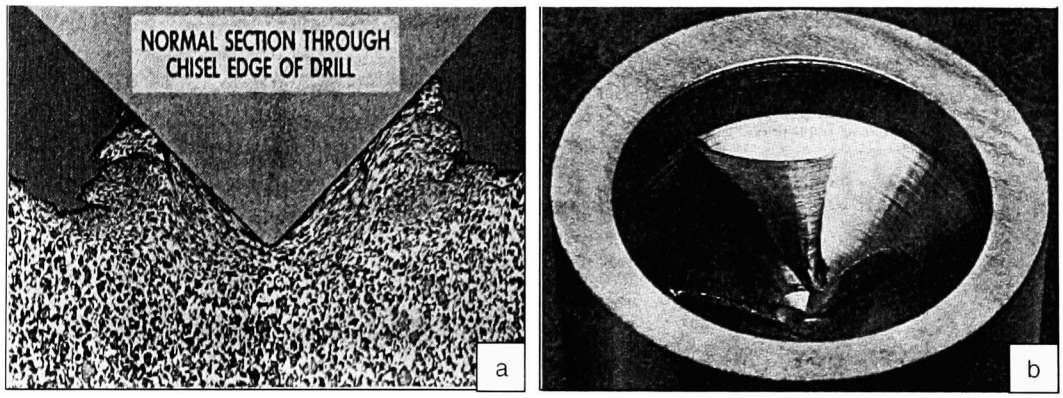

Figure 2.2: Chip formation in drilling (a) Along chisel edge (b) Along cutting edges [15].

- ☞ The conical chips produced in drilling are evacuated through the flute space with the help of cutting fluids.

The helix angle (δ), the point angle (2ρ), the web thickness ($2w$) and the clearance angle (θ) play an important role in determining drill performance in terms of cutting mechanics and chip conveyance. These terms are briefly described below, a detailed account of which is provided by Galloway [16].

Helix Angle (δ)

The helix angle is defined as the acute angle between the drill axis and the leading edge land (Figure 2.1) and is an important variable in drill design. Since the helix angle varies along the radius of the drill it is always specified at the

periphery of the drill. An increase in helix angles greatly assists chip evacuation, but also weakens the cutting edges. Hence as a compromise between satisfactory chip evacuation and cutting edge strength, the helix angle is optimized to a value between $28^0 - 32^0$ at the periphery [17].

Point Angle (2ρ)

The point angle is the sum of the acute angles between the axis of the drill and the lines joining the outer corner to the corresponding corners of the chisel edge (Figure 2.1). Each of the acute angles is referred to as "Half Point Angle" and must be equal. The point angle enables the drill to be fed gradually into the workpiece and influences chip flow direction. A typical value for the point angle for solid carbide drills is $135^0 - 140^0$ [12]. The cutting edge length is inversely proportional to the point angle.

Web Thickness ($2w$)

The web thickness is defined as the minimum dimension of the web measured at the point end of the drill (Figure 2.1). The web thickness is influenced by the length of the chisel edge and directly impacts the thrust forces in drilling. Any reduction in web thickness will reduce the thrust forces, thereby improving centering accuracy of the drill, however a larger web improves torsional rigidity and also provides resistance to chipping. The web thickness varies according to the type of tool and workpiece material, and the point geometry employed.

Clearance Angle (θ)

The clearance angle is the angle between the flank face and a plane perpendicular to the drill axis (Figure 2.1). The clearance angle is always specified at periphery of the drill and in general is in the range of $8^0 - 12^0$

The above parameters influence the grinding of the chisel edge and cutting lips of the drill [16]. Torque, power consumption and temperature generated during drilling are affected by the design of the cutting edges (lips). The positioning accuracy and thrust forces are governed by the design of the chisel edge. Since these attributes are of paramount importance in ascertaining the performance of the drill, a wide variety of drill point and body configurations have been developed and still continues to evolve, a review of which is beyond the scope of this research.

2.3 Properties of Alloy Steels

Alloy steels contain elements other than carbon like nickel (Ni), manganese (Mn), chromium (Cr), tungsten (W), molybdenum (Mo), vanadium (V) etc to enhance one or more of their properties. Addition of alloying elements usually influences several properties of plain carbon steels simultaneously. The extent of their effect on a given property however depends on the type and amount of element added. Some of the most important influences of alloying elements are detailed below.

- ☞ Most alloying elements are soluble in ferrite (pure iron) to a certain extent and form solid solutions. These solid solutions are harder and stronger than pure metals and hence greatly influence the strength and hardness of the alloy. Phosphorus (P), Silicon (Si), Manganese (Mn) and Nickel (Ni) are effective solid solution strengtheners.

- ☞ Some alloying elements combine with carbon and form the respective carbides. While these elements do not directly influence the hardness and strength of the alloy steel (Figure 2.3), they increase wear and abrasion resistance due to the formation of hard alloy carbide particles. Molybdenum (Mo), Vanadium (V), Tungsten (W) and Chromium (Cr) have such an influence.

☞ One of the most important effects of alloying elements (except cobalt) is the lowering of the critical cooling rate thereby increasing the hardenability of steel. Elements such as Manganese (Mn), Molybdenum (Mo), Nickel (Ni) and Chromium (Cr) have the greatest influence on improving hardenability.

Alloy steels used specially for working, shaping and cutting of metals are categorized as Tool Steels by the American Iron and Steel Institute (AISI). These steels share a fundamental requirement of being hard, tough and wear resistant, however, exact requirements differ based on the intended service conditions [18]. The following refers to the basic characteristics of cold work tool steels with an emphasis on AISI D2 steel upon which the current work is based.

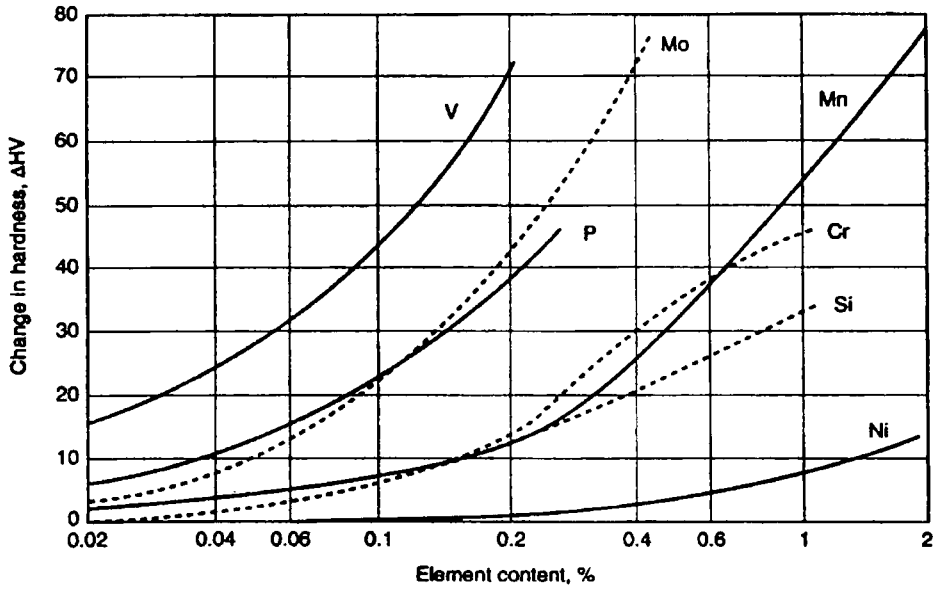

Figure 2.3: Hardening effects of alloying elements dissolved in pure iron [18] [19].

2.3.1 Cold Work Tool Steel

As the name implies, cold work tool steels are intended for cold forming of metals and demonstrate excellent hardness and wear resistance at lower temperatures.

Depending upon their hardening characteristics they are classified into sub-groups as water hardening steels (W-Series), oil hardening steels (O-Series), air hardening steels (A-Series) and high-carbon, high-chromium steels (D-Series). Some of the property enhancements of cold work tool steels due to alloying elements are discussed below [12] [18]:

- Cold work tool steels have good hardenability characteristics which ensures that the steel can be uniformly through hardened without the use of quenching techniques that may induce cracks and cause damage.
- Better resistance to wear and abrasion by precipitating alloy carbides that are coarse and hard, which also improves corrosion and oxidation resistance.
- Some alloying elements combine with oxygen to prevent the formation of blow holes and ensure more uniform properties throughout.
- Ability to resist deformation and distortion during heat treatment.

In conclusion it can be stated that alloying elements impart some very unique properties to cold work tool steels making them suitable for cold forming applications.

2.3.2 AISI D2 Tool Steel

The AISI D-Series of steels are also known as high-carbon, high-chromium (HCHC) steels because they have chromium as their main alloying element which increases their hardenability. Upon hardening, chromium forms carbides which increases the hardness and imparts wear resistance. Chromium increases corrosion and oxidation resistance by forming a thin film of chromium oxide (Cr_2O_2) on the surface under oxidizing environments. Development of D-Series steels was undertaken primarily as a replacement for cutting tools made from high speed steels. They were

however commercially unsuccessful as cutting tools due to their high brittleness, but were well suited for cold forming applications.

The typical chemical composition of AISI D2 is given in Table 2.1 and the physical properties as a function of temperature are listed in Table 2.2.

%C	%Si	%Mn	%Cr	%Mo	%V
1.55	0.3	0.4	11.8	0.8	0.8

Table 2.1: Chemical composition of AISI D2 cold work tool steel [20].

Physical Data (Hardened and tempered to 62 HRC)			
Temperature	*20°C*	*200°C*	*400°C*
Density kg/m^3	7700	7650	7600
Coef. of thermal expansion - low temperature tempering (°C from 20°C) - high temperature tempering (°C from 20°C)		$12.3 \cdot 10^{-6}$ $11.2\ \ 10^{-6}$	$12 \cdot 10^{-6}$
Thermal conductivity W/m°C	20.0	21.0	23.0
Modulus of elasticity GPa	210	200	180
Specific heat J/kg°C	460		

Table 2.2: Physical properties of AISI D2 tool steel at various temperatures [20].

The distinctive property of AISI D2 characterized by superior wear resistance, high compressive strength and excellent hardenability are ideally suited for the manufacture of forming dies and molds, which are preferably machined from hardened stock. Hard part machining is rapidly gaining importance due to the advantages derived in terms of manufacturing flexibility and better product quality. Along with the development of super hard cutting tools and advancements in machine tool technologies, hard machining provides a competitive alternative to grinding and electrical discharge machining, eliminating the need for polishing translating into savings in production time and overall machining costs. The wear resistance of AISI D2 in its

hardened state is imparted by the presence of hard chromium carbide particles formed during the hardening process, which however inhibit its machinability.

2.4 Hard Machining

Hardened steel components are often employed in high performance applications and need to satisfy stringent quality requirements. The functional behavior of these machined components is strongly influenced by the finishing process. On account of the higher cutting forces and prohibitive chip tool interface temperatures, certain technological elements are imperative for successful hard machining and are discussed below:

- Depending upon the workpiece material hardness the temperature in the tool-chip interface can range anywhere from 800 ^{0}C to 1050 ^{0}C thus necessitating higher hot hardness of the tool. The cutting tool substrates must also possess high hardness without compromising fracture toughness to endure high stresses and the abrasive nature of the workpiece material [1] [21].

- The ratio of the thrust force (F_Q) to the cutting force (F_P) in hard machining is 2 as compared to 0.5 in soft machining. This can aggravate tool deflection and necessitate increased machine tool stiffness [1] [21].

- In order to provide adequate strength to the cutting edge, negative rake tools are generally employed while machining hardened steels [1].

- Chip formation in hardened steels is generally considered to be due to periodic crack initiation from the free surface along the shear plane that stops in the vicinity of the tool tip due high hydrostatic pressure therein. This results in saw-tooth type chips in contrast to continuous chips produced while machining soft steel (Figure 2.4) [2] [22] .

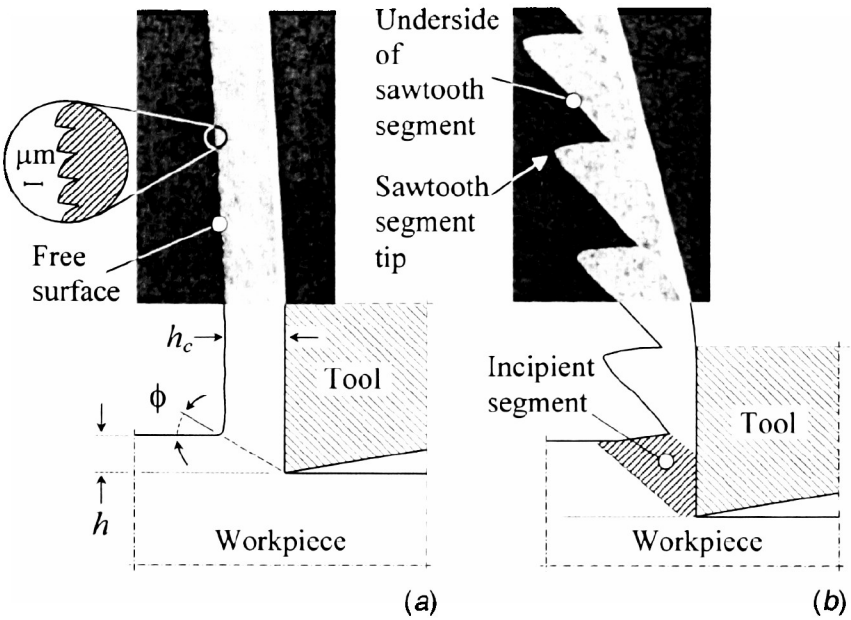

Figure 2.4: (a) Continuous chip (b) Saw-tooth chip [22].

- ☞ Saw-tooth type chip formation is usually accompanied with large amplitude dynamic forces causing forced excitation of the machine tool system. The machine tool has to be rigid enough to withstand the forces and prevent vibrations, that could prematurely limit tool life [1].

- ☞ Tool wear in hard machining of tool steels is characterized primarily by severe abrasion of the flank face, attrition wear and micro-chipping of the cutting edge. The work material properties influence the dominance of a particular wear mechanism over another [1].

It may be noted that hard machining is a complex process that not only demands exceptional toughness, wear resistance and hot hardness from the cutting tool, but far greater rigidity from the machine tool as well as the tool and workpiece holding system. Although hard machining requires an entire setup change and not merely switching to super hard cutting tools, the economic gains achieved by elimination

of follow-up operations such as EDM, grinding, polishing etc. outweigh some of the challenges proposed by adopting such a new technology.

2.5 Review of Machining Hardened AISI D2

One of the very first investigations into the machinability of hardened (60 HRC) AISI M2, D2 and D6 tool steels was undertaken by Hodgson et. al. [23] in 1980. They investigated the influence of work material hardness, rake angles, cutting speeds and feeds on the life of PCBN inserts. They found out that at lower cutting speeds (25 m/min) and feeds (0.1 mm/rev), tool life with negative rake (-6^0) inserts was much higher than those with neutral (0^0) and positive ($+6^0$) rake inserts. However at higher cutting speeds and chip loads, the rake angle had a negligible effect on tool life. It was concluded that the variation in tool life could not be solely attributed to the hardness of the workpiece and that the influence of alloying elements on the chemical and mechanical properties of the work material need be investigated. Experimental results indicated PCBN inserts with chamfered cutting edges to correspond to poor tool life, although detailed explanation of this phenomenon was not provided by the researchers.

Boehner et. al. [24] analyzed the influence of work material microstructure on tool performance under high speed machining conditions. Cutting tests were performed using coated and uncoated carbide ball end mills of diameter 12.7 mm at a feed rate of 0.1 mm/tooth and a spindle speed of 10,000 rpm. Massive flank wear along the entire length of contact was observed while machining AISI D2. An interesting observation was the chipping of the cutting edges at the maximum tool/work contact point which corresponds to highest cutting speed and chip load along the cutting edge of the ball end mill. Observation of the rake face indicated attrition wear caused by the removal of tool material fragments, a feature not observed while

machining AISI H13 and was attributed to the presence of carbide particles in the D2 microstructure (Figure 2.5) propagating microcracks along the tool rake face. Metallographic investigations into the microstructure of AISI D2 hardened at 55 HRC reveal perceptible amounts of undissolved carbide and martensite particles compared to AISI H13 that exhibit traces of very fine undissolved carbides. Numerical simulation indicated the cutting temperature at the tool chip interface to be around 800 ^{0}C which accelerates tool wear. In line with Hodgson's [23] observation, Boehner et. al. [24] concluded that the microstructure of the workpiece material severely influences the performance characteristics of the tool.

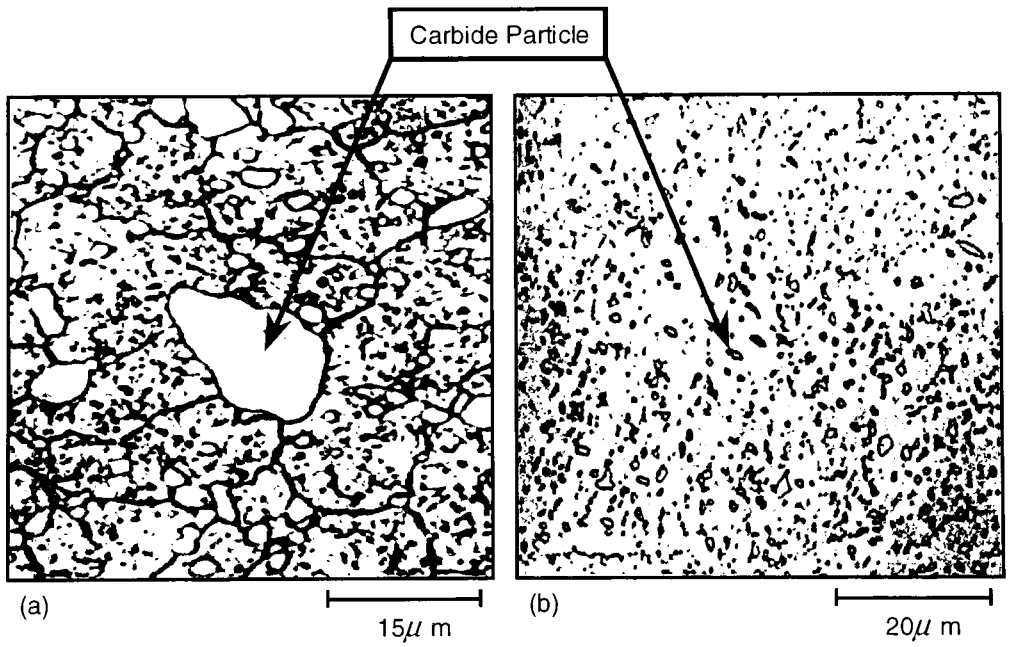

Figure 2.5: Microstructure of hardened tool steels: (a) AISI D2, and (b) AISI H13 [25].

In continuation with their study on the effects of carbide tool grades and cutting edge geometry on tool life of hardened (62 HRC) AISI D2, Boehner et. al. [26] concluded that a sharp cutting edge preparation combined with a neutral rake are best suited for machining hardened D2 steels. However this judgment is somewhat

flawed as negative rake tools were not tested for comparison in their work contradicting the results reported by Hodgson et. al. [23]. At lower cutting speeds, fine grade uncoated carbide with a neutral rake produced progressive flank wear as compared to catastrophic flank wear obtained with titanium aluminum nitride (TiAlN) coated carbide grades. In concurrence with their previous work [24], attrition wear was the primary wear mechanism combined with thermal wear at the maximum tool/work contact point. Statistical analysis was used to corroborate the influence of cutting speed, axial depth of cut (a_p) and tilt angle on tool life. Reduction in tool life with increase in cutting speed is not atypical, however the influence of axial depth of cut (a_p) was marginal. Thus using a higher axial depth of cut (a_p) reduces the number of passes needed to remove the same amount of material thereby improving tool life and reducing cutting time. The statistical trend on the influence of tilt angle on tool life deduced a negative effect with an increase in tilt angle. In order to realize a stable cutting process with longer tool life, it was recommended that a combination of cutting speeds, feeds, axial depth of cut (a_p) and tilt angle was necessary.

In the first of a two part investigation into the surface integrity of hardened die materials in high speed machining, El-Wardany et. al. [27] performed micrographical analysis of chips and surface produced by machining hardened ($60 - 62$ HRC) AISI D2 using sharp and worn PCBN tools. Studies on chip morphology indicated that at small depths of cut, continuous (flow-type) rather than saw-tooth chips are formed. These continuous chips exhibit minute cracks that do not propagate through the chip cross-section and are obtained only with a sharp cutting edge. It was identified that saw-tooth chips were obtained only when the critical pressure in the cutting direction exceeded 4000 MPa. White layer (Figure 2.6b) evident under the machined surface of hardened D2 steel, increased with progression of flank wear which is influenced by the cutting speed and hence its occurrence was concluded to be influenced by

the magnitude of flank wear. Distortion of the grain boundaries in the direction of feed and deformation of carbide grains at high cutting speeds (350 m/min) indicated generation of high cutting temperatures. Due to poor deformability of the carbide grains, microcracks were generated, further deteriorating the generated surface.

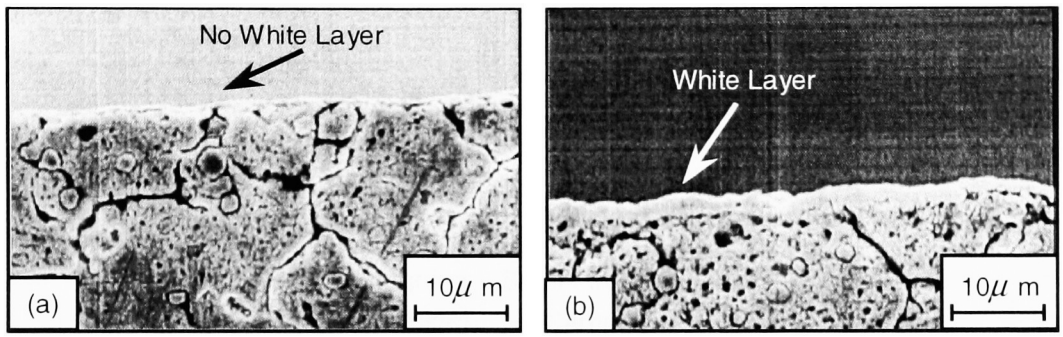

Figure 2.6: Influence of flank wear on white layer formation in hardened AISI D2 tool steel (a: Flank wear $\approx$ 0 mm, b: Flank wear = 0.5 mm) [27].

Becze et. al. [28] analyzed the effects of complex tool paths on chip morphology, tool wear, surface integrity and tool life associated with high speed five axis milling of hardened (63 HRC) D2 tool steel. The experiments were carried out dry with coated carbide tools with a rake angle of 0^0 for roughing and semi-finishing operations, and PCBN tools with a sharp edge preparation and a rake of -10^0 for finish milling. The spindle rotational speed was kept constant at 6000 rev/min for roughing and 10,000 rev/min for finishing. It was comprehended that the chip formation process remains unaffected by five axis rough milling, similar to that obtained in a linear test producing saw toothed chips with residual white layer. Tool life (Figure 2.7) realized in five axis machining was comparable to that of a linear test, with flank wear being the predominant wear mechanism in roughing and semi-finish milling. Nose wear accompanied by micro chipping of the cutting edge at point of highest cutting speed was the principal wear mode for finish five axis milling. The constant variation of the tilt angle, characteristic to five axis machining changed the contact area of the point

of engagement, increased the tool life in finish milling.

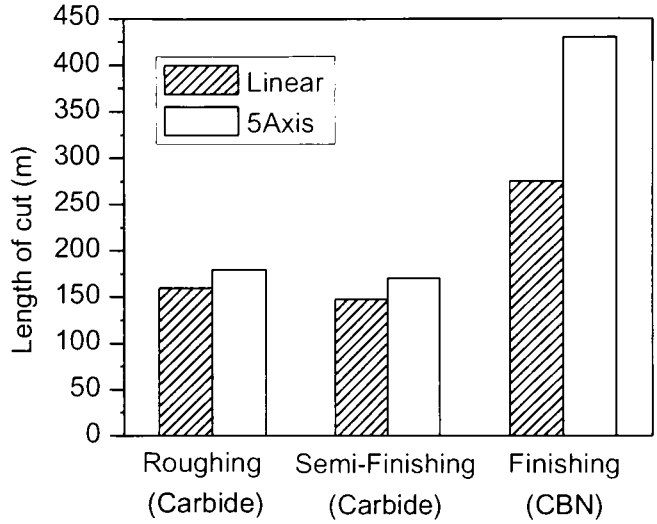

Figure 2.7: Comparison of tool life in linear and 5-axis milling of AISI D2 [28].

Kishawy [29] investigated the effects of process parameters on the temperature generated on the cutting edge under high speed hard turning of D2 tool steel using a tool embedded thermocouple technique. As expected, cutting speed had a marked influence on temperature (Figure 2.8a) at the tool chip interface, which increased from approximately 480 ^{0}C at 140 m/min cutting speed to over 1000 ^{0}C at 500 m/min. Increasing the feed rate did not have a pronounced effect as that of cutting speed. Temperature was found to increase with decrease in tool nose radius owing to decline in area available for heat conduction with smaller tool nose radius which also augmented the tensile residual stresses. The research also investigated the influence of rake angle on the temperature generated (Figure 2.8b). Reducing the rake angle from 0^0 to -20^0 leads to reduction in temperature generated at the cutting zone. This is due to the increase in the area available for heat conduction as the rake angle is rendered negative. However with further reduction in the rake angle, the increase in area of conduction is outweighed by the higher cutting pressure and frictional forces

associated with negative rake angle thereby increasing the temperature.

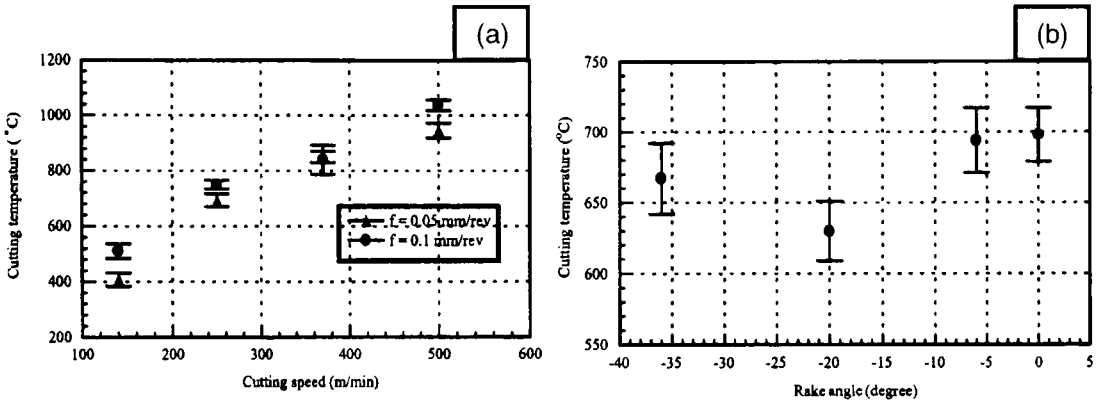

Figure 2.8: (a) Effect of cutting speed and feed on cutting edge temperature (b) Effect of rake angle on cutting edge temperature [29].

Koshy et. al. [7] conducted machining experiments on hardened ($\sim$ 58 HRC) AISI D2 and AISI H13 in order to document tool wear and appropriate cutting parameters. The majority of tools tested involved two flute coated carbide and cermet ball end mills in solid and indexable insert configurations. In line with the observations of previous researchers such as Hodgson [23] et. al., Becze et. al. [28] and Kishawy et. al. [29], an indexable ball end mill assembly with a negative rake of -10^0 was chosen, while the solid carbide tools presented positive axial rake of 0.5^0 to 3^0 and a radial rake of -16^0, -2.5^0 and $+3^0$. Better tool life was observed at intermediate feed (0.1 mm/tooth) suggesting that at lower feeds (0.05 mm/tooth), there is insufficient undeformed chip thickness promoting rubbing rather than cutting, thus affecting tool life. Tool life with negative radial rake solid carbide tools was better as compared to positive radial rake tools at lower cutting speeds (50 m/min), the effect of which was rather insignificant at higher cutting speeds (200 m/min). They concluded that indexable tools with a negative rake of -10^0 combined with coating of PVD TiCN (3 μm) is ideally suited for machining of hardened ($\sim$ 58 HRC) AISI D2. Tool life was an order of magnitude lower than that for AISI H13 and was

largely attributed to the hard and abrasive microstructure of D2. The governing wear mechanism was flank wear combined with chipping and attrition of the cutting edge. For predictable tool life and stable cutting process, they recommended that cutting speeds be restricted to less than 100 m/min.

Poulachon et. al. [30] [31] investigated the performance and wear mechanism of PCBN tools while turning four different hardened steels of the same hardness (54 HRC). While machining these steels under identical cutting parameters, the tool life varied significantly, establishing that cutting parameters and hardness of the material are not solely responsible for the deterioration of the cutting edge. In analyzing flank wear as a function of cutting time for the four materials, they observed X155CrMoV12 (AISI D2 equivalent) to correspond to higher tool wear rates. Flank wear morphology was found to exhibit deep grooves (Figure 2.9a) resulting from the abrasive action of the carbides. The size of the major grooves was approximately $10 - 15$ μm, which correlated well with the size of the hard carbide particles (Figure 2.5a) found embedded in the matrix of the hardened AISI D2 tool steels. The machining of X155CrMoV12 produced saw toothed chips even with a new tool (Figure 2.9b) indicating that the critical pressure in the cutting direction to exceed 4000 MPa as reported by El-Wardany et. al. [27] and can be ascribed to the chamfer provided on the tools used in the work. The research inferred that microstructure of hardened D2 tool steels consisting of hard and abrasive carbides particles are the main contributors to the wear of PCBN tools.

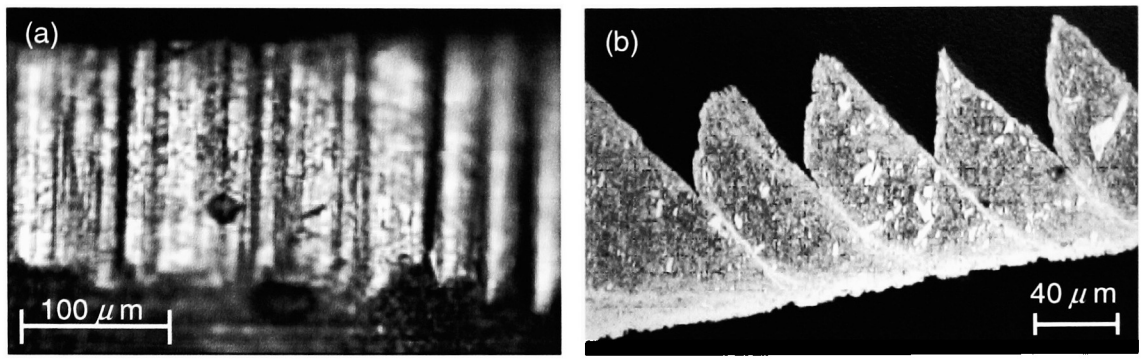

Figure 2.9: Flank wear (a) and saw-tooth chip morphology (b) obtained while turning X155CrMoV12 at V=180 m/min, f=0.08 mm/rev [30] [31].

In investigating the machinability of X210Cr12 (equivalent to AISI D2) cold worked tool steel hardened to 62 HRC in an end milling operation with neutral axial rake tools, Aslan et. al. [32] compared the performance of coated cemented carbide, coated cermets, Al_2O_3 ceramic and PCBN tools. Employing cutting a speed of 50 m/min for coated carbides and cermets, and 200 m/min for PCBN, the experiments were performed dry with a flank wear criterion of 0.3 mm. The hard and abrasive microstructure of the workpiece material is believed to be the contributing factor to the poor tool life (1200 mm^3) obtained with coated carbide and cermet tools with flank wear ranging from 0.79 to 0.55 mm respectively (Figure 2.10a). Flank wear on ceramic tools progressed smoothly to 0.135 mm for a volumetric tool life of 8400 mm^3, and failed thereafter because of excessive chipping (Figure 2.10b). This was attributed to the microcracks developed due to high mechanical loads during machining hardened D2 tool steels coupled with the brittleness of the tool material which limits its application. PCBN inserts portrayed a more uniform flank wear progression combined with $6-7$ times higher tool life (Figure 2.10c) as compared to ceramics and is best suited for machining of D2 tool steel. Surface finish obtained with coated carbide and cermet tools despite their catastrophic wear progression and

poor tool life was better than PCBN and ceramic inserts, the reason behind this is not clearly presented in the paper.

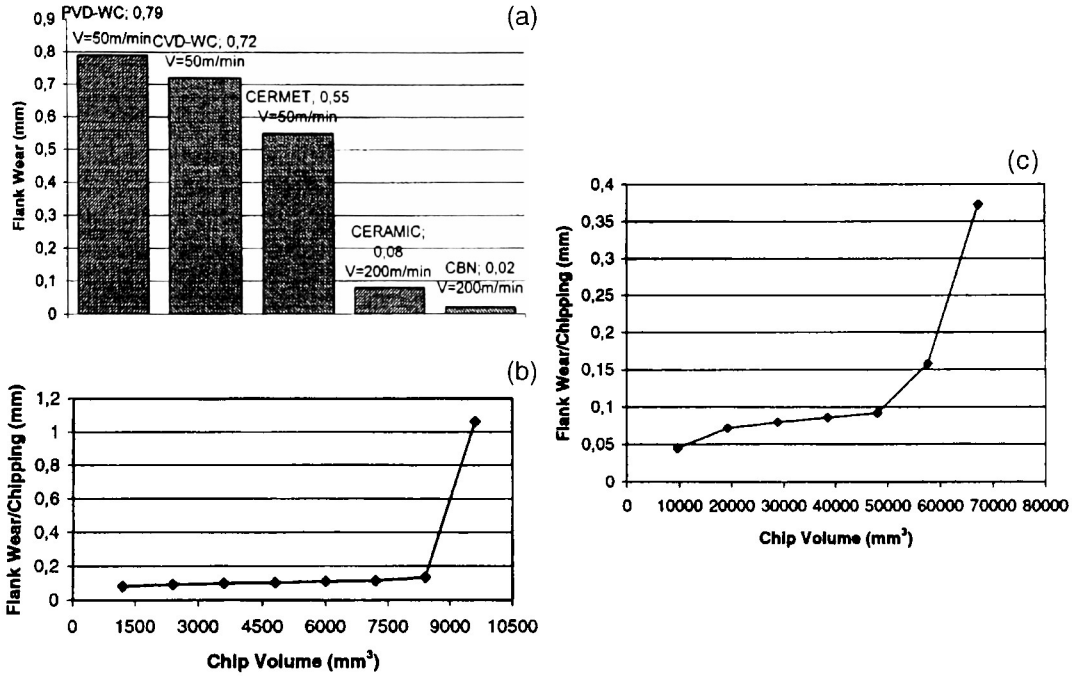

Figure 2.10: (a) Tool wear measured after removing a volume of 1200 mm^3 Progression of flank wear: (b) Ceramic and (c) PCBN [32].

2.6 Review of Hard Drilling of AISI D2

One of the very first research investigations into drilling of ferrous materials in their hardened ($50 - 70$ HRC) state was undertaken by König et. al. [1]. In their attempt to drill four different steels heat treated to 55 HRC (50CrMo4 heat treatable steel, 16MnCr5 case hardened steel and fully hardened 90MnV8 and X210Cr12 tool steels), using PCBN inserts, they realized tool life to vary by a factor of seven despite employing similar cutting parameters. Investigations revealed tool life to be inversely proportional to the percentage of martensite and the size and composition of carbide phase in the workpiece microstructure. The hard carbides impart maximum wear

resistance to tool steels but inhibit machinability as indicated by the poor tool life. While initial results on drilling of fully hardened (through hardened) thread rolls and plates were reasonably successful, the same could not be said in case of case hardened steels. It was observed that drilling performance deteriorated as the hardness values of the work material decreased in case hardened steels resulting in premature failure of the tool. The poor performance in drilling case hardened steels was attributed to the ductile chip formation in the softer zone causing clogging and seizure, and consequent failure. For successful machining of ferrous alloys in their hardened state, they recommended the use of negative rake tools ($\geq -10^0$) with a high wedge angle ($\geq 90^0$). Although this research presented the possibility of drilling steels in their hardened (50 – 70 HRC) state, it was concluded that tool life and hence overall performance remain strictly influenced by the material microstructure.

In order to fully understand the machining of hardened materials with geometrically defined cutting edges, in continuation of their previous work, König et. al. [33] employed higher cutting parameters and modified tool geometry to provide a negative rake angle (-6^0) while drilling four types of hardened (62 HRC) steels. Identical cutting parameters were employed in order to study the influence of material microstructure on the machinability of these steels. For a drilling depth of 2 mm, the authors reported a decrease in tool life (Figure 2.11a) influenced by the material microstructure with maximum tool life for case hardened steel (16MnCr5E) followed by cold worked tool steels (X100CrMoV51 and X210CrW12), high speed steel (S6-5-2) and least tool life with nitriding steel (31CrMo12). The drilling depth selected for all steels corresponded to the case depth of case hardened steel, thereby avoiding failure associated with drilling of a softer core with PCBN inserts as previously reported [1]. Although through holes were not drilled, it was expected that on account of the higher cutting and thrust forces involving negative rake tools, work material

breakouts at the hole exit would be inevitable limiting its application to blind holes. The authors concluded that the fundamental problem in drilling of hardened steels with a hard carbide matrix stemmed from the drop in cutting speed to zero near the center coupled with development of very high stress values along the cutting edge due to the carbide particles enhancing the flow strength of the workpiece. In order to address this issue, they proposed increasing the cutting speed so as to increase the temperature in the cutting zone, stimulating thermal softening of the work material, facilitating drilling (Figure 2.11b). The authors also recommended the use of cutting fluid while drilling hardened steels to flush the chips away from the cutting zone.

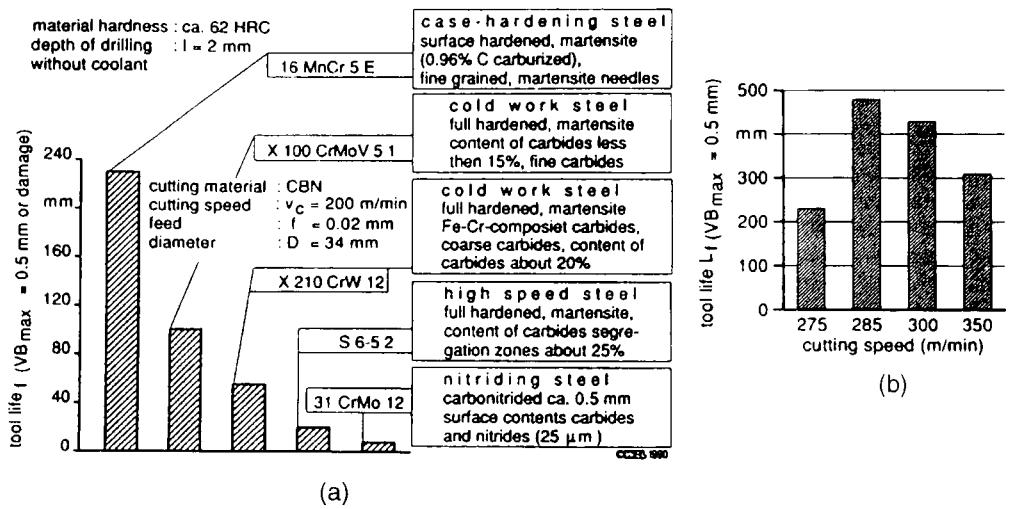

Figure 2.11: (a) Influence of material structure on tool life when drilling with PCBN (b) Influence of cutting speed on tool life [33].

In order to evaluate the impact of high pressure coolant, Arai et. al. [4] studied drilling of hardened SKD 11 (JIS equivalent of AISI D2), heat treated to values from 350 HV ($\sim$ 35 HRC) to 620 HV ($\sim$ 55 HRC). Coolant was supplied through the SKH 51 (JIS equivalent of Molybdenum High Speed Tool Steel AISI M2) twist drill at pressures of 1 and 7 MPa. Drilling to a depth 30 mm with a 6 mm twist drill at 350 HV ($\sim$ 35 HRC) at a spindle speed of 1100 rpm and a feed rate of 0.15 mm/rev,

they noted that the flank wear incurred was minimum ($\leq$ 0.075 mm) after 10 holes when high pressure coolant was employed. Maintaining constant cutting parameters and merely increasing the workpiece hardness up to 530 HV ($\sim$ 50 HRC) demonstrated an exponential increase in flank wear even with the supply of high pressure coolant, indicating the influence of work-material microstructure on flank wear (Figure 2.12a). The authors measured drilling temperatures to exceed 700 ^{0}C as the work hardness approached 60 HRC, rendering drilling impracticable, despite through-drill application of high pressure cutting fluid (Figure 2.12b).

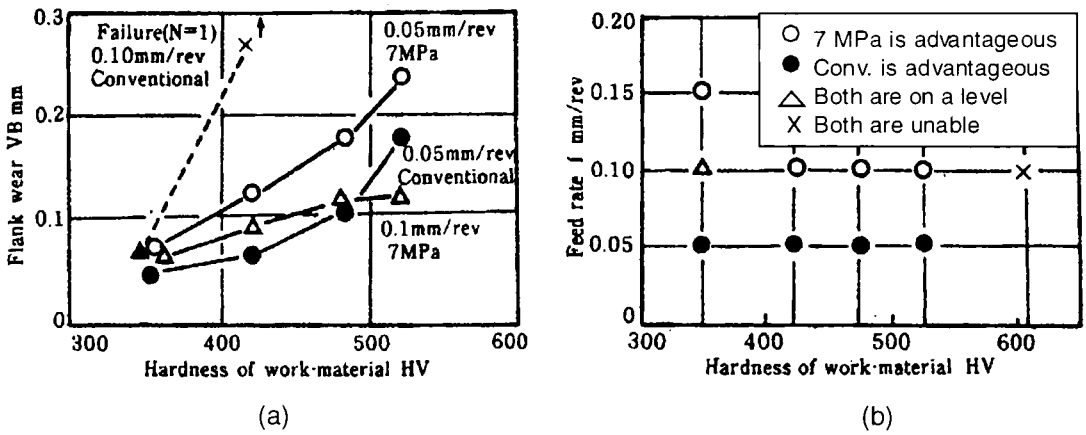

Figure 2.12: (a) Effect of work material hardness and feed rate on flank wear (8 holes) (b) Drilling conditions for hardened SKD 11 [4].

Coldwell et. al. [5] investigated the performance of long (7 mm diameter) and short (6.8 mm diameter) series coated (TiCN + TiN) solid carbide drills with respect to tool life when drilling hardened (60 HRC) AISI D2 steel plates of thickness 28 mm. Pressurized (1 MPa) cutting fluid supplied through the drill and peck drilling (14 mm peck depth) were employed during the machining trials. Using a screech criterion for determining end point of the test, the authors realized a tool life of 0.168 mm (6 holes). In comparing tool life it was observed that deflection due to smaller core diameter was the root cause of higher flank wear on long series drills consequently

resulting in poor tool life. Regardless of employing $3-6$ times higher cutting speeds while drilling AISI H13 than that for AISI D2, higher tool life ($\sim$ 18 times) was achieved with the former. The inferior performance when drilling D2 tool steel was attributed to its hard and abrasive microstructure.

2.7 Chapter Synopsis

The current chapter presented an overview of the complex drilling mechanics and highlighted the difficulties in hard drilling. Each of the drill attributes described in this chapter, namely: the helix angle (δ), the point angle ($2p$), the web thickness (2ω) and the clearance angle (θ) clearly influence the design of the cutting lips and the chisel edge and in turn affect drill performance. Alloying elements such as Chromium (Cr) and Molybdenum (Mo) not only improve hardenability of AISI D2, but also combine with carbon to form respective carbides which increases their wear and abrasion resistance. Characteristics of machining of hardened ($\geq$ 60 HRC) AISI D2 tool steel can be summarized as:

- Negative rake tools ($\geq -10^0$) along with a high wedge angle ($\geq 90^0$) are best suited for machining hardened D2 tool steel.
- Temperatures generated while machining hardened D2 tool steel can be as high as 1050 ^{0}C, necessitating high hot hardness of the cutting tools.
- Due to the use of negative rake tools, cutting forces are higher and demand high degree of stiffness from tooling, tool holding systems and machine tools to minimize the impact of deflection on tool life and product quality.
- A sharp cutting edge preparation is desired while machining hardened AISI D2 using PCBN tools in order to maximize tool life, while a chamfer or hone edge preparation may be provided on carbide tools to strengthen the cutting edge.

- ☞ Tool wear rate is heavily influenced by the carbide content of the work material and the cutting parameters employed. Saw-tooth chip forms are obtained when the pressure in the cutting direction exceeds 4000 MPa.

- ☞ Attrition wear at the maximum tool-work contact point was the predominant wear mechanism. Depending on cutting parameters employed, chipping and catastrophic failures were also observed.

- ☞ Although the process of drilling has evolved over time with the development of multifaced point geometries and tool substrates, drilling of hardened AISI D2 steel still presents a major challenge.

In light of the above, it is evident that a novel drilling process needs to be developed to addresses the fundamental issues with hard drilling of D2 tool steel. The following chapters discuss the adaptation of helical milling to handle the complexities posed by conventional drilling of hardened D2 tool steel.

CHAPTER 3
EXPERIMENTAL

3.1 Introduction

This chapter presents the experimental work conducted to evaluate the efficacy of helical milling of hardened AISI D2 tool steel in comparison to conventional drilling. Drilling of this material proved to be a formidable task, as indicated in Chapter 2 and hence was selected as the work material in this investigation. The current chapter builds on the concept of helical milling, explained in Chapter 1, providing details of process characteristics relevant to machining experiments. The experiments were designed to facilitate the investigation of tool life, cutting forces / torque, modes of tool wear and hole quality obtained in helical milling process. Information on the type of cutting tools used along with the selection of cutting parameters employed in machining experiments are detailed in the following sections.

3.2 Work Material and Tooling

Holes of 16.0 mm diameter were drilled in square plates of side 254 mm and thickness 13.8 mm, through hardened to 60 HRC. The work material surfaces were ground to remove any scales and distortions left behind due to heat treatment. This further facilitated proper clamping of the workpiece on the machine table, and assessing the quality of the hole at the exit surface.

In order to compare the effectiveness of the helical milling process vis-à-vis drilling, four types of twist drills and two types of end mills were utilized (Table 3.1).

Tool	Style	Tool Diameter (mm)	Substrate (Grade)	Operation
Tool 1	Solid	16.0	Tungsten Carbide (P10 – P30)	Conventional Drilling
Tool 2	Solid	16.0	Tungsten Carbide (P30)	Conventional Drilling
Tool 3	Solid	16.0	Tungsten Carbide (K40)	Conventional Drilling
Tool 4	Indexable	16.0	Tungsten Carbide (Not known)	Conventional Drilling
Tool 5	Indexable	12.0	Tungsten Carbide (P05 – P20)	Helical Milling
Tool 6	Solid	12.0	Tungsten Carbide (P05 – P20)	Helical Milling
Manufacturers Tool Code				
Tool 1: R840 – 1600 – 30 – A1A 1220 [34]				
Tool 2: B224A – 16000 KC7215 [35]				
Tool 3: Series 5510 – 5510 – 16.00 [36]				
Tool 4: DCM0630 – 205 – 063B – 3.5D (Body), IDI0.630 – SGIC908 (Insert) [37]				
Tool 5: R216 – 12A20 – 045 (Body), R216 – 1202M – M1025 (Insert) [34]				
Tool 6: R216.26 – 12050CAC26H 1610 [34]				

Table 3.1: Tooling used in experimental work.

The tools utilized in the current research are composed of ultra fine grained (grain size $\leq$ 0.5 μm) carbide substrates. These fine grains impart higher toughness without compromising hardness or wear resistance. thus facilitating machining of hardened steels with geometrically defined cutting edges [3].

3.2.1 Conventional Drills

Drilling experiments involved one each of four types (3 solid and 1 indexable insert) carbide drills (Figure 3.1) specifically meant for drilling of hardened steels as recommended by four different reputed manufacturers and are considered to be state-of-the-art in industry. All the drills incorporated a wear resistant coating, as shown in Table 3.2 that also lists the drill point geometries.

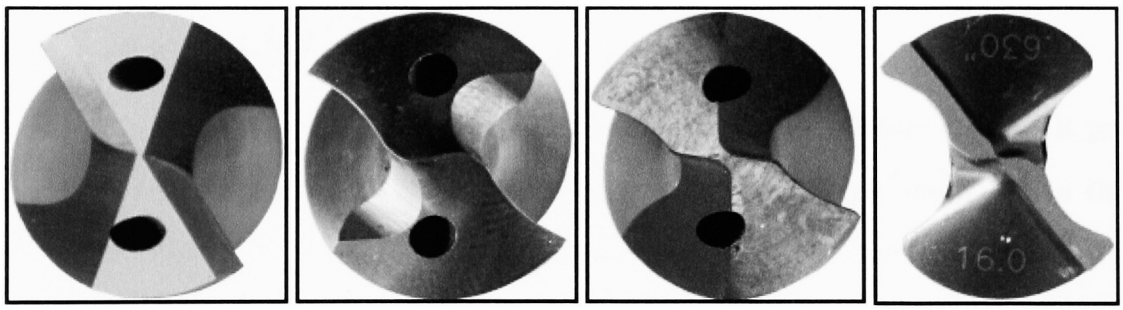

Figure 3.1: Drilling tool point geometries (a) Tool 1, (b) Tool 2. (c) Tool 3. (d) Tool 4.

Tool 1 supported a base coating of TiAlN with a topcoat of TiN, whereas Tools 2 and 4 were coated with a monolayer TiAlN coating, while Tool 3 was coated with multi-layer TiAlN consisting of alternating films of TiN + TiAlN to a thickness of around $3 - 6$ μm with the top stratum composed of TiAlN. It is interesting to note that but for the point angle of 140^0, the geometric elements of drills deemed suitable for drilling hardened steel varied over a wide range from one manufacturer to another.

	Tool 1	Tool 2	Tool 3	Tool 4
Helix Angle (δ)$^{\diamond}$	35^0	30^0	30^0	15^0
Point Angle (2ρ)	140^0	140^0	140^0	140^0
Clearance Angle (δ)$^{\diamond}$	9.6^0	10.6^0	13.0^0	9.2^0
Web Thickness (2ω)	0.28mm	5.40mm	0.78mm	0.28mm
Coating$^{\triangle}$	TiAlN + TiN	TiAlN	TiAlN (Multi-layer)	TiAlN
Diametral Tolerance	+0.007mm/ +0.025mm	+0.007mm/ +0.025mm	+0.007mm/ +0.025mm	Not available
$^{\diamond}$: Values specified at the periphery of the drill $^{\triangle}$: Physical Vapor Deposition (PVD) coating with a thickness of $3-6\mu$m				

Table 3.2: Characteristics of drills tested.

3.2.2 Helical Milling Tools

The tool path in helical milling follows a helical course (Figure 3.2a) as it proceeds into the workpiece. The tool used has to be of a diameter smaller than that of the machined hole (Figure 3.2b). The minimum machined hole diameter can be assumed to be 1.2 times the tool diameter and the maximum machined hole diameter would in general be restricted to 1.9 times the tool diameter, based on the following two factors:

- At minimum Bore to Tool ratio $(D_H/D_T)_{min}$, the hole diameter (D_H) should be at least 1.2 times the tool diameter (D_T), to ensure sufficient radial clearance between the tool and the hole for chip evacuation.

- At maximum Bore to Tool ratio $(D_H/D_T)_{max}$, where the hole diameter (D_H) is 1.9 times the tool diameter (D_T), the hole radius is less than the tool diameter. This ensures that the hole is not annular in profile.

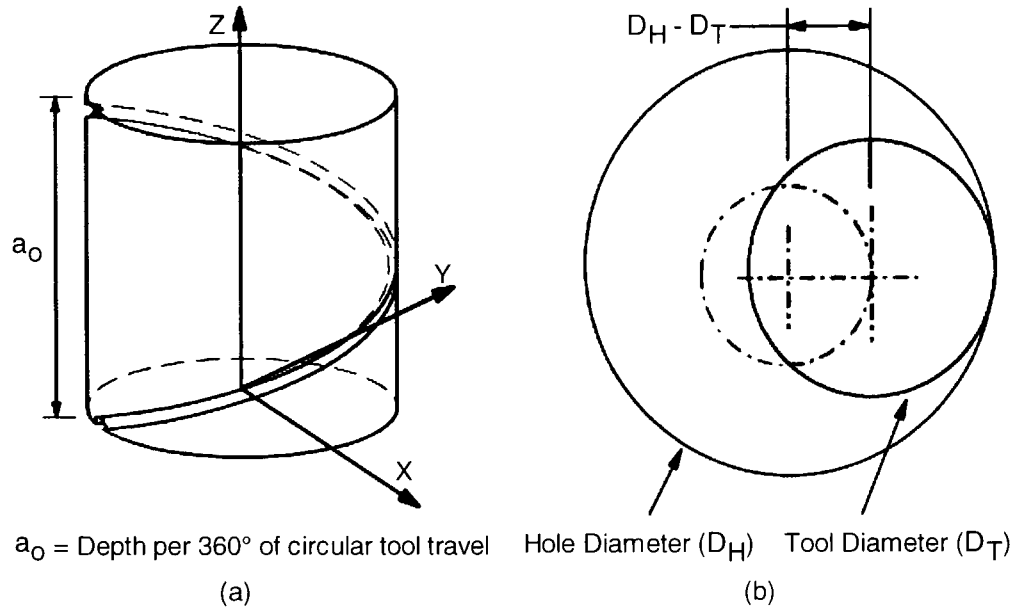

Figure 3.2: (a) Tool path in helical milling, (b) Tool / Hole diameter variation.

Considering that ball nose end mills are widely used in the tool and die industry, this tool type was selected for the helical milling trials with a view to minimizing tool changes and inventory. A 12 mm tool diameter (D_T) was used to machine a hole diameter (D_H) of 16 mm, thereby providing a bore to tool ratio (D_H/D_T) of 1.33. The geometrical details of helical milling tools are listed in the Table 3.3. One of the helical milling tools (Figure 3.3a) tested uses indexable inserts fastened to the cutter body. An unique design feature of this tool is the central insert that extends to the centreline of the cutter and the peripheral insert that stops short of the centreline. The indexable inserts were coated with TiCN with a topcoat of TiN.

Since the manufacturing tolerance on the indexable tool is rather high (Table 3.3) by design, it would have an influence on the final machined diameter. Hence a TiAlN coated, non-center-cutting solid carbide end mill with a negative axial rake of -8.5^0 and a helix angle of 50^0 with a much smaller tolerance was also employed for auxiliary machining trials.

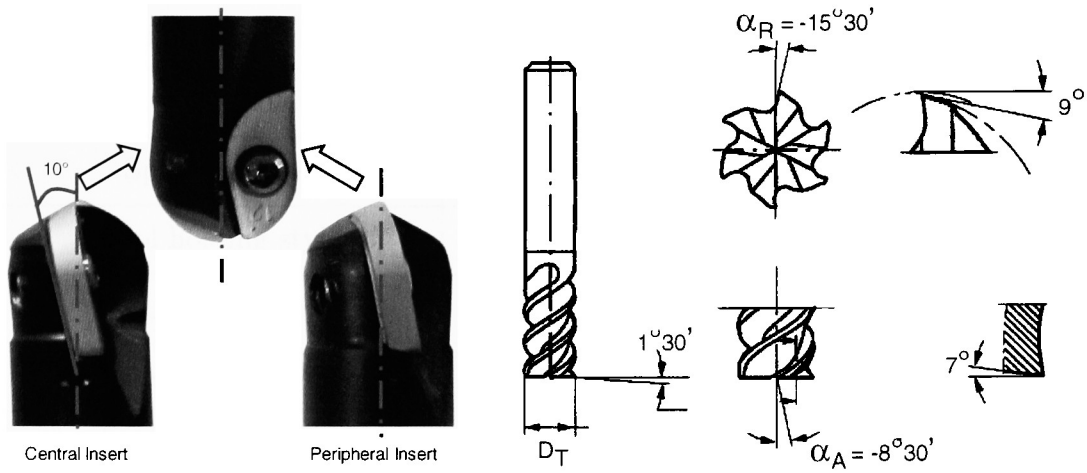

Figure 3.3: Helical milling tools used (a): Indexable insert ball nose end mill, (b): Solid carbide end mill [34].

	Helix	Axial Rake	Radial Rake	Primary Clearance	Wear Resistant Coating□	Diametral Tolerance
Tool 5	0^0	-10^0	0^0	$+9^0$	TiCN + TiN	+0.07 mm/ −0.23 mm
Tool 5	0^0	-10^0	0^0	$+9^0$	FUTURA® TiAlN◇ [38]	+0.07 mm/ −0.23 mm
Tool 6	50^0	-8.5^0	-15.5^0	$+9^0$	TiAlN	0.000 mm/ −0.070 mm
□ : Physical Vapor Deposition (PVD) coating with a thickness of $3-6$ μm ◇ : FUTURA® Multi-layer titanium aluminum nitride (TiAlN) coating $3-6$ μm						

Table 3.3: Configuration of helical milling tools.

3.3 Machine Tool Specification

Experiments were conducted on a Makino MC56-5XA, five axis milling center, as it satisfied the power / torque requirements suggested by the cutting tool manufactures for the parameters selected for machining of hardened steels. Owing to horizontal spindle orientation of the machine tool, the fifth axis (B Axis) was used to align the square face of the workpiece normal to the spindle axis. The technical details of the machine tool is detailed below (Table 3.4).

Maximum feed rate	15 m/min (Rapid)
Maximum spindle speed	15000 RPM
Spindle power	30 kW (40 HP)
Tool holding style	HSK 100A
Maximum travel	X : 510 mm, Y : 635 mm, Z : 635 mm
4^{th} Axis tilt (A Axis)	$+20^0$ to -100^0
5^{th} Axis tilt (B Axis)	360^0
Control	Fanuc 16
Movement Increment	0.0001 mm
Machine Features • Simultaneous 5-Axis Control • High Pressure Through Spindle Coolant and Air	

Table 3.4: Machine tool specification.

It is well understood that machining of hardened steels produces large thrust forces [39] [40] [41] [42] and hence in order to ensure adequate tool holding with minimal slippage and radial runout, the cutting tools were held in CoroGrip© high precision power chuck [34]. As illustrated in the schematic diagram (Figure 3.4), it consists of a moveable sleeve (2) which is moved up and down against a straight bore, tapered shank inner body (1) to facilitate clamping. In order to clamp the tool, an external hydraulic pump is used to generate a pressure of 70 MPa (700 bar), pushing the moveable sleeve (2) up against the tapered shank (1). The high pressure used for the movement of the sleeve activates a self locking mechanism and clamps the tool. For unclamping (Figure 3.4), pressurized oil is supplied in the reverse direction consequently moving the sleeve (2) down the tapered body thus releasing the tool.

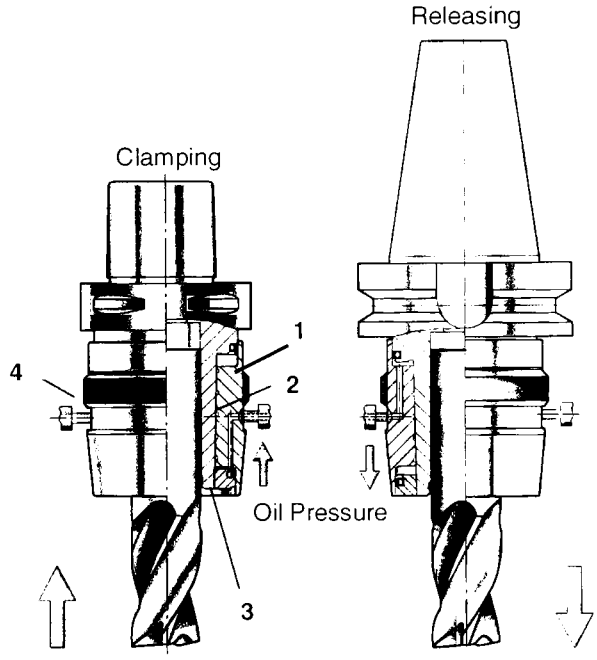

Figure 3.4: Cutting tool holder (adapted from [34]).

The rigid design and symmetrical clamping force limited the radial runout in the current experiments to $3 - 5$ μm for a tool overhang of $4 \times D_T$ (D_T being the tool diameter) and highest axial position stability. The clamping force of CoroGrip© precision chucks is considerably higher than that of shrink fit and hydraulic tool holders and incorporates the precision of shrink fit tool holders.

3.4 Material Removal Rate (MRR)

Material removal rate (MRR) can be computed by multiplying the cross-sectional area of the chip by the linear travel rate of the tool along the length of the workpiece. In order to compute the material removal rate for a given process, the relationships between the cutting parameters must be clearly understood, which is clarified in the following sections.

3.4.1 MRR - Conventional Drilling

Performance of a drilling operation depends extensively on the nature of the materials involved, drill geometry and the cutting parameters employed in the process. The relationships between the cutting parameters in drilling (Figure 3.5) are discussed as follows:

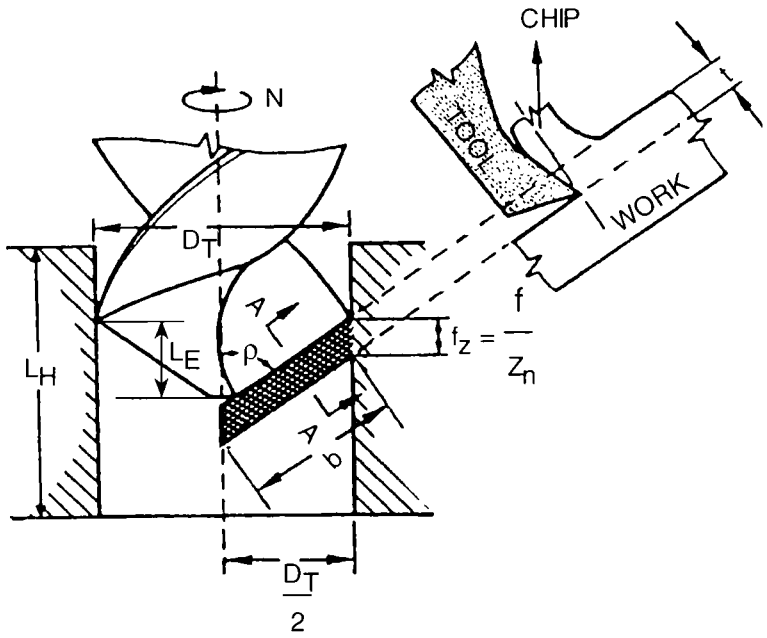

Figure 3.5: Mechanics of drilling (adapted from [11]).

The cutting speed (V) in drilling is given by

$$V = \frac{\pi \times D_T \times N}{1000} \qquad \text{(m/min)} \tag{3.1}$$

where D_T is the drill diameter and N is the spindle speed in rev/min. Feed (f) in drilling is usually specified as distance traveled per unit revolution of the drill which depends on the feed per tooth f_z and the number of cutting edges Z_n.

$$f = f_z \times Z_n \qquad \text{(mm)} \tag{3.2}$$

The feed rate (V_f) in drilling is given by

$$V_f = f_z \times Z_n \times N \quad = \quad f \times N \qquad (\text{mm/min}) \tag{3.3}$$

The material removal rate ($MRR\,|_{CD}$) in conventional drilling is given by:

$$MRR\,|_{CD} = \frac{\pi \times (D_t)^2 \times V_f}{4} \qquad (\text{mm}^3/\text{min}) \tag{3.4}$$

Drilling time $T\,|_{CD}$ is given by,

$$T\,|_{CD} = \frac{L_H + L_E}{f_z \times N \times Z_n} \quad = \quad \frac{L_H + L_E}{V_f} \qquad (\text{min}) \tag{3.5}$$

where, L_H is the length of the hole and L_E is twice the projection of the drill, required to engage the full diameter of the drill at the top and bottom of the hole.

3.4.2 MRR - Helical Milling

Although helical milling is employed to machine a hole, it follows the basic rules of milling and like any other machining process, its performance is affected by the cutting parameters adopted. In helical milling since the tool rotates about its own axis while simultaneously moving in the axial and radial directions, it is important to specify the axial depth per 360^0 of circular tool travel (a_o) as shown in Figure 3.6,

$$a_o \; = \; \pi \times (D_H \; - \; D_T) \times \tan(\theta_R) \qquad (\text{mm}) \tag{3.6}$$

where D_H is the diameter of the machined hole, D_T is the tool diameter and θ_R is the ramping angle recommended by the tool manufacturer. The ramping length L_R per 360^0 of circular tool travel (Figure 3.6) can be calculated as:

$$L_R \; = \; \sqrt{(a_o)^2 \; + \; [\pi \times (D_H \; - \; D_T)]^2} \qquad (\text{mm}) \tag{3.7}$$

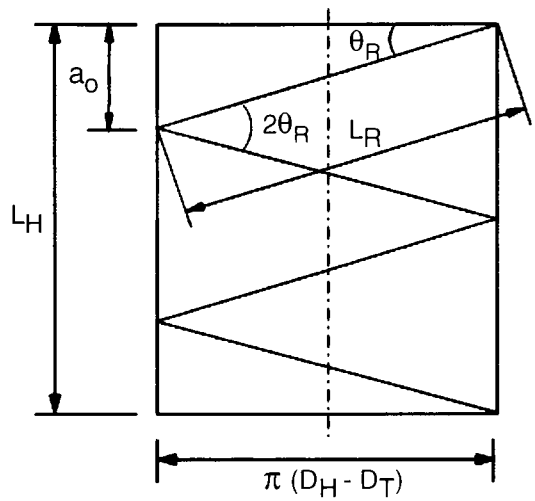

Figure 3.6: Tool travel in helical milling.

Substituting the value of a_o from equation 3.6, we get,

$$L_R = \sqrt{[\pi \times (D_H - D_T) \times \tan(\theta_R)]^2 + [\pi \times (D_H - D_T)]^2}$$

$$= \pi \times (D_H - D_T) \sqrt{\tan(\theta_R)^2 + 1}$$

$$\therefore \quad L_R = \frac{\pi \times (D_H - D_T)}{\cos(\theta_R)} \quad \text{(mm)} \tag{3.8}$$

Since the tool traverses a helical path, the total length of tool travel (L_T) is much greater than the length of the hole (L_H).

$$L_T = \frac{\pi \times (D_H - D_T)}{\cos(\theta_R)} \times \frac{L_H}{a_o}$$

$$= \frac{\pi \times (D_H - D_T)}{\cos(\theta_R)} \times \frac{L_H \cos(\theta_R)}{\pi \times (D_H - D_T) \times \sin(\theta_R)}$$

$$\therefore \quad L_T = \frac{L_H}{\sin(\theta_R)} \quad \text{(mm)} \tag{3.9}$$

Hence from equation 3.9 it can be comprehended that for a given hole depth (L_H), the total length of tool travel (L_T) in helical milling is inversely proportional to sine of the ramp angle (θ_R).

In the current experiments, ball nose end mills were employed wherein, quite often the full diameter of the tool (D_T) is not engaged in the work. It can be seen from Figure 3.7 that as the axial depth per 360^0 of circular tool travel (a_o) is varied, the effective cutting diameter (D_{eff}) changes accordingly and in general is always smaller than the tool diameter (D_T).

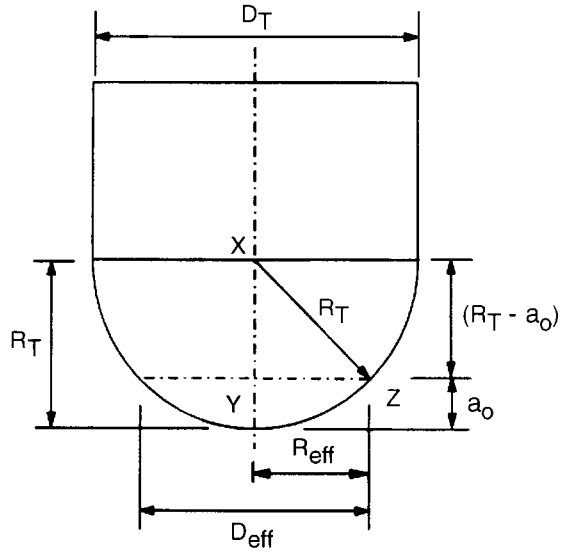

Figure 3.7: Effective cutting diameter in ball nose end mills.

Considering triangle XYZ in figure 3.7, the effective cutting radius (R_{eff}) of the ball nose end mill is given by:

$$R_{eff}{}^2 = R_T{}^2 - (R_T - a_o)^2 \quad = 2R_T \cdot a_o - a_o{}^2$$

We know that $2 \times R_T = D_T$ and $2 \times R_{eff} = D_{eff}$, where R_T is the radius of the tool and D_{eff} is the effective cutting diameter of the ball nose end mill.

$$\text{Substituting, we get} \quad \frac{{D_{eff}}^2}{4} = a_o(D_T - a_o)$$

$$\therefore \qquad D_{eff} = 2 \times \sqrt{a_o(D_T - a_o)} \qquad \text{(mm)} \tag{3.10}$$

Hence the effective cutting speed (V_{eff}) in helical milling is given by:

$$V_{eff} = \frac{\pi \times D_{eff} \times N}{1000} \qquad \text{(m/min)} \tag{3.11}$$

In most CNC machines the feed rate required for programming a contour (circular or helical) is calculated based on the center line of the tool. When the tool is moved along a straight line, the feed rate along the center of the tool and the cutting edge are identical. However in case of helical milling since the tool moves along a circle, there is a difference in the feed rate between the tool center and periphery (Figure 3.8) and is accounted for as follows:

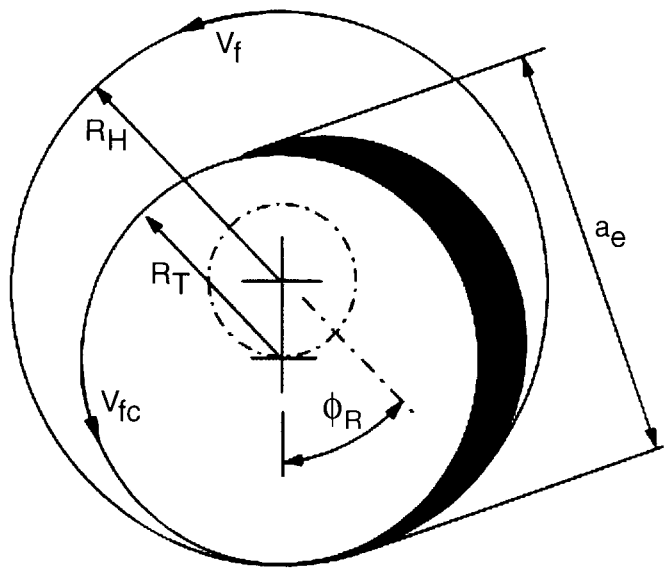

Figure 3.8: Effective feed rate in helical milling.

For a circular tool path, machining time (T) will be given as,

$$T = \frac{\text{Length of travel}}{\text{Feed rate}}$$

$$= \frac{\pi \times D_H}{f_z \times Z_n \times N}$$

$$\therefore \quad T = \frac{\pi \times D_H}{V_f} \quad \text{from equation 3.3} \quad \text{(min)} \tag{3.12}$$

Similarly in helical milling, machining time ($T\,|_{HM}$) is given by,

$$\text{Machining time } (T\,|_{HM}) = \frac{\text{Length of travel of tool center}}{\text{Circular feed rate at tool center}}$$

$$= \frac{\pi \times (D_H - D_T)}{V_{fc}} \quad \text{(min)} \tag{3.13}$$

where V_{fc} is the feed rate at the center of the tool and can be computed from equations 3.12 and 3.13.

$$\therefore \quad V_{fc} = [\frac{(D_H - D_T)}{D_H}] \times V_f \quad \text{(mm/min)} \tag{3.14}$$

The radial engagement (a_e), (Figure 3.8) is given by,

$$a_e = \frac{\text{Total area to be removed}}{\text{Length of tool travel}}$$

$$= [\frac{\pi}{4} \times {D_H}^2] \times [\frac{1}{\pi \times (D_H - D_T)}]$$

$$\therefore \quad a_e = \frac{{D_H}^2}{4 \times (D_H - D_T)} \quad \text{(mm)} \tag{3.15}$$

Metal removal rate in helical milling ($MRR\,|_{HM}$) is given by,

$$MRR\,|_{HM} = a_o \times a_e \times V_{fc} \qquad (\text{mm}^3/\text{min}) \tag{3.16}$$

Hence from equations 3.9 and 3.13 the total time required in helical milling ($T\,|_{HM}$) to machine the hole is:

$$(T\,|_{HM}) = \frac{L_T}{V_{fc} \times \sin\theta_R} \qquad (\text{min}) \tag{3.17}$$

3.5 Process Strategy and Cutting Parameters

Down (climb) milling technique was followed in all helical milling experiments. In helical milling, different bore to tool ratios (D_H/D_T) correspond to different material removal rates (MRR) despite constant cutting parameters, as reported by Tönshoff et. al. [8] [9], during their investigation into the effect of Bore to Tool ratio on hole quality.

Figure 3.9 indicates, two different tool diameters used to machine the same hole diameter by helical milling for bore to tool ratios (D_H/D_T) of 1.33 and 1.88. In a given situation where the spindle speed (N), ramp angle (θ_R), feed per tooth (f_z) and number of cutting edges on the tool (Z_n) are maintained constant for both the instances, the material removal rate (MRR) is higher for higher bore to tool ratios. The material removal rate (MRR) in helical milling (eq 3.16) depends upon the axial depth per 360^0 of circular tool travel (a_o), radial engagement (a_e) and the circular feed rate at tool center (V_{fc}). Equations 3.6, 3.15 and 3.14 suggest that any increase in the bore to tool ratio (D_H/D_T) would increase the axial depth per 360^0 of circular tool travel (a_o) and circular feed rate at tool center (V_{fc}) while decreasing the radial engagement (a_e). The increase in the axial depth per orbit and feed rate at tool center far outweigh the reduction in radial engagement thereby increasing the metal removal

rate (eq. 3.16). Higher metal removal rate results in higher machining forces, thus increasing the deflection of the tool and influencing form and diametral deviation. This is an important aspect to be considered in the selection of tool diameter in helical milling.

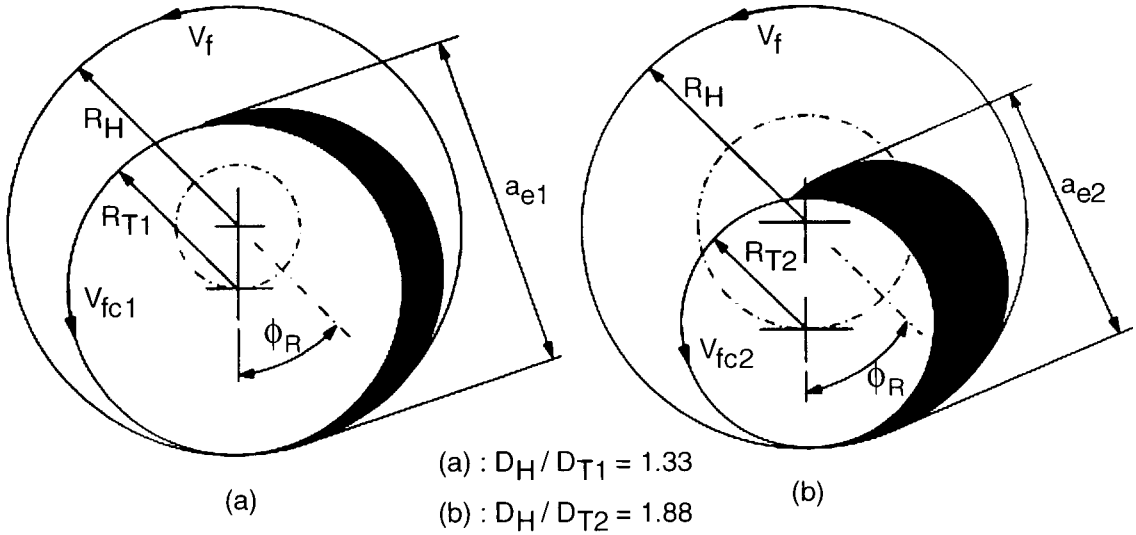

Figure 3.9: Influence of Bore to Tool ratio. (a): $D_H/D_T = 1.33$, (b): $D_H/D_T = 1.88$

In order to evaluate the process strategy in conventional drilling, pilot drilling trials were conducted considering three distinct scenarios.

- In the first scenario, trials conducted under dry conditions with no peck, resulted in poor performance with catastrophic failure of the cutting edges.
- The application of cutting fluid through the coolant holes in the drill body with no peck was attempted next. The cutting fluid assisted in the removal of chips, but did not significantly improve drill performance.
- Finally peck drilling combined with the application of cutting fluid was employed resulting in the best performance, and hence was adopted for all the

drilling experiments. The peck depth was chosen so as to ensure that the full diameter of the drill was engaged during each peck cycle.

3.5.1 Cutting Parameters

In order to minimize the impact of tool overhang on tool life and the occurrence of chatter [5], short series drills were chosen and tool overhang was restricted to 48 mm for all the tools tested. The cutting parameters for drilling was based on the generic recommendations of the manufacturers, as specified in Table 3.5,

Cutting Speed (V)	30 m/min
Spindle Speed (N)	600 rpm
Feed per Tooth (f_z)	0.06 mm/edge
Number of Cutting Edges (Z_n)	2
Feed Rate (V_f)	72 mm/min
Drilling Method	Peck Drilling
Peck depth	3 mm

Table 3.5: Drilling parameters.

Since the cutting speed (V) has the maximum influence on tool wear [12], the same was maintained for helical milling. The feed per tooth however was increased in helical milling from that in drilling based on the recommendations of the cutting tool manufacturer. The cutting parameters employed to test the performance of helical milling is listed in Table 3.6. It should be noted that the choice of ramp angles depends upon the design of the cutting tool and is usually based on the recommendation of the tool manufacturer.

	Ball Nose End Mill	Flat End mill
Cutting Speed (V)	$30^{\square}$, $37^{\square}$, $47^{\square}$ m/min	$66^{\square}$ m/min
Ramp Angle$^{\diamondsuit}$ (θ_R)	3^0	3^0
Axial Depth$^{\diamondsuit}$ (a_0)	0.659 mm	0.659 mm
Effective Diameter (D_{eff})	5.47 mm	12 mm
Spindle Speed (N)	$1740^{\square}$, $2160^{\square}$, $2760^{\square}$ rpm	$1740^{\square}$ rpm
Feed per Tooth (f_z)	0.10 mm/tooth	0.033 mm/tooth
Number of Cutting Edges (Z_n)	2	6
Linear Feed Rate (V_f)	348, 432, 552 mm/min	348 mm/min
Feed Rate at Tool Center (V_{fc})	87, 108, 138 mm/min	87 mm/min
$\square$: Parameter considered at the Effective Diameter (D_{eff}) $\diamondsuit$: Parameter considered per 360^0 of circular tool travel		

Table 3.6: Helical milling parameters.

Center cutting end mills are preferred in order to take advantage of higher ramp angles which translates in shorter machining times (equation 3.14). Also in cases where blind holes are required, use of non center cutting end mills would leave a small undesirable protrusion near the center of the hole.

3.5.2 Test Conditions and Force Measurement

Arai [4] and Kishawy [29] deduced through numerical simulation and experimentation that the temperatures in machining of hardened steel range from 700 ^{0}C to 1000 ^{0}C, depending upon the cutting parameters employed. Research into drilling of hardened steels has shown that for drilling depths over 10 mm, application of cutting fluid is essential to cool the tool and to flush the chips away [4] [5] [43]. This was reinforced by the results obtained during pilot drilling trials that necessitated the

need for employing a cutting fluid (water soluble oil, 10% by volume) at a pressure of 7 bar (0.7 MPa) through the coolant ducts in the drill body.

In view of the high temperatures involved, pilot helical milling experiments were also conducted with a cutting fluid (water soluble oil, 10% by volume), supplied externally, at a pressure of 7 bar (0.7 MPa). This however resulted in severe tool chipping, attributable to thermal cycling [12]. Hence helical milling trials involved just an air blow at a pressure of 8.3 bar (0.83 MPa), so as to cool the cutting edge and blow the chips away from the cutting zone.

The end of tool life for helical milling was characterized by a flank wear (V_B) criterion of 300 μm. Upon reaching the wear criterion, the tools were examined under an optical microscope for chipping on the flank and rake faces, notch wear and the flank wear (V_B) land width was measured. In the case of conventional drilling a screech criterion, which occurred prior to catastrophic failure, was used to determine the end of the trial and wear morphology was investigated [5].

The helical milling inserts obtained from the manufacturer were coated with TiCN + TiN (Table 3.3) and in order to establish correspondence with the drilling tool coatings, uncoated inserts were applied with BALINIT® FUTURA (TiAlN) coating from an external source other than the tool manufacturer. Their performance was evaluated not only in comparison to conventional drilling but also to that obtained by helical milling with TiCN + TiN coating. Considering that four different types of drills were tested, no attempt was made to repeat the tests. However, helical milling trials were replicated to assess the performance consistency in terms of tool performance and wear progression.

In order to facilitate measurement of torque and cutting force components, a Kistler quartz three-component dynamometer (model 9255B) was used. The holes machined using helical milling were sectioned for measurement and analysis of surface

finish using the Zygo Newview 5000, a non-contact surface testing machine. Prior to characterization of surface finish, measurement of hole quality characteristics, namely roundness and hole tolerance were undertaken on the Zeiss Prismo 900 co-ordinate measuring machine.

3.6 Chapter Synopsis

The current chapter details experimental set-up and cutting parameters employed to test the benefits envisaged in helical milling of hardened AISI D2 tool steel. In case of conventional drilling, the recommendations of four highly reputed cutting tool manufacturers was considered while selecting drill geometry and machining parameters.

As pointed out earlier, apart from the point angle (2ρ), none of the other geometric attributes of the drills were similar, which were considered to be state of the art for hard drilling. Helical milling tools consisted of a indexable ball nose end mill and a solid carbide end mill, that are commonly used in the die and mold industry and were smaller in size than the drills.

Since cutting speed is known to have the maximum impact on tool life, the same was maintained for helical milling, whereas other parameters such as ramp angle (θ_R), feed per tooth (f_z) were based on the recommendations of the tool manufacturer. Helical milling trails were performed dry with pressurized air supplied externally, while drilling experiments were conducted wet with cutting fluid supplied through the coolant holes of the drill.

In order to prevent slippage of the tools owing to high thrust forces associated with machining of hardened steels and to restrict radial runout, a high precision power chuck was used to hold the tools.

The experimental set-up, metal removal calculations and process strategy discussed in this chapter are critical for this research since they govern the reliability of the results. Since two completely different machining process are compared in this research, utmost care has been taken to ensure that the elements of variability are reduced to the minimum.

CHAPTER 4
RESULTS AND DISCUSSION

4.1 Introduction

The difficulty in drilling of hardened AISI D2 steel is due to the hard and abrasive microstructure of the work material leading to catastrophic tool failure resulting in poor tool life. The information presented in this chapter consists of validation of the process of helical milling for hole making in hardened AISI D2 steel. Cutting tests were conducted to compare drilling and helical milling in terms of attainable tool life, cutting forces, tool wear characteristics and hole quality. Based on the drill geometry, a hypothesis for the failure of drilling tools is put forth and verified. The impact of tooling configuration (indexable versus solid carbide) on the hole quality achieved in helical milling is also addressed.

4.2 Drilling of Hardened AISI D2

In the first phase of experimental work, drilling trials were undertaken employing cutting parameters described in Table 3.5. Experimental trials conclusively established the ineffectiveness of conventional drilling of hardened AISI D2 tool steel. The drilling process was characterized by a loud shriek from the time of drill engagement with the workpiece signifying imminent tool failure, which increased as the drill progressed into the hole. Even in the event that a single hole was conventionally drilled, tool life variation in terms of the length of hole drilled was as high as 35%, that can primarily be attributed to the geometrical characteristics (helix angle, point angle, web thickness, shape of the cutting lip) of the drill affecting its cutting mechanics and is discussed in this chapter.

4.2.1 Wear Modes in Conventional Drilling

The wear pattern of drilling tools 1 and 4 (Figures 4.1, 4.2) indicates catastrophic fracture of the cutting edges at the periphery. The point geometry of tool 1 is similar to that of a Four-Facet Chisel Edge design formed by the intersection of the primary and secondary relief planes ensuring reduction in thrust forces and improvement in centering accuracy. Tool 4 was ground to a modified split point geometry with "S" shaped cutting edges and web thinning for enhanced performance [11].

The tools (1 and 4) have the same web thickness of 0.28 mm (Table 3.2) and their respective cutting edge geometries advocate a positive cutting action with the rake angle equal to the helix angle of the drill at the periphery. High normal rake angles (α_n) and clearance angles (θ) (Table 3.2) at the periphery of the drills reduces their respective wedge angles (ξ) leaving the cutting edges vulnerable to failure due to reduced edge strength and is observed in the wear pattern of these drills (Figures 4.1, 4.2).

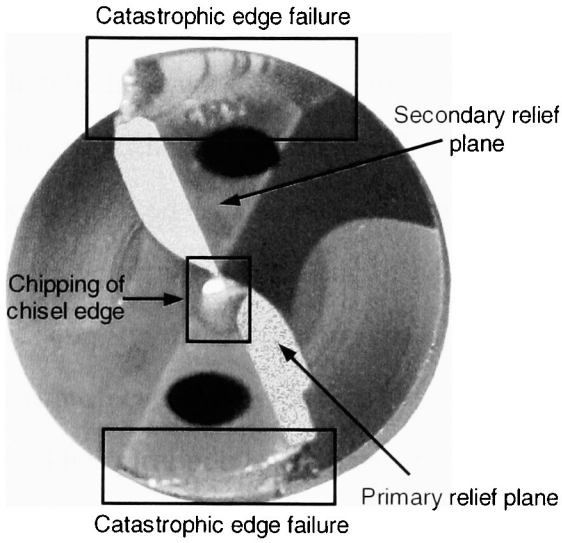

Figure 4.1: Drill wear mode Tool 1.

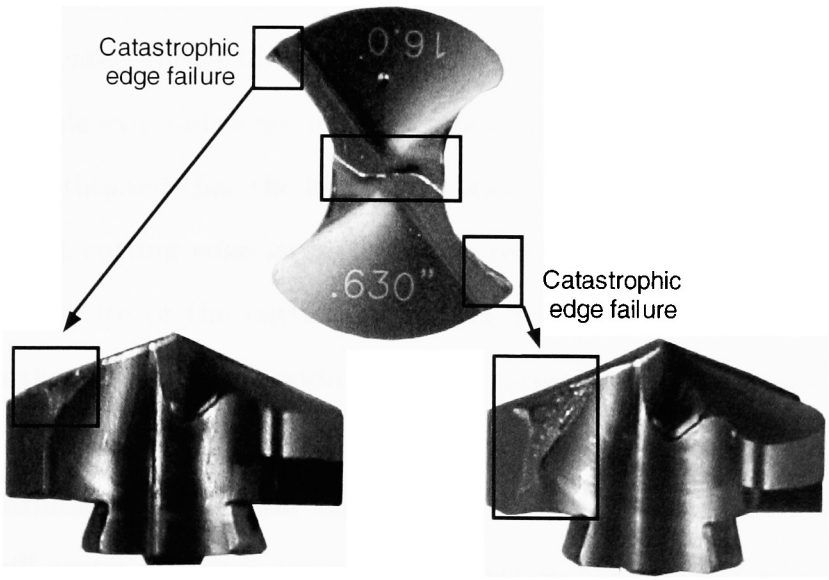

Figure 4.2: Drill wear mode Tool 4.

The failure of the cutting edges is attributed to extremely high cutting forces generated due to the presence of carbide particles in the workpiece microstructure impeding dislocation mobility thereby increasing the flow strength of the material coupled with poor cutting edge strength. Although drilling depths of 11.8 mm and 6.5 mm respectively were attained with these tools, the wear pattern realized is highly undesirable and hence these tools are unsuitable for drilling of hardened D2 tool steels.

Tool 2 underwent complete disintegration after drilling a depth of approximately 11 mm, with the fracture surface inclined roughly 45^0 to the drill axis indicating failure in torsion (Figure 4.3). The spiral point geometry ("S" shape chisel edge) of the drill (Figure 3.1) increases the web thickness of the tool as compared to conventional twist drills. Any increase in web thickness has a direct influence on the thrust forces generated in drilling and would be speculated as the cause of failure of the tool [3]. However the spiral point geometry of the chisel edge of Tool 2, provides a lower negative normal rake angle (α_n) than that of a conventional (straight) chisel edge promoting cutting rather than extrusion at the drill center. Due to the cutting action near the drill center, thrust forces are lower, which also translates into reduced burr formation at hole exit and hence improving hole quality [11].

It is hypothesized that the hard and abrasive nature of work material coupled with insufficient cutting edge strength due to reduced wedge angle ($\xi \sim 58^0$) cause chipping or fracture of the cutting edges. In addition, the concave cutting edge exacerbates the problem by providing a sharp corner that is susceptible to chipping [44], increasing the cutting forces. As a result, the torque acting at a given radial location in drilling, defined as the sum of the cutting forces multiplied by its distance from the drill center increases causing failure across the plane of maximum normal stress. The carbide tool substrate material being brittle in nature, is weaker in tension than in shear with the plane of maximum tension occurring along surfaces at 45^0 to the

shaft axis causing catastrophic failure of the tool. Although Tool 4 sported a concave cutting edge as Tool 2 (Figure 3.1), it provided a stronger wedge angle ($\xi \sim 75^0$) that prevented such a catastrophic failure.

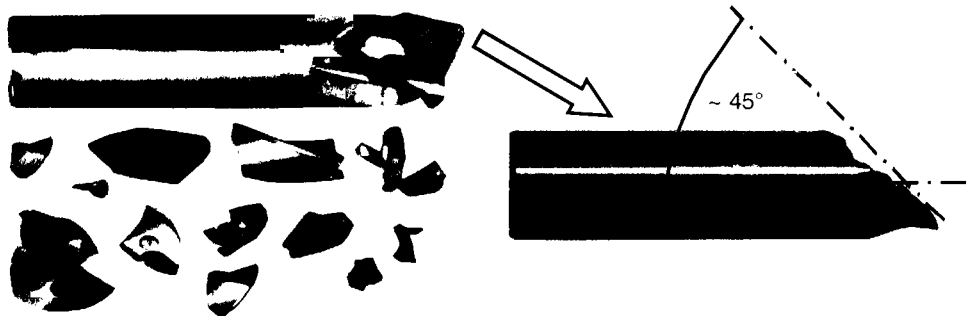

Figure 4.3: Drill wear mode - Tool 2.

The best outcome among the four drills tested corresponded to tool 3 (Figure 4.4) that yielded just a single hole, but incurred rake face wear in excess of 300 μm. Modified Split Point configuration with an "S" shaped cutting edge geometry similar to tool 4 was ground on the drill, but demonstrated a higher web thickness (Table 3.2) as compared to tools 1 and 4. The increased web thickness is due to adoption of notch type web thinning procedure which produces two small cutting edges on each side of the chisel edge, improving edge security and reducing thrust forces. Observation of the drill periphery indicated micro-chipping of the cutting edges in line with the results obtained for tools 1 and 4 albeit not as severe as in the previous cases. The improved performance of tool 3 is attributed to the cutting edge correction in the form of edge honing provided at periphery and the application of tougher (K40) carbide grade which improves toughness by $50 - 60\%$ preventing premature failure [36]. The increased toughness helps in resisting fracture caused by high mechanical loads, but comes at the expense of hardness of the tool, affecting its wear resistance. The rake face wear of the cutting edges exceeded the wear criterion of 300 μm restricting the application of this tool for drilling of hardened D2 tool steel.

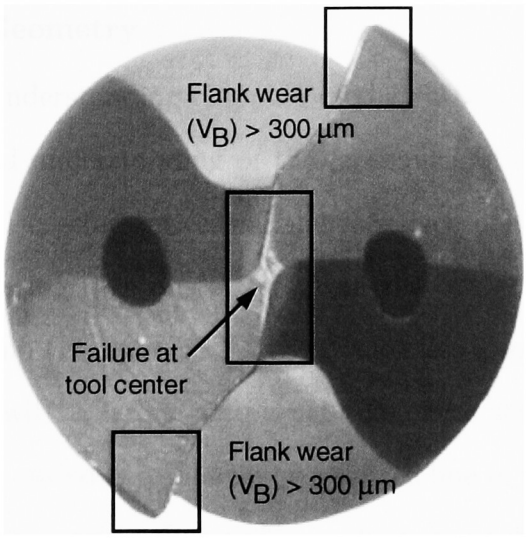

Figure 4.4: Drill wear mode - Tool 3.

It can be seen that none of the drills tested followed the desired wear pattern of a conventional drill (Figure 4.5). The wear profiles experienced in case of conventional drilling of hardened D2 tool steel indicate catastrophic fracture caused due to excessive mechanical loads acting along the cutting edges. The location of the fracture is consistently observed to be along the periphery on the flute face (except for tool 2 that disintegrated completely) and is discussed in the following section.

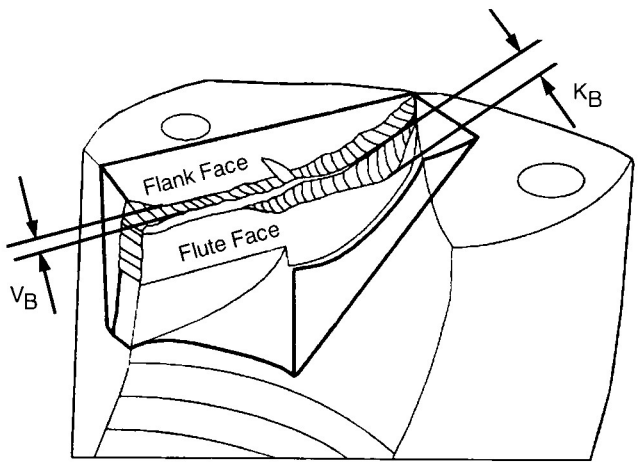

Figure 4.5: Conventional twist drill wear pattern (adapted from [34]).

4.2.2 Twist Drill Geometry

With a view to understanding chipping of the cutting lips of the drill (Figure 4.1, 4.2, 4.4), a detailed understanding of the mechanics of drilling is necessary. In contrast to other metal cutting processes, the rake face of a twist drill is not flat, but twisted with increasing rake angle (α_n) from the center towards the periphery producing a rotating chip (Figure 4.6). Cutting velocities also vary along the cutting edge, which combined with a larger peripheral rake cause strong side curling of the chip. This strongly side curled chip, shown by a dotted line in the figure 4.6, is further forced to curl when it encounters obstruction in the form of drill web and the wall of the hole as it progresses into the workpiece forming a conical helical chip. The chip is subjected to angular velocities ω_c, ω_r and ω_z along the drill axis and along the X and Z directions respectively (Figure 4.6). The resultant of these three velocity identities imparts helical motion to the chip at an angular velocity of ω [45].

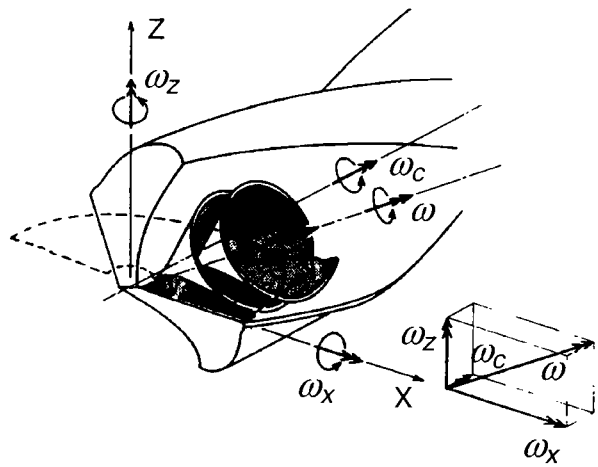

Figure 4.6: Conical helical chip produced by twist drill [45].

Chip formation in drilling occurs by extrusion / indentation around the chisel edge, and cutting along the lips of the drill. The inherent geometry of the cutting edges of the drill cause a variation in the helix angle (δ), the clearance angle (θ) and

the wedge angle (ξ) along the drill lip. The normal rake angle (α_n) at any radial location (r) along the cutting edge of the drill is given by the relationship [46] [47]:

$$\tan(\alpha_n) = \frac{\tan(\delta)}{\sin(\rho)}[\cos(\beta) + \sin(\beta)\tan(\beta)\cos(\rho)^2] - [\tan(\beta)\cos(\rho)] \tag{4.1}$$

where ρ is half point angle of the drill; δ is the helix angle at radial location r and β is the web angle at the same radial location (r) under consideration.

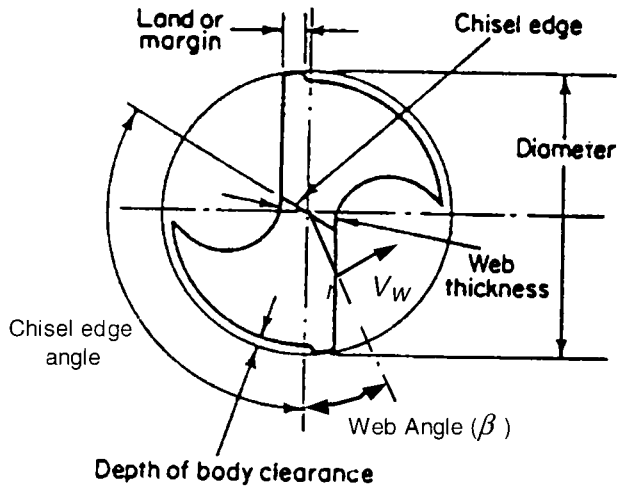

Figure 4.7: Web angle (β) of a drill (adapted from [48]).

The web angle (β) varies along the cutting edge (Figure 4.7) and is expressed as [12] [46] [47]:

$$\sin(\beta) = \frac{w}{r} \tag{4.2}$$

where r is the radial location along the cutting edge and w is half the web thickness of the drill. The helix angle (δ) can be written as [12] [46] [47]:

$$\tan(\delta) = \frac{2\pi r}{L} \tag{4.3}$$

where L is the lead of the helix and is constant for a given drill. Since this information

is usually not supplied by the drill manufacturer it can easily be computed as:

$$L = \frac{2\pi R_T}{\tan(\delta_o)} \tag{4.4}$$

where R_T is the radius of the drill and δ_o is the helix angle at the periphery of the drill.

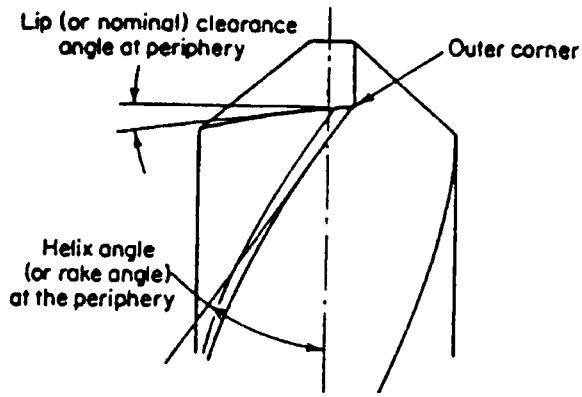

Figure 4.8: Clearance angle (θ) and Helix angle (δ) of a drill at the periphery [48].

It is apparent from equation 4.1, that the normal rake angle (α_n) will vary with any variation in helix angle (δ) and web angle (ξ) along the cutting edge. Similarly, the clearance angle (θ) also varies along the cutting edge and hence is always specified at the periphery of the drill. It can be computed using the expression [46] [47]:

$$\tan(\theta) = \frac{\cos(\rho)[\cos(\beta_1)\tan(\beta) - (\tan(\beta_o) - \tan(\theta_o)\tan(\rho))]}{\cos(\beta_o) + \tan(\beta)\cos(\rho)^2[\tan(\beta_o) - \tan(\theta_o)\tan(\rho)]} \tag{4.5}$$

where θ_o is the clearance angle at the drill periphery and β_o is the web angle at the periphery of the drill, given by the relationship [12] [46] [47]:

$$\sin\beta_o = \frac{w}{R_T} \tag{4.6}$$

The wedge angle (ξ) defined as the angle between the rake face and clearance face of

the tool can be computed as:

$$\xi = 90 - \alpha_n - \theta \tag{4.7}$$

Using the above relationships, variation in normal rake (α_n), clearance angle (θ) and wedge angle (ξ) for the drilling tools used in the current research were mapped using MATLAB® and is shown in Figure 4.9.

It can be seen that the normal rake angle (α_n) attains very high negative values close to the chisel edge and gradually approaches a value equal to the helix angle (δ_o) towards the periphery of the drill. The clearance angle (θ) and wedge angle (ξ) however decrease from the chisel edge to the outer corner of the drill lip. The cutting edge in drilling is formed by the intersection of the flute and flank faces and its shape is strongly influenced by the point angle, helix angle and the flute contour. Galloway [16] observed the shape of the cutting lip to vary from a convex shape at a point angle (2ρ) of 60^0 to concave at 150^0. At a point angle (2ρ) of 118^0, a straight cutting lip was obtained which facilitates maximum tool life. The flute contour and the helix angle are on the other hand are designed so as to provide this straight cutting edge for a point angle (2ρ) of 118^0 [11] [16] [48].

The drilling tools (Figure 3.1) used in this research have a point angle (2ρ) of 140^0 advocating a concave cutting edge for improved chip breaking except for tool 1 which sported a straight cutting edge [11] [44]. Even though the relationships developed to study the variations in drill angles are based on a straight cutting edge, Chayan et. al. [49] reported that they can very well be applied to concave and convex cutting edge designs of the conventional twist drill. The effect of the variation on the wedge angle (ξ) (Figure 4.9) in terms of catastrophic tool failure is discussed in the next section.

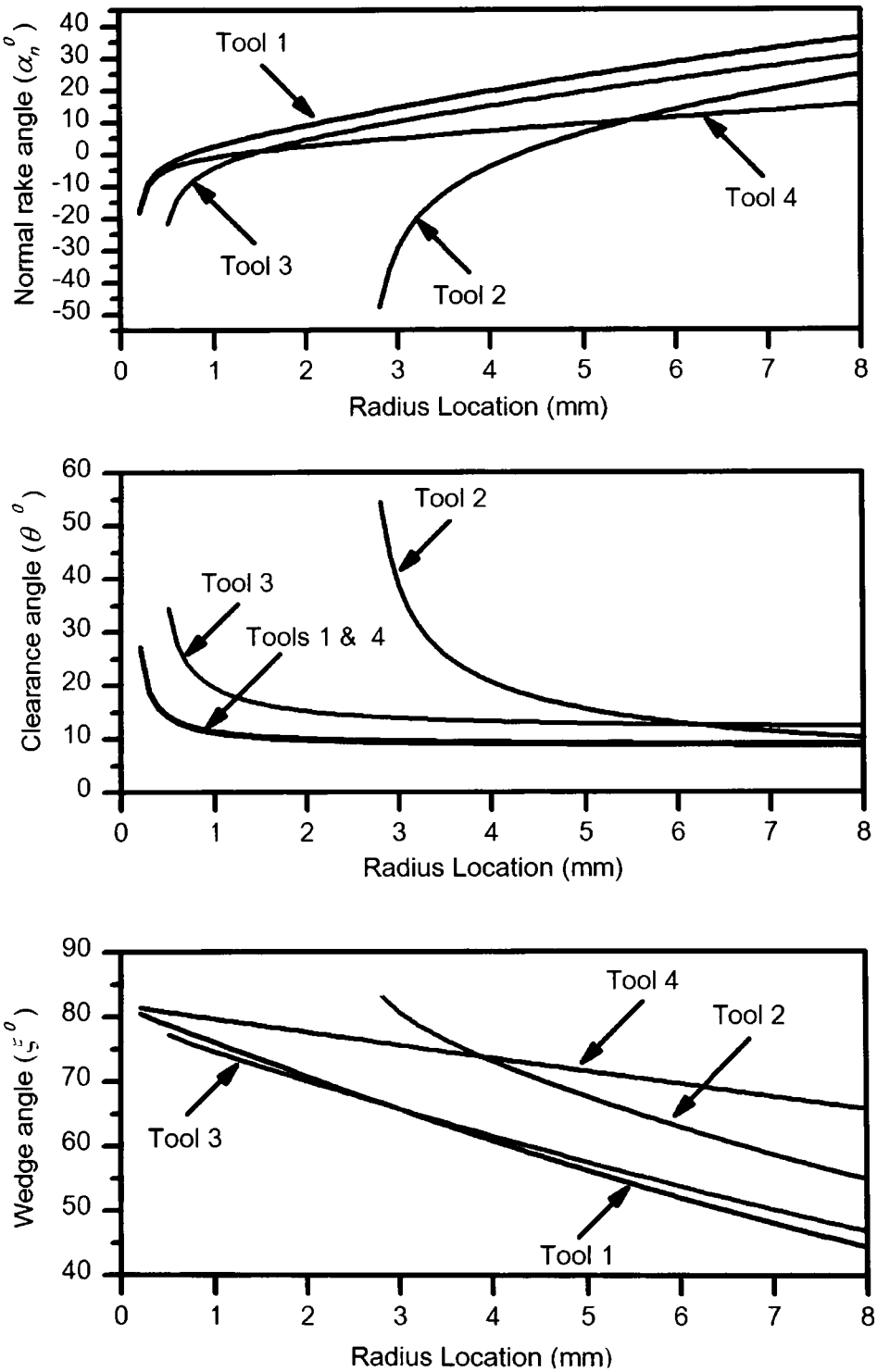

Figure 4.9: Variation of normal rake angle (α_n), clearance angle (θ) and wedge angle (ξ) along the cutting edge of the drills tested.

4.2.3 Influence of Work Material

While investigating the flow stress of hardened AISI D2 using the Compressive Split Hopkinson Bar technique (CSHB), Becze et. al. [50] observed the material to undergo significant strain hardening at low (3.5×10^3 s^{-1}) and high (5×10^4 s^{-1}) strain rates owing to carbide particles (Section 2.3.2) in the steel impeding mobility of dislocations. Temperature had a marginal effect on the shear flow stress of the material which was measured to be in excess of 1300 MPa at an ambient temperature and approximately 1100 MPa at 500 ^{0}C. Although benign from the point of view of augmenting the wear resistance of the material, the carbide particles significantly hinder machinability by increasing its flow strength and inducing abrasive wear.

The increased flow strength of the material necessitates the use of a stronger cutting edge. The intrinsic variation of the normal rake angle (α_n) in drilling from being highly negative (typically about -23^0, Figure 4.9) near the drill center to being positive at the drill periphery corresponds to lower wedge angles ($\xi \sim 45^0$ to 70^0 Figure 4.9) of the cutting edges at the periphery, weakening the overall strength of the cutting edge. Consequently, this is also the location of failure (Figures 4.1, 4.2, 4.4) in most of the drills tested. Although a positive rake (α_n) is obliging in terms of reducing the cutting forces and temperatures, it compromises the strength of the cutting edge (Figure 4.10) which is paramount in this application.

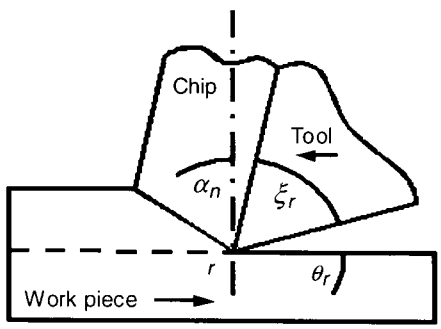

Figure 4.10: Wedge angle (ξ) at radial location r (r = Drill periphery).

Chipping of the cutting edges at the drill periphery (Figures 4.1, 4.2, 4.4) has further been investigated in light of the stresses developed along the cutting edges. The stresses developed along the cutting edge while machining hardened AISI D2 and AISI H13 tool steels was studied by Ng [51] using finite element analysis. Simulations were performed for a normal rake angle (α_n) of 35^0, which is equivalent to the helix angle at the periphery (δ_o) for tool 1 (Table 3.2). Clearance angle at the periphery (θ_o) corresponded to 10^0 giving a wedge angle (ξ) of 45^0 and cutting speed (V) was maintained at 30 m/min for an uncut chip thickness of 0.06 mm. Using Arbitrary Lagrangian Eulerian formulation and Johnson-Cook constitutive model to characterize the non-linear thermo-plastic work material behavior, the finite element simulation indicated the highest maximum tensile principal stresses for a tool with no flank wear to be on the order of 2 GPa (Figure 4.11).

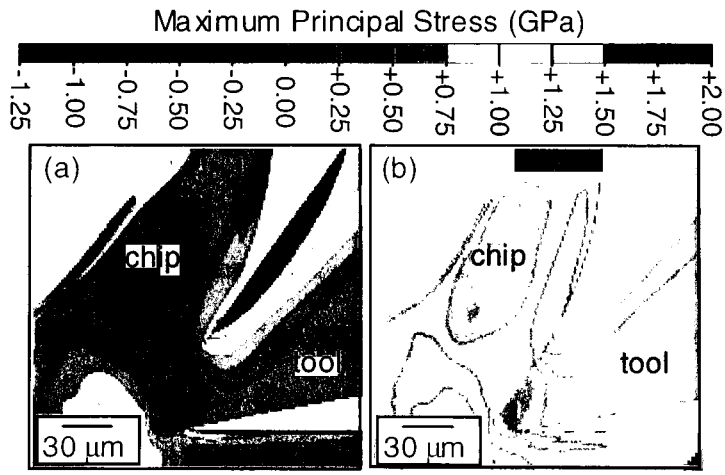

Figure 4.11: Stress field when machining : (a) D2 and (b) H13 tool steels [51].

The transverse rupture strength (TRS) of commercially available fine grain carbide varies in the range of $1.5 - 2.5$ GPa at ambient temperature [52]. Due to abrasive nature of the material, tool wear progresses rapidly increasing the maximum stresses on the tool. Arai at. al. [4] showed the temperature to approach 700 ^{0}C while drilling

D2 at a hardness of 520 HV ($\sim$ 51 HRC) and is envisioned to be higher in the current research, as higher hardness of the work material and cutting speeds are employed. The increase in temperature, would further decrease the TRS of the cutting tool elucidating chipping of the cutting edges. The TRS of submicron grade cemented carbides can be as high as 3.5 GPa [52], however, the higher end of the TRS spectrum generally corresponds to a lower hardness that compromises its wear resistance, which is unfavorable in reference to the abrasive carbides in D2 that are of hardness 2400 HV, which is three times that of martensite. It can be seen from Figure 4.11 that the maximum stress developed while machining AISI H13 is only half of that of AISI D2, which explains why drilling of hardened AISI H13 does not involve any of the problems associated with D2 [5]. The stress analysis emphasizes the need for negative rake (α_n) tools corresponding to sufficient wedge angles (ξ) when machining hardened AISI D2 tool steel.

Additional problems in drilling arises from the drop in the cutting speed (V) to zero at the drill center leading to material removal by extrusion rather than cutting. The chisel edge configurations influence the thrust forces, rigidity of the drill and its centering capabilities. Although, all the tools tested incorporated modern point configurations designed to reduce the problems associated with the chisel edge, tools 1, 3 and 4 show chipping at the tool center (Figures 4.1, 4.2, 4.4). The hardness of the work material combined with an abrasive microstructure further exacerbates the problem. Difficulties with drilling of hardened steel can be comprehended with reference to the works of König et. al. [33] and Coldwell et. al. [5], who reported drill life to vary by a factor of over 30 and 7 respectively depending upon the work material microstructure.

4.2.4 Possible Drill Geometry Modifications

The stress analysis presented in the previous section pointed to the preferred need for negative rake (α_n) tools that correspond to sufficient wedge angles (ξ) to provide the necessary strength to the cutting edge when machining hardened D2 tool steel. It is seen from equation 4.1 that of all the geometrical parameters of the drill, the helix angle (δ) and the point angle (2ρ) would have the most influence on the normal rake angle (α_n) along the cutting edge of the drill. This section examines the possibility of rendering the drill geometry to correspond to adequate wedge angle (ξ).

The simulation results for variation in helix angles at the periphery (δ_o) of the drill and variation in point angles (2ρ) is shown in Figures 4.12 and 4.13 respectively. It can be seen from Figure 4.12 that as the peripheral helix angle (δ_o) is changed from 28^0 to 0.1^0, the variation in normal rake angle (α_n) from the drill center to its periphery tends to be less acute. In fact at a peripheral helix (δ_o) of 0.1^0, the normal rake (α_n) is negative all along the cutting edge with minimal variation in the wedge angle (ξ). The variation of clearance angle (θ) along the cutting edge of the drill (4.12) depends upon the point angle (θ) and the web angle (β) as reported in Equation 4.5 and remains unaffected by variations in the peripheral helix angle (δ_o).

Variation in the point angles (2ρ) are seen to have a marginal effect on the normal rake angle (α_n) and the clearance angle (θ) as seen from Figure 4.13. At a point angle (2ρ) of 179^0, there is almost no variation in the normal rake (α_n) or clearance angle (θ) and the drill resembles a center cutting end mill, providing a stronger wedge angle (ξ). This would however lead to a highly concave cutting edge shape, which is prone to chipping at the periphery of the drill [16] [44]. Moreover, thrust forces are minimum at a point angle (2ρ) of 118^0 and increase parabolically with further increments in point angle (2ρ) [11] resulting in work material breakouts at hole exit leading to poor part quality.

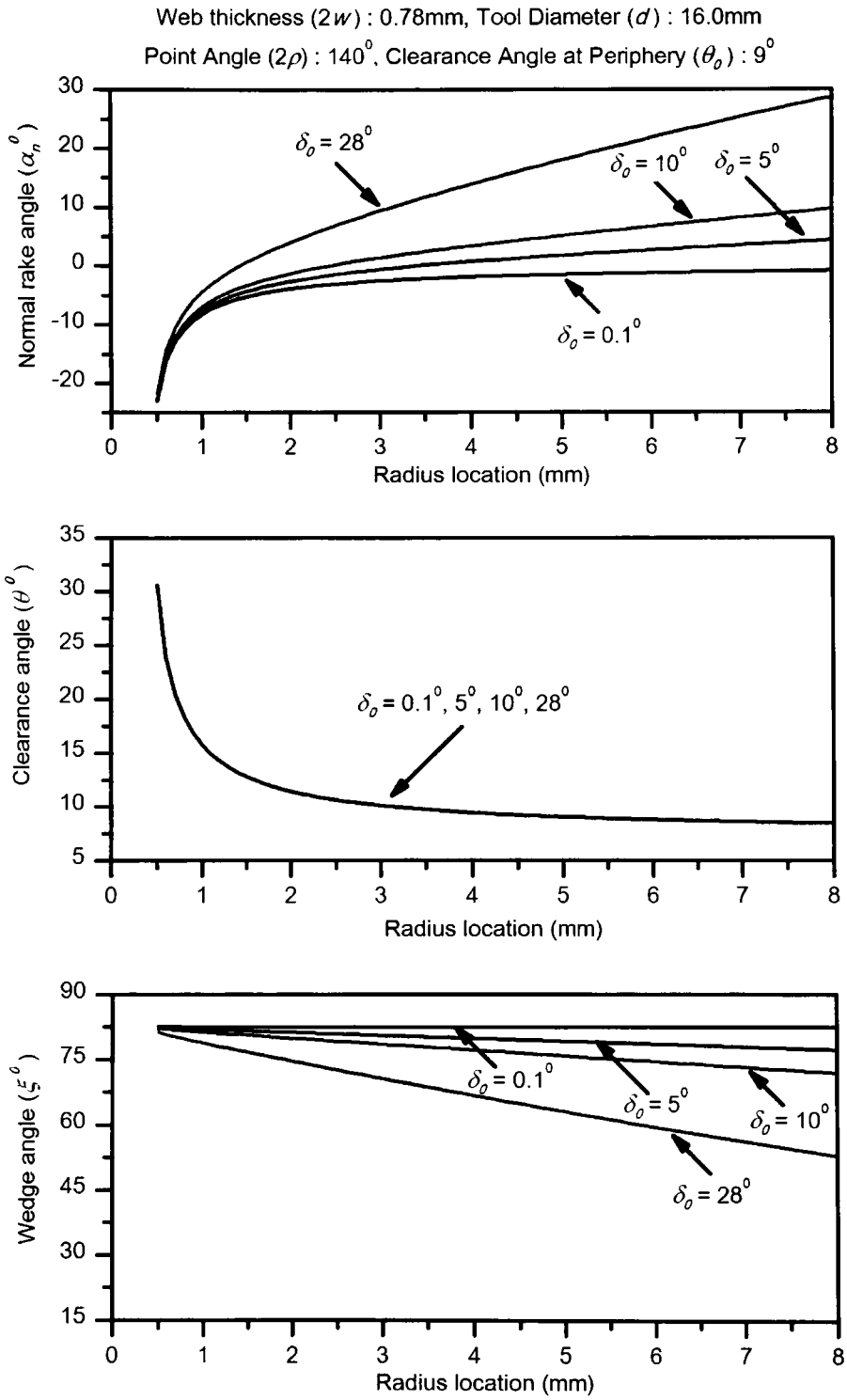

Figure 4.12: Variation in normal rake angle (α_n), clearance angle (θ) and wedge angle (ξ) along the cutting edge with variation in peripheral helix angles (δ_o).

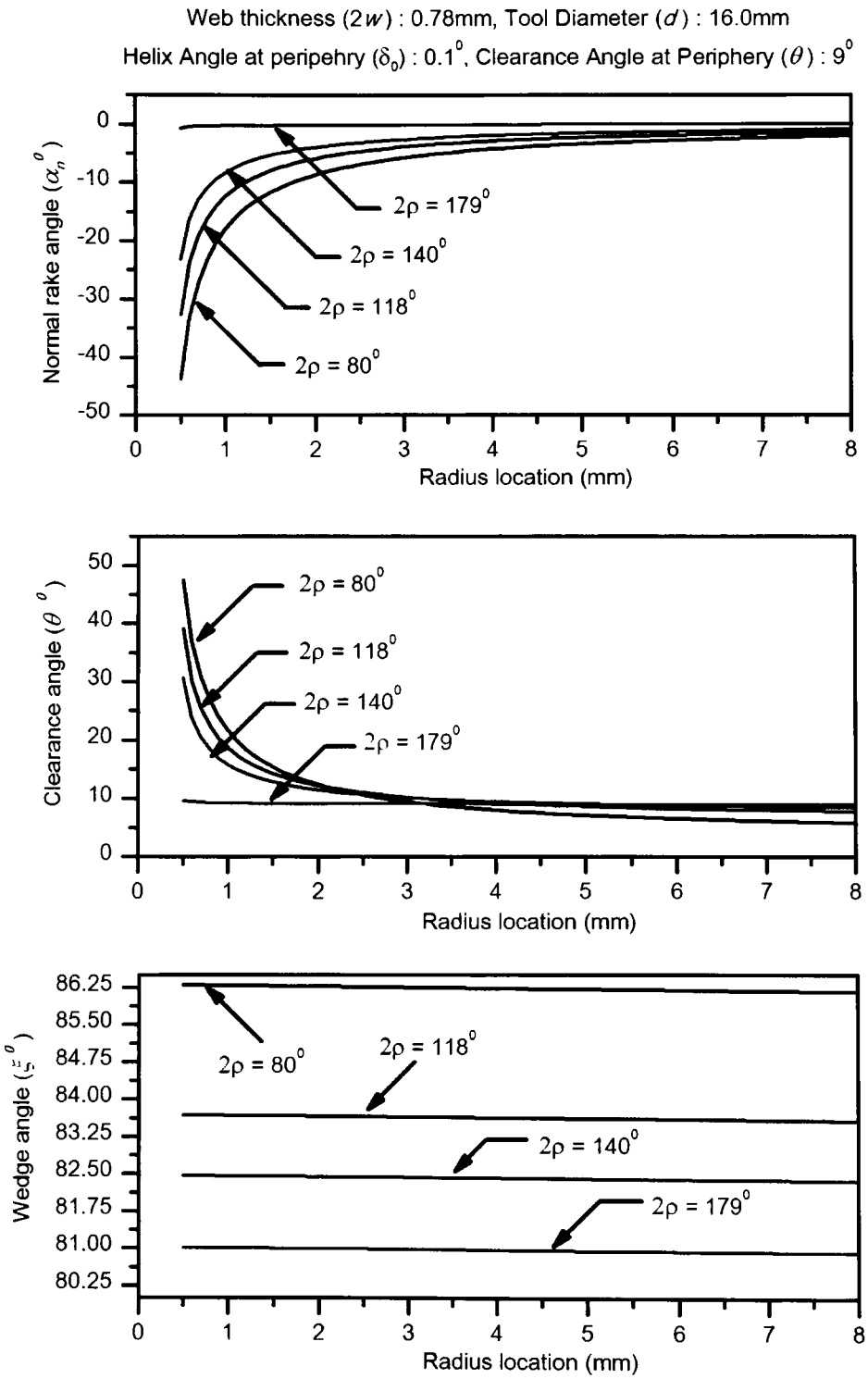

Figure 4.13: Variation in normal rake angle (α_n), clearance angle (θ) and wedge angle (ξ) along the cutting edge with variation in point angles (2ρ).

A reduction in helix angle at the periphery of the drill (δ_o) not only has the most pronounced effect in terms of achieving a suitable rake angle (α_n) variation throughout the cutting edge length, but also affects the rigidity and chip evacuation capability of the drill. The maximum cutting force that a drill can withstand depends upon its torsional stiffness, which in turn depends upon the cross sectional area and the geometric form of the drill, influenced by the helix angle [53]. Narasimha et. al. [17] observed the torsional stiffness of the drill to vary parabolically with the helix angle (δ_o) and reach a maximum value at 28^0 (Figure 4.14). Lower helix angles also increase the thrust forces in drilling increasing the chances of edge breakouts at hole exit. Furthermore, a negative rake would tend to push the chips into the hole, causing build up and hence affecting chip ejection. Although using a smaller (0.1^0) helix angle (δ_o) increases the edge security of the drill, it affects its torsional stiffness and chip evacuation capabilities thereby seriously affecting its applicability in drilling of hardened steels.

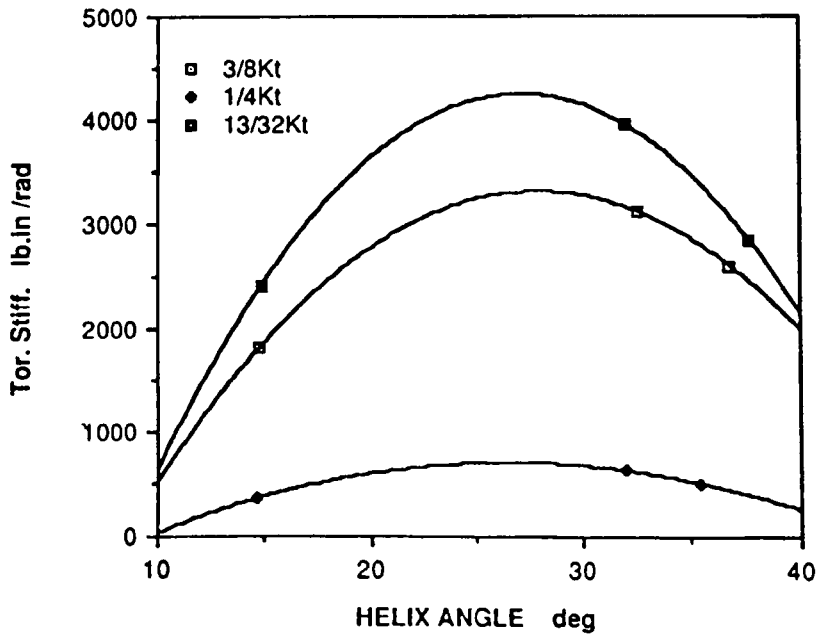

Figure 4.14: Effect of helix angle on the torsional stiffness of the drill [17].

In light of the geometry inherent to drills, it can be seen that it is infeasible to supplement the wedge angle (ξ) along the cutting edge of drill by provision of a continuously negative rake angle (α_n). It was shown that any variation in the geometrical parameters seriously affects the design of the drills. Since the design of drills is essentially a compromise between, overall tool stiffness, chip evacuation and cutting efficiency, it can be concluded that a completely negative rake (α_n) cannot be incorporated rendering it impossible to drill hardened AISI D2 tool steel. Although drilling of hardened D2 tool steels is currently not possible, it can successfully be milled [7] indicating the possibility of employing helical milling for machining holes in hardened AISI D2 steel.

4.3 Helical Milling of Hardened AISI D2

In stark contrast to conventional drilling that was characterized by a loud squeal accompanied by catastrophic tool failure which yielded just a single hole at best, the number of holes that could be machined in helical milling with TiCN + TiN coating was 10 holes (Figure 4.15).

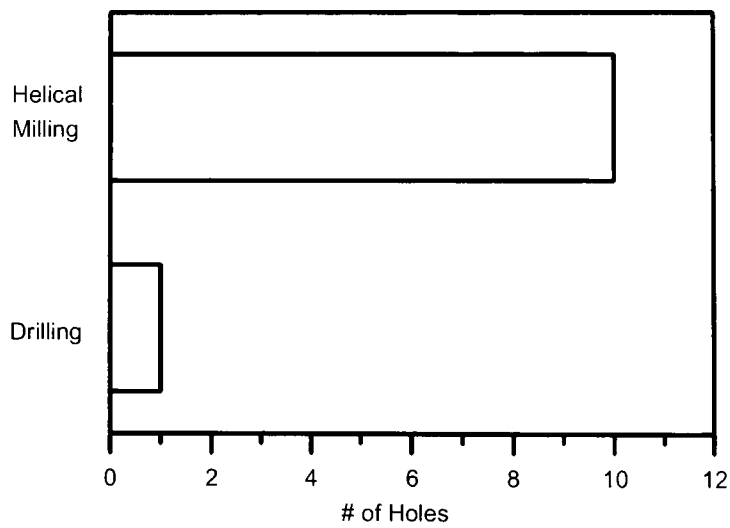

Figure 4.15: Tool life obtained in conventional drilling and helical milling.

The influence of tool coating on the performance outcome in helical milling is presented in Figure 4.16. Since TiAlN inserts were not available as a part of the standard product program, uncoated inserts were coated with a TiAlN coating from an external source other than the tool manufacturer. Despite possessing better tribological properties than TiCN and TiN coatings, poor tool life was obtained with TiAlN coating at an effective cutting speed (V_{eff}) of 30 m/min. Visual inspection of the inserts show spalling of the coating on the rake face exposing the substrate carbide surface (Figure 4.21) limiting their tool life. The performance of TiAlN coatings improved with increase in effective cutting speeds (V_{eff}) as seen in Figure 4.16.

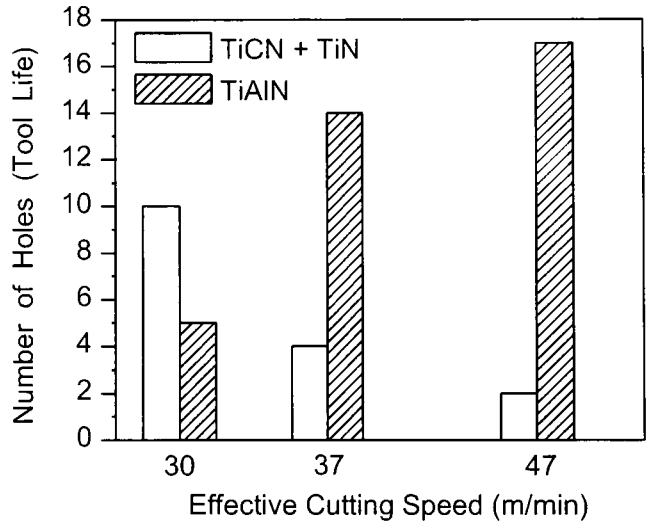

Figure 4.16: Influence of coating on tool life in helical milling.

While evaluating the hot-hardness of titanium nitride (TiN), titanium carbo nitride (TiCN) and titanium aluminum nitride (TiAlN) coatings from 25 ^{0}C to 1000 ^{0}C, Jindal et. al. [54] illustrated that TiCN has the highest room temperature hardness which gradually deteriorated with an increase in temperature (Figure 4.17). The maximum service temperature of TiCN coating is restricted to 400 ^{0}C as compared

to 900 ^{0}C for TiAlN coatings [38], implying that the latter can withstand higher cutting temperature environments with minimal detriment to its properties. Moreover at elevated temperatures, a thin layer of aluminum oxide (Al_2O_3) is formed on the tool surface preventing tribo-oxidation of the coating, thus reducing tool wear and improving tool life [55]. However with an increase in effective cutting speeds (V_{eff}), the increasing cutting temperatures depreciate the hardness of TiCN coating and degrade their performance.

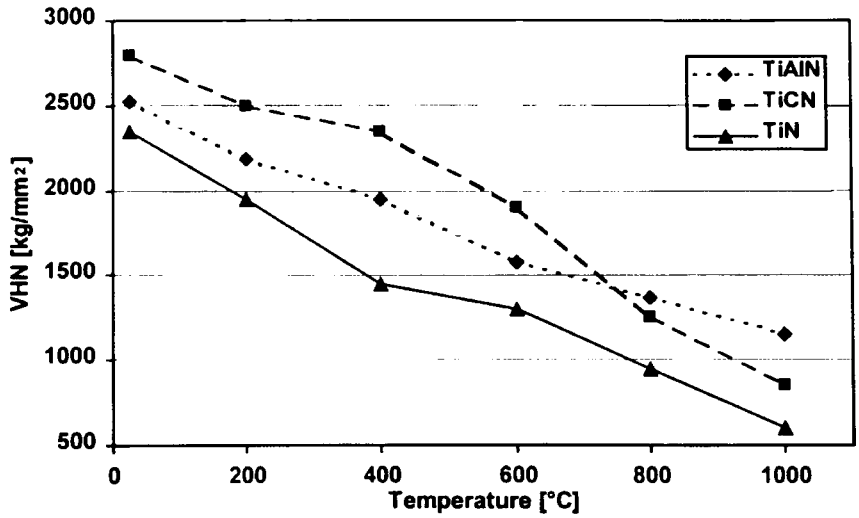

Figure 4.17: Coating micro-hardness (HV) as a function of temperature [54].

Replication of machining trials involving TiCN + TiN coated inserts revealed performance variation of 10% in helical milling (Figure 4.15). Trials with TiAlN inserts were however inconsistent owing to coating peel off and is attributed to the coating process. As temperature increases, the differences in thermal expansion coefficient between the coating and the tool substrate give rise to large thermoelastic stresses in the coating causing it to peel off exposing the substrate [11]. It is interesting to note that the location of the coating peel off is at the point of maximum cutting speed entailing the highest temperature along the cutting edge.

The results obtained in the current research is compared to that obtained by König et. al. [1] [33] in Figure 4.18. Since there is a large variation in the cutting parameters and tool configurations, a more generic methodology of comparison in terms of the volume of metal removed is adopted. Coldwell et. al. [5] employed a cutting speed of $5 - 10$ m/min with a feed (f) of $0.05 - 0.08$ mm/rev and achieved a volumetric tool life of approximately 6 cm^3. Although the flank wear (V_B) measured was only 0.1 mm, the cutting edges showed micro-chipping and hence were withdrawn from further use. König et. al. [1] [33], developed an indexable drilling tool (diameter = 34 mm) incorporating negative rake (α_n) PCBN inserts to machine holes in hardened X210CrW12 (DIN equivalent of AISI D2) steel. Although an exceptional tool life of 500 mm was achieved for a blind hole depth of 34 mm, the negative rake (α_n) susceptible to hole exit failures restricted its application. Furthermore, König et. al. [1] [33] and Coldwell et. al. [5] employed cutting fluid to flush the chip away from the cutting area and also to provide cooling to the cutting edge. Pressurized air was employed in case of helical milling which translates into additional savings in terms of elimination of fluid disposal and protecting the environment.

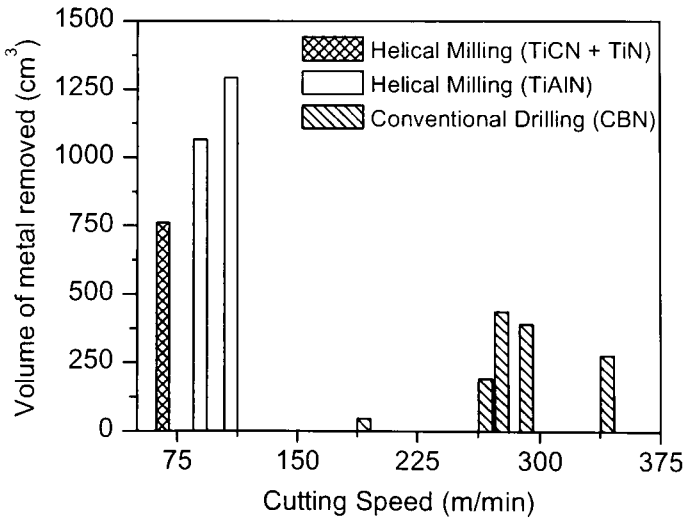

Figure 4.18: Tool life comparison with respect to previous research work.

4.3.1 Wear Modes in Helical Milling

Unlike drilling, wherein the predominant wear mode was catastrophic fracture of the cutting edge, helical milling displayed a progressive wear pattern. The governing wear mechanisms as a result of the mechanical and thermal load acting on the cutting edge during helical milling of hardened D2 tool steel, are discussed below:

- *Abrasion Wear* . This type of wear is caused by the hard particles in the workpiece material. Abrasive wear is usually controlled by increasing the hardness of the tool material. Flank wear, notch wear on the leading edge and nose radius wear are typical examples of abrasive wear and is desirable since it progresses uniformly [12] [56].

- *Attrition Wear :* This type of wear occurs at relatively low cutting parameters formed by the built up edge (BUE) formed along the cutting edge of the tool. Under intermittent cutting conditions (like milling), BUE is formed between the chip and the cutting edge, with successive layers from the chip being welded and hardened becoming part of the cutting edge. Upon subsequent engagement, the strongly bonded work / tool material is torn away from the tool surface and is characterized by a rough and uneven plucked surface on the tool rake face [56] [57]. This form of wear mechanism is called attrition and is primarily adhesive in nature.

Depending upon the cutting conditions and workpiece microstructure, either one or a combination of the factors listed above is responsible for tool wear. In case of hardened D2 tool steel, wear is influenced by the conspicuous presence of hard (2400 HV) $(Fe, Cr)_7C_3$ carbides of particle size $5 - 25$ μm that are embedded in the martensite matrix [30]. The wear progression of TiCN + TiN coated indexable ball

nose end mill at a effective cutting speed (V_{eff}) of 30 m/min and that of TiAlN inserts at a cutting speeds (V_{eff}) of 30 m/min , 37 m/min and 47 m/min are as shown in Figure 4.19. In stark contrast to conventional drilling where tool failure was catastrophic macro fracture, helical milling displayed progressive flank wear arising due to abrasion and attrition wear comprising micro-cracks along the rake face (Figures 4.20, 4.21, 4.22, 4.23, 4.24, 4.25).

Although flank wear progressed uniformly in all these tests, trials with TiAlN inserts at a effective cutting speed (V_{eff}) of 30 m/min had to be terminated at a flank wear (V_B) of 0.125 mm (central) and 0.119 mm (peripheral) due to flaking of coating on the rake face. Observation of the rake face (Figure 4.21) indicates failure due to spalling attributed to the problems in coating procedures. As the exposed surface is more likely to fail catastrophically, the trials were discontinued although the flank wear criterion (V_B) of 300 μm was not reached.

The wear progression for TiCN + TiN inserts at effective cutting speeds (V_{eff}) of 37 m/min and 47 m/min were not plotted due to poor tool life obtained rendering their application ineffective above 30 m/min effective cutting speed (V_{eff}). The wear mode (Figure 4.22 and 4.24) shows chipping along the rake face around the vicinity of maximum cutting speed. TiCN has an maximum operating temperature of 400 ^{0}C above which it loses its properties [38] and as cutting speed increases, the temperature generated along the cutting edge also increases causing failure of the coating and exposing the carbide substrate along the rake face instigating wear. In both the cases, the rake face wear supersedes the flank wear criterion restricting the performance of these tools. TiAlN coated inserts on the other hand show no such defects at elevated cutting speeds (Figure 4.23 and 4.25) and display uniform flank wear (Figure 4.19) due to its inherent properties discussed in Section 4.3.

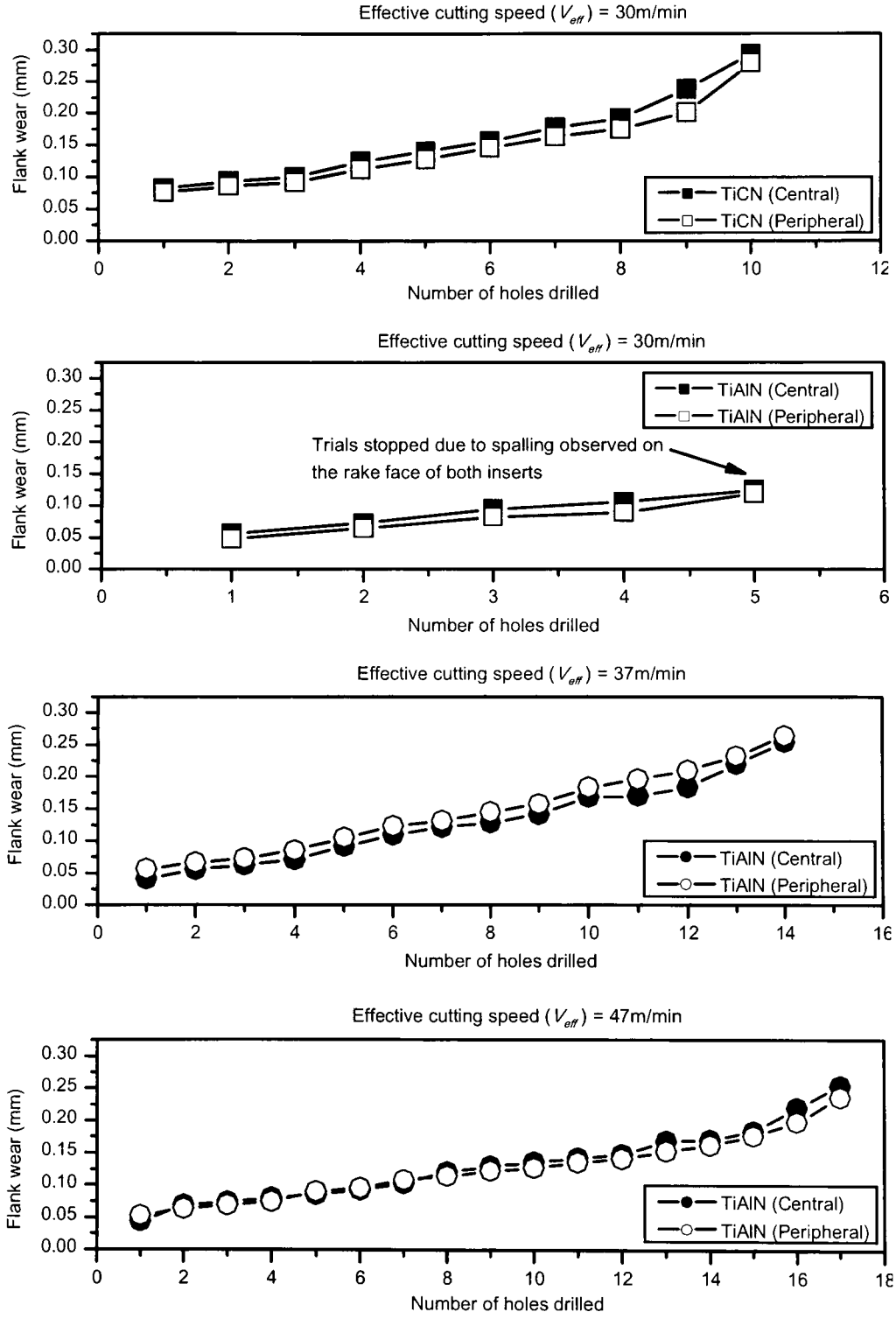

Figure 4.19: Flank wear progression in coated indexable insert ball end mills.

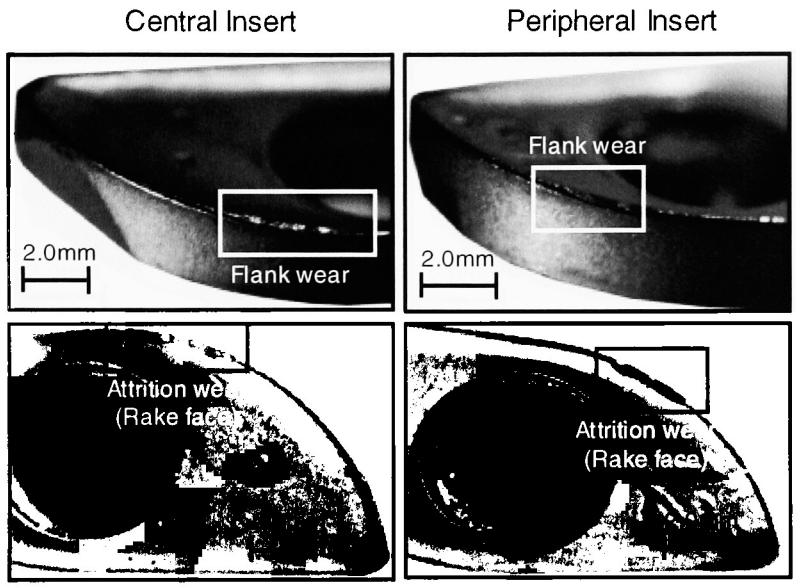

Figure 4.20: Wear mode of TiCN coated inserts in helical milling at $V_{eff} = 30$m/min.

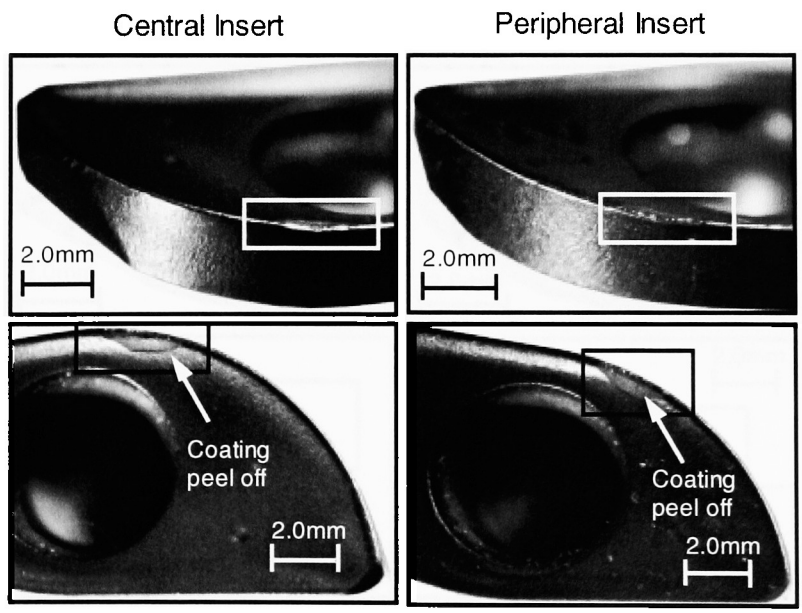

Figure 4.21: Wear mode of TiAlN coated inserts in helical milling at $V_{eff} = 30$m/min.

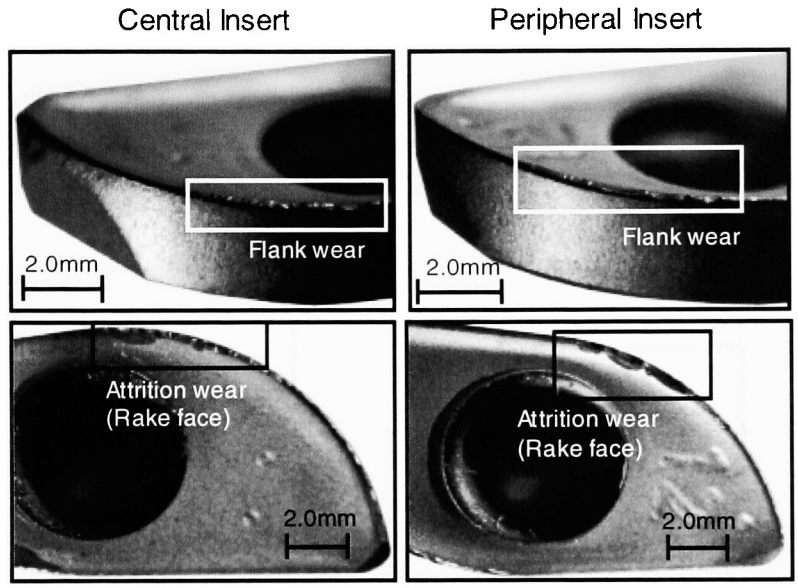

Figure 4.22: Wear mode of TiCN coated inserts in helical milling at $V_{eff} = 37$m/min.

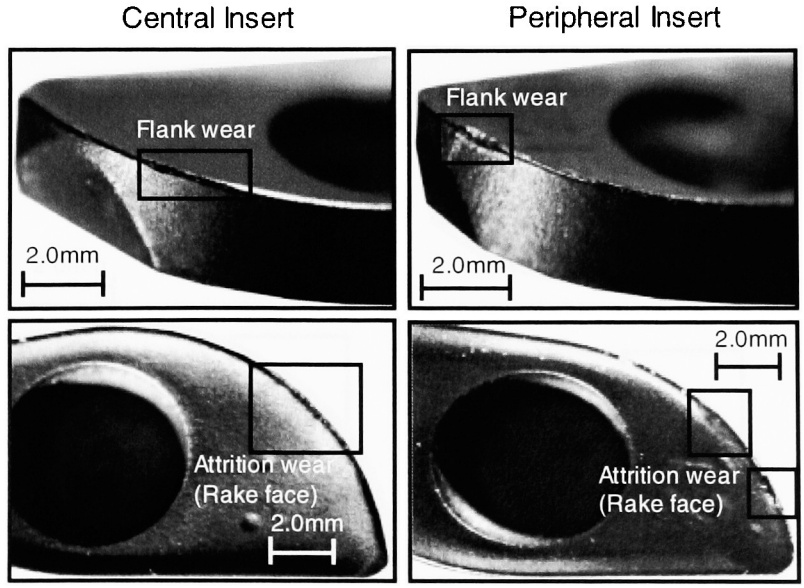

Figure 4.23: Wear mode of TiAlN coated inserts in helical milling at $V_{eff} = 37$m/min.

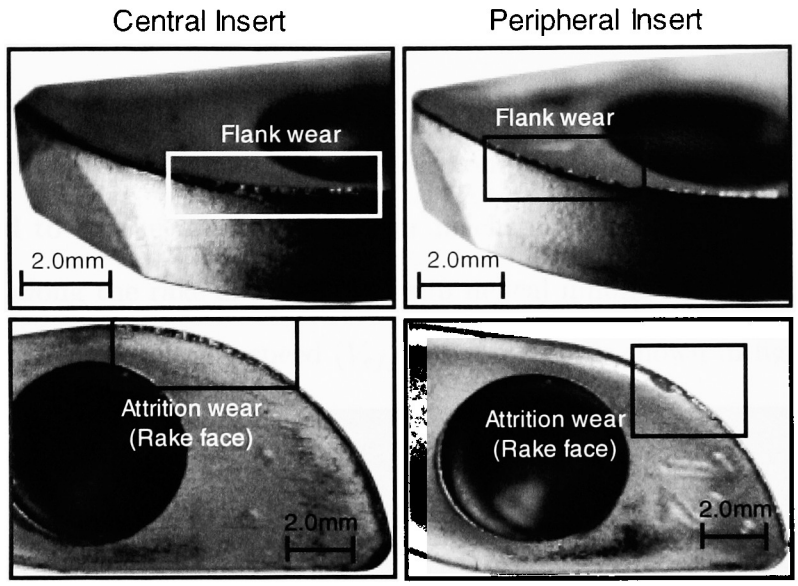

Figure 4.24: Wear mode of TiCN coated inserts in helical milling at $V_{eff} = 47$m/min.

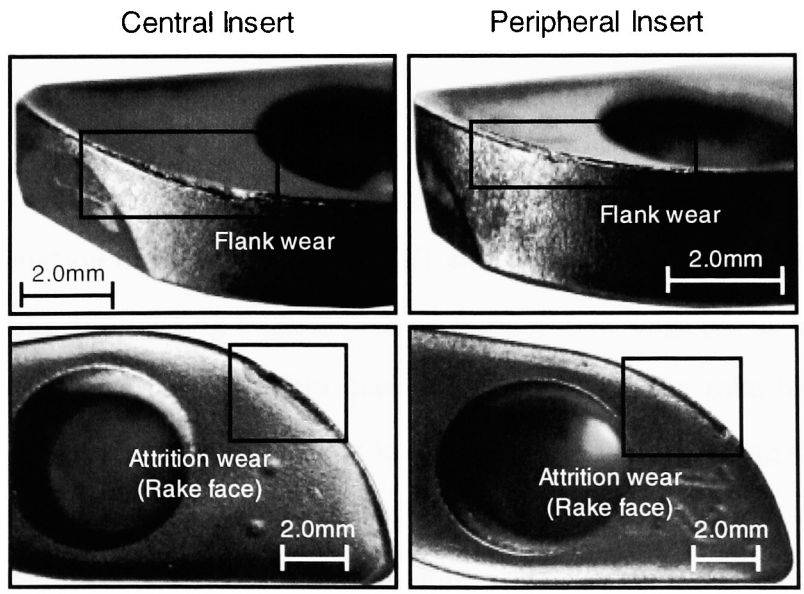

Figure 4.25: Wear mode of TiAlN coated inserts in helical milling at $V_{eff} = 47$m/min.

Observation of wear modes in helical milling (Figures 4.20, 4.21, 4.22, 4.23, 4.24, 4.25) indicates a peculiar pattern inherent to ball nose end mills while machining hardened tool steels [58] [39] [41]. Attrition wear in the form of micro chipping around the vicinity where full diameter of the ball comes into contact with the workpiece was observed to be the predominant wear mechanism in helical milling. The wear morphology along the rake and flank faces in helical milling for TiCN + TiN coated inserts at an effective cutting speed (V_{eff}) of 30m/min is shown in figure 4.26.

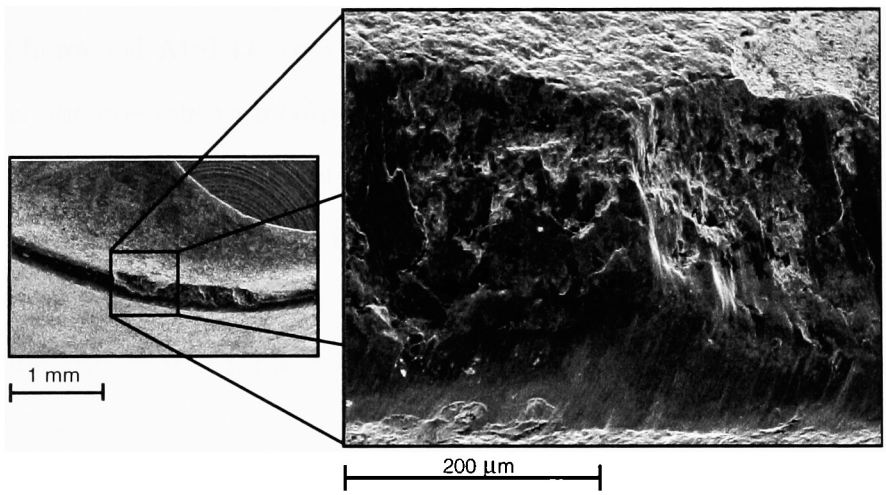

Figure 4.26: Wear morphology along the rake and flank faces in helical milling.

When machining at relatively low cutting speeds, low machining temperatures facilitate formation of built up edge (BUE) along the cutting edge of the tool. BUE is formed along the cutting edge in helical milling as it engages in the cut due to welding of successive layers of chip material flowing past the rake face. The BUE becomes a part of the cutting edge as it disengages the cut. During the next entry, the localized tensile stresses imposed by the flowing work material over the BUE elicits fragmentation of the cutting edge along the rake face exhibiting a very rough surface [57] and can be observed from the wear morphology shown in Figure 4.26. Attrition wear is not accelerated by higher cutting speeds and temperatures owing

to lower BUE formation over the tool rake face, as observed by the wear pattern of TiAlN inserts at higher cutting speeds (Figures 4.23, 4.25). On the other hand TiCN rapidly oxidizes at higher cutting speeds due to rise in temperatures exposing the substrate and thus limiting its tool life as explained previously.

4.3.2 Helical Milling Tool Geometry

The analysis of stresses acting along the cutting edge (Section 4.2.3) did impress upon the need for negative rake angle (α_n) for strengthening the cutting edge when machining hardened AISI D2 tool steel. It was reported in Section 4.2.4 that such a provision is not possible to incorporate in conventional drills, but is possible in end mills. Figure 4.27 shows an orientation similar to the helical milling tool, except for the radial rake (α_r), which is neutral (0^0) and in this case is depicted as negative. The helical milling tool assembly provides a negative axial rake (α_a) of -10^0 and a side clearance (θ) of 9^0 (Table 3.3). Using equation 4.7, we can deduce the wedge angle (ξ) to be 91^0.

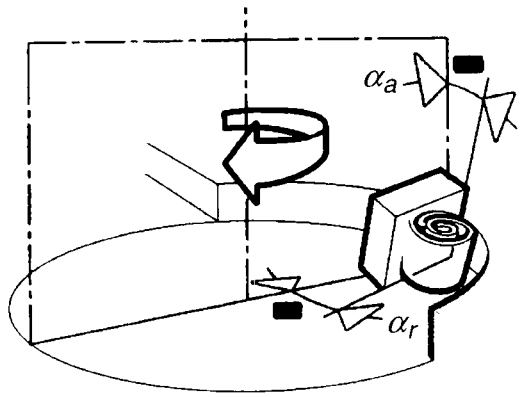

Figure 4.27: Axial (α_a) and radial (α_r) rake in milling (adapted from [56]).

Unlike conventional drilling, the normal rake angle (α_n) does not vary in end mills thereby facilitating a constant negative rake (α_n) along the entire cutting edge imparting strength by providing a constant and higher wedge angle (ξ). In addition

to higher wedge angle (ξ), the orientation of the cutting edge (Figure 4.27), protects the tool tip from the initial shock during engagement with the workpiece (Figure 4.28). It also changes the direction of the resultant force away from the cutting tip and towards the body of the tool hence arresting chipping.

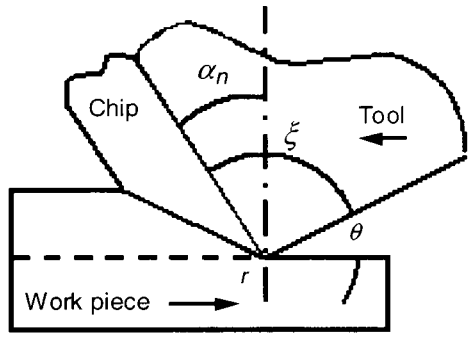

Figure 4.28: Wedge angle (ξ) in milling.

The negative rake (α_n) also reduces the cutting edge temperatures by providing a larger area for heat conduction [29]. Although high negative rakes ($\alpha_n \geq 20^0$) would greatly supplement the cutting edge, they are not preferred due to nature of forces generated during machining. At a normal rake angle (α_n) of -20^0, the thrust force (F_Q) is approximately twice the cutting force (F_P) demanding high tool holding stiffness in order to avert chipping due to tool deflections [1], [59]. A larger clearance angle (θ) on the other hand would also weaken the cutting edge making it susceptible to chipping. The optimum clearance angle (θ) and radial rake angle (α_r) for solid carbide non-center cutting end mill designed to machine hardened (45 HRC) AISI D2 are -14^0 each respectively [60]. The axial rake (α_a) forms the governing normal rake (α_n) for all face milling operations, while the radial rake (α_r) assumes the position of normal rake (α_n) during peripheral milling. The success of helical milling in machining holes in hardened D2 steel can be attributed to the facilitation of negative rake (α_n), which is not possible in conventional twist drills.

4.4 Cutting Forces

The success of helical milling of hardened D2 tool steel in terms of tools and wear progression is mainly accredited to the negative rake angle (α_n) that corresponds to sufficient cutting edge strength. The process kinematics of helical milling guarantees that material removal near the tool center does not occur by extrusion as in drilling thereby reducing the thrust forces. In addition, the interrupted cutting process provides respite to the cutting edge from the imposed thermal and mechanical loads. The maximum thrust force in helical milling is almost an order of magnitude lower that in conventional drilling (Figures 4.29, 4.30). High thrust forces (~ 9 kN) observed in conventional drilling are a consequence of the material removal by extremely negative normal rakes (α_n) near the chisel edges and zero cutting speed near the drill center causing material removal by extrusion.

During the fifth peck cycle (Figure 4.29), intense screeching sound was heard, indicating imminent tool failure. In order to prevent catastrophic failure of the cutting edge, the tool was fed at a reduced feed rate thereby increasing the peck cycle time. The tool was withdrawn from further use as the chipping at the periphery was observed exceeding the wear criterion (VB) of 300 μm.

The torque developed in both the machining processes are compared in Figures 4.31, 4.32. The torque in helical milling is higher than that in conventional drilling due to the negative rake angle (α_n) along the cutting edge. Furthermore this also increases the radial forces in helical milling (Figure 4.33). A similar force trace was observed in the "Y" direction as well, necessitating the use of a rigid tool holding systems to counter tool deflections. The torque trace in conventional drilling indicates periodic chipping of the cutting edge in each of the peck cycle in the form of spikes.

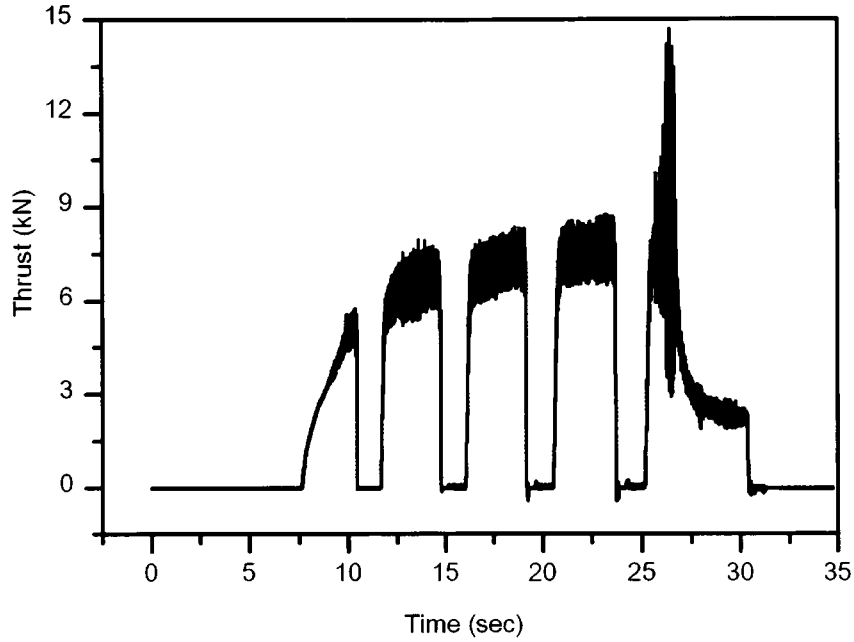

Figure 4.29: Thrust forces and machining time in conventional drilling.

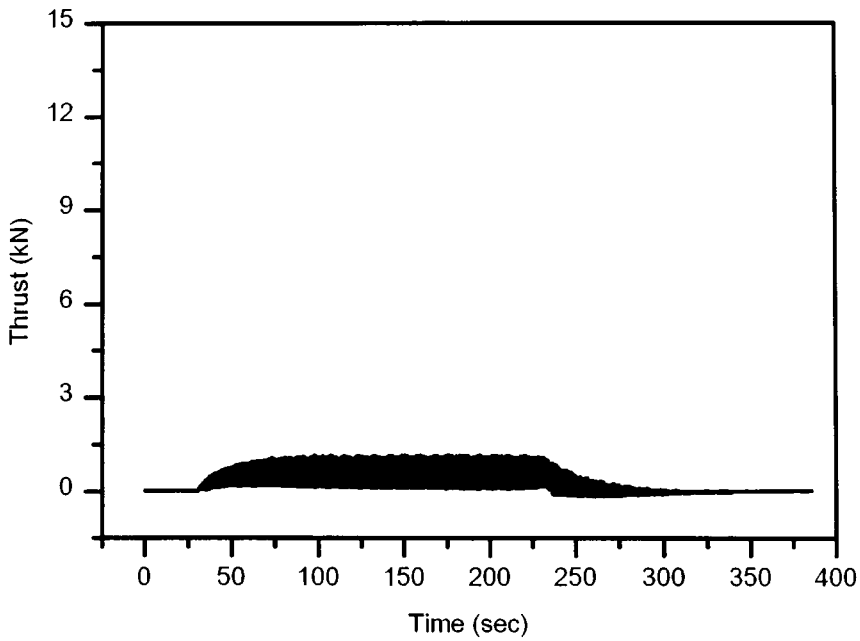

Figure 4.30: Thrust forces and machining time in helical milling.

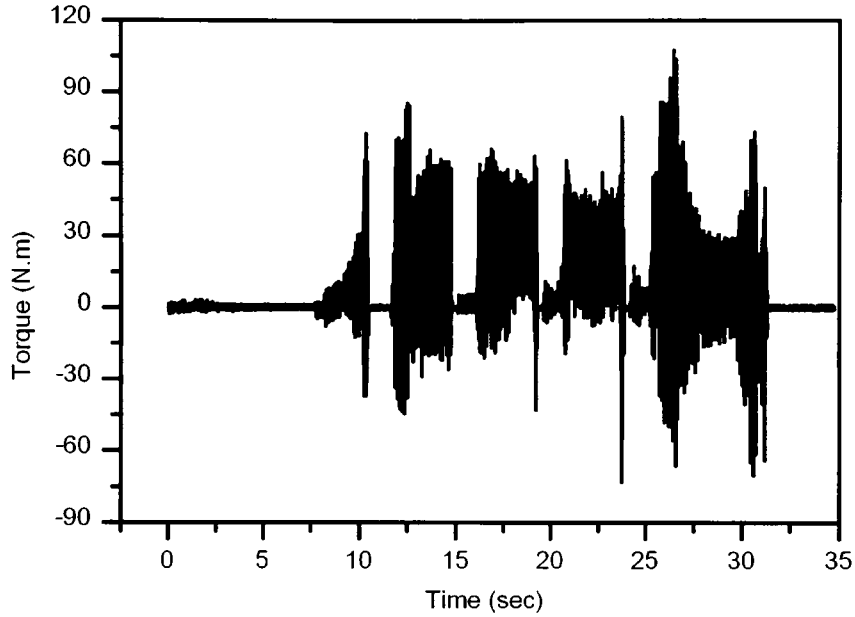

Figure 4.31: Torque in conventional drilling.

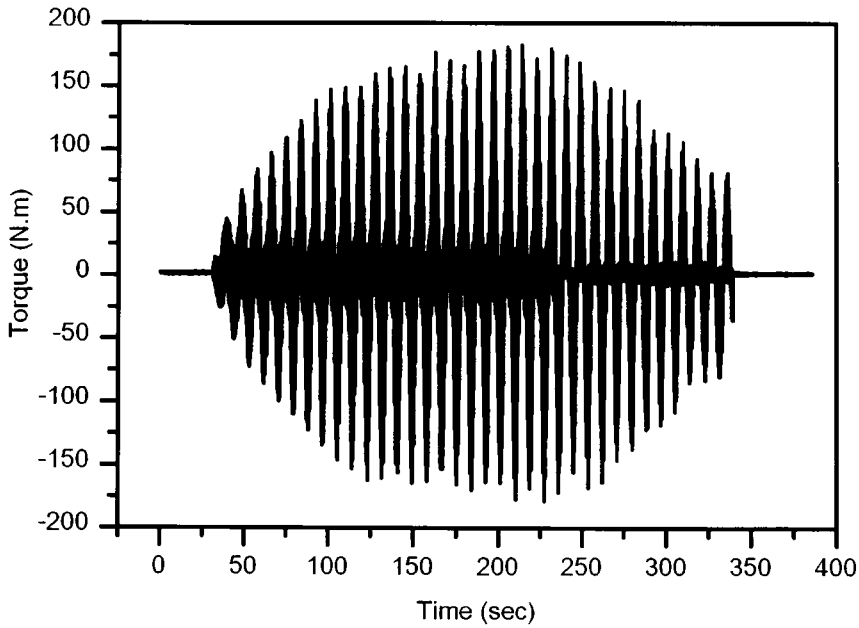

Figure 4.32: Torque in helical milling.

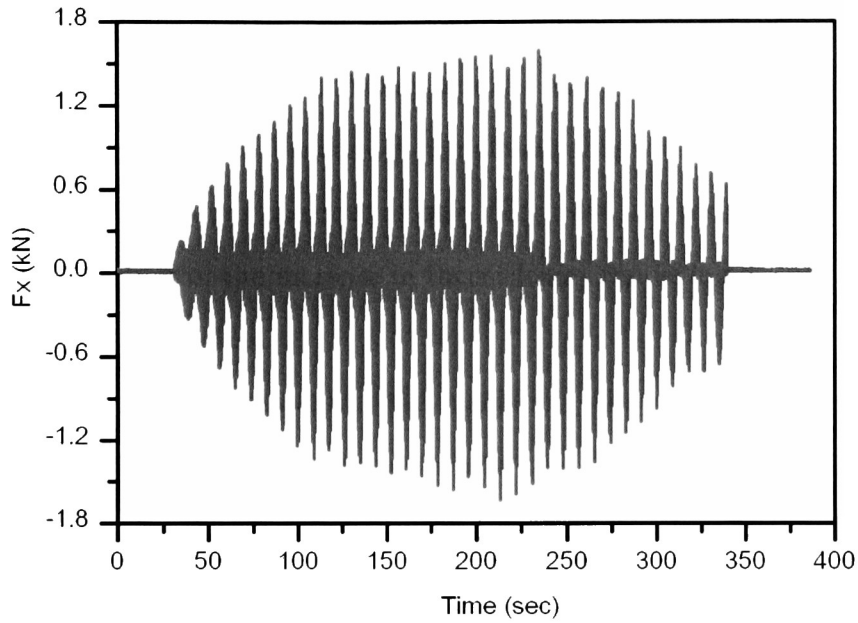

Figure 4.33: Forces in the "X" direction in helical milling.

The maximum thrust forces generated in conventional drilling are higher than that in helical milling (Figures 4.29, 4.30) on account of metal removal by extrusion near tool center, precipitating material breakout at the exit of the hole, Figure 4.34, whereas no such defects were observed with helical milling.

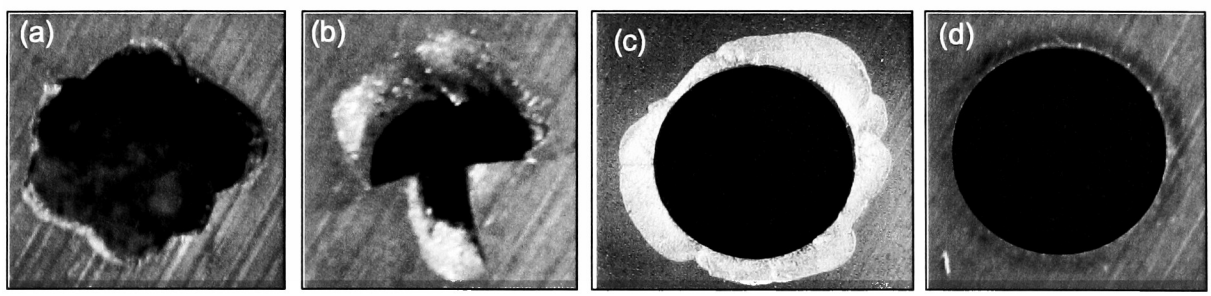

Figure 4.34: Material breakout at the exit of the hole (a): Tool 1; (b): Tool 2; (c): Tool 3; (d): Helical Milling.

It can seen from material exit profiles (Figure 4.34) that unlike Tool 3, Tools 1 and 2 did not even complete a single hole and failed catastrophically highlighting

poor performance of the drilling process. The provision of lip correction in the form of edge hone provided on Tool 3 to strengthen the edge, resulted in most severe edge breakout suggesting a further increase in the already high thrust forces. Providing a negative rake angle (α_n) along the cutting edge (Figure 4.12) would further exacerbate this problem on account of the increase in thrust forces rendering drilling of hardened AISI D2 tool steel impossible.

For similar cutting parameters, the machining time corresponding to helical milling would be significantly higher as seen in the Figures 4.29 and 4.30. This is due to the helical path traced by the tool as opposed to linear distance in conventional drilling which increases the distance traveled in helical milling by a factor of $[1/\sin(\theta_R)]$, where θ_R is the ramp angle. Hole making time is not a major issue in applications involving hardened D2 tool steels since drilling is not successful and is impractical. The current process of helical milling is severely restricted by the design of cutting tools, limiting the use of higher ramp angles. Since the distance traveled in helical milling is inversely proportional to the sine of the ramp angle (θ_R) employed, it is evident that tool designs that permit the use of higher ramp angles would reduce machining time significantly. Nevertheless milling tools with as many as six flutes (cutting edges) can also be employed, increasing the feedrate and thereby decreasing machining time.

Die and mold components generally entail several holes of varying diameters and forms (eg. counter-sink, recess for bolt head etc.) that could be accomplished using a single tool in helical milling. This translates into overall cycle time savings, in comparison to drilling, wherein a separate tool needs to be employed for a given hole diameter and even then may not be able to machine all the forms prescribed in the hole. Not only does this increase the overall cycle time due to time spent in changing tools, it also leads to increased tooling inventory and overall costs. Tönshoff et. al.

[9] have shown in the manufacture of an aluminum component entailing several hole sizes and accuracies that the net machining time savings accrued by helical milling employing three tools to be 25% in comparison to the conventional sequence of high speed drilling followed by reaming requiring 12 different tools.

4.5 Hole Accuracy in Helical Milling

Measurement of hole quality characteristics, namely roundness and hole tolerance at a effective cutting speed (V_{eff}) of 30 m/min were undertaken on the Zeiss Prismo 900 co-ordinate measuring machine (CMM). The hole accuracies obtained in helical milling using TiCN + TiN coated indexable insert type tooling were compared to that obtained by a TiAlN coated solid carbide end mill. The indexable ball nose tool assembly related to a diametral tolerance of 0.3 mm producing a machined hole tolerance of 0.34 mm. In the second part of the investigation, machining was carried using a solid carbide end mill with a diametral tolerance of 0.07 mm. The machined hole tolerance was measured to be 0.017 mm which corresponds to a hole quality of H7, thereby eliminating the need for reaming. It can hence be concluded that in applications wherein hole quality is of primary importance, helical milling can best be accomplished using solid carbide tooling.

A comparison of out-of-roundness for both of helical milled holes using indexable and solid carbide tooling respectively is presented in Figure 4.35. The indexable tooling assembly corresponded to an out-of-roundness of 25 μm compared to 10 μm with solid carbide tooling. The radial forces (Figure 4.33) have the highest impact on the roundness profile as they influence deflection. In case of the indexable tool assembly, the tool body is made up of hardened steel as opposed to tungsten carbide body for solid carbide tooling which offers higher core stiffness and resistance to deflection translating into better roundness profiles.

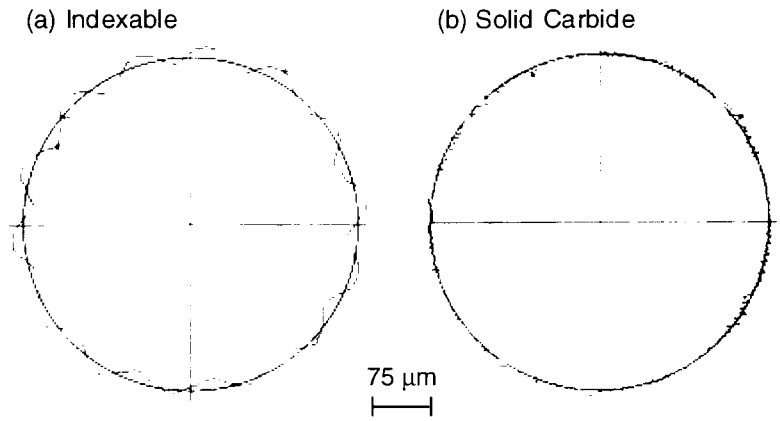

Figure 4.35: Roundness profiles of helical milled holes.

Tönshoff et. al. [8] have indicated that the geometrical characteristics of helical milled holes are governed by the interpolation capability and quality of the machine tool. Form errors are caused by quadrant change over of the machine tool axes and momentary stoppage of the tool at the change over between the two spirals of the helical course leaving an indentation on the surface of the hole. For elimination of these errors, the machine tool controller must be equipped with feed rate compensation parameters and curve smoothing options respectively, stressing the need for a quality machine tool.

Surface finish obtained in helical milling is using indexable insert and solid carbide type tooling is presented in Figures 4.36 and 4.37 respectively. It can be seen that under comparable cutting conditions, the surface finish (R_a value) obtained with indexable tooling is approximately an order of magnitude higher than that with solid carbide tools. The clearance between the trailing edge along the length of the insert and the full diameter of the ball, generates feed marks on the generated hole surface and can be seen in form of a scallop in the oblique plot for indexable tool (Figure 4.36). It is attributed to the design of the end mill with the distance between successive feed marks equal to the axial depth per 360^0 of circular tool travel (a_o).

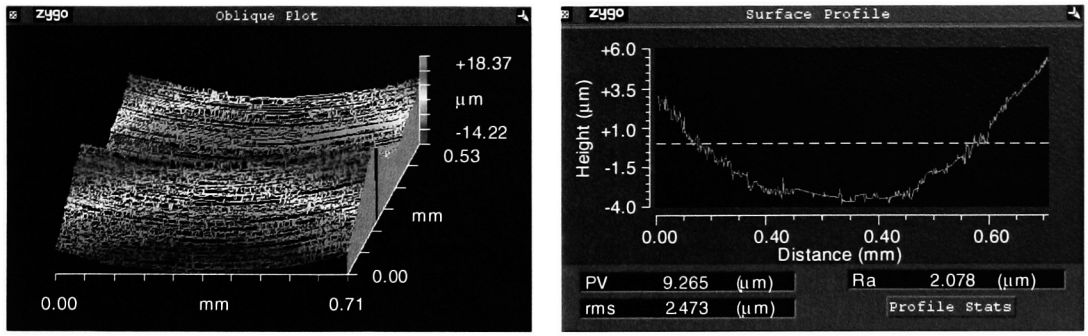

Figure 4.36: Surface finish obtained in helical milling using indexable ball nose end mill.

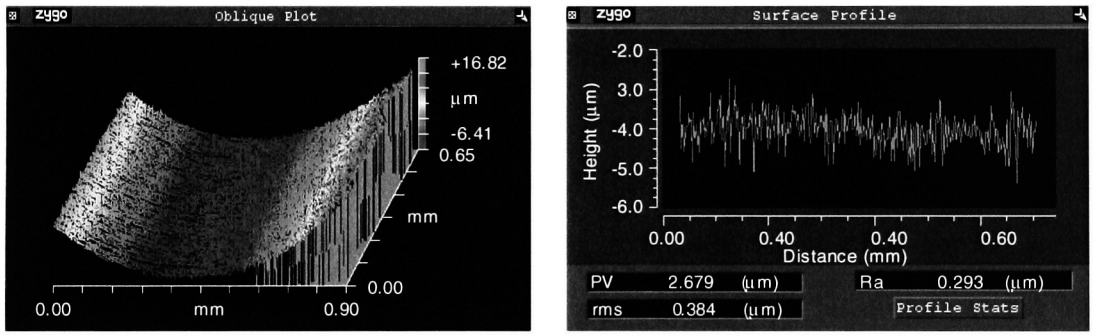

Figure 4.37: Surface finish obtained in helical milling using indexable ball nose end mill.

4.6 Chapter Synopsis

Catastrophic fracture of the cutting tool directly influences part quality and tooling costs and hence are often the most important practical considerations in the selection of cutting tools and machining process. It was conclusively ascertained from results of the machining trials that conventional drilling of hardened D2 tool steel was ineffective establishing helical milling as a true enabling technology for such applications. The machining process for all the four drills tested was characterized by a loud squeal right from the outset of drill engaging the work piece, signifying impending tool failure. Helical milling on the other hand referred to consistent performance with a smooth cutting action. Moreover the uniform wear progression accompanied by an order of magnitude higher tool life, firmly establishes helical milling as a viable

process for machining holes in hardened D2 tool steel.

It was observed that high stresses ($\geq$ 2 GPa) acting along the cutting edge necessitates the need for enhanced edge strength when machining hardened D2 tool steel. The normal rake angle (α_n) in conventional drilling varied from negative -20^0 near the chisel edge to a positive value that is equal to the helix angle (δ_o) at the periphery along the cutting edge. This gave rise to a smaller wedge angle (ξ), weakening the cutting edge at the periphery of the drill abetting catastrophic failure. The provision of a negative rake (α_a) in helical milling not only imparted exceptional strength to the cutting edge, but also arrested chipping by directing the resultant forces away from the cutting edge into the body of the tool.

Numerical simulation revealed that reducing the peripheral helix angle (δ_o) would have the best influence in providing a negative rake angle throughout the cutting edge of the drill. Adopting such a change would increase the cutting forces and reduce the stiffness of the drill and seriously compromise the design of the drill rendering it impractical. On the other hand, since flute space is not required for transport of chips from the cutting zone, helical milling tools offered higher stiffness than their drilling counterparts and withstood the deflections caused by the use of negative rake (α_n) angles.

Owing to the unique process kinematics of helical milling preventing material removal near the center of the tool by extrusion, lower thrust forces were reported in comparison to conventional drilling. Unlike in drilling, wherein excessive thrust forces in the vicinity of the drill center cause exit breakouts in the work material, helical milling produced a clean hole exit further establishing itself as an enabling technique for machining holes in hardened tool steels. The indexable insert ball nose tools used in helical milling experiments related to a poor diametral tolerance (0.34 mm) as compared to solid carbide tools (0.017 mm) indicating that the hole geometry

characteristics were dependent not only on the interpolation capability of the machine tool, but also on the tool assembly. It was hence concluded that when hole quality was of primary concern, helical milling should be accomplished using a solid carbide tooling.

Since the tool diameter (D_T) is always smaller than the hole diameter (D_H) in helical milling, a single tool can be employed to machine a range of hole sizes and forms providing incentive for savings in the form of reduction in tooling inventory and costs. This also reduces the overall machining time by cutting non productive time spent on tool changes ultimately translating into cost savings. The experimental results in terms of tool life, wear morphology and hole quality characteristics reinforce the effectiveness of helical milling process in machining of holes in hardened AISI D2 tool steel.

CHAPTER 5
CONCLUSIONS AND FUTURE WORK

5.1 Conclusions

Experimental work presented in this thesis established that successful drilling of hardened AISI D2 steel is not feasible with the current state of drilling technology. This presents a major process chain bottleneck inhibiting hard machining of die and mold components. To this end, the current research presents the proof-of-concept of helical milling an enabling technology for machining precision holes in fully hardened (60 HRC) AISI D2 tool steel. The performance of helical milling in terms of tool life, wear modes and mechanisms, progression of tool wear and cutting forces is studied and compared against that obtained in conventional drilling of hardened AISI D2 tool steel.

Conventional drilling of hardened D2 tool steel, characterized by a loud squeal right from the outset of using a new drill, was observed to be ineffective with poor tool life predominantly due to large scale chipping at the outer edge of the cutting lips.

One of the drills tested (Tool 2) disintegrated completely with a fractured surface at roughly 45^0 to the tool axis alluding to failure in torsion. The best outcome among the four drills tested corresponded to the drill of grade K40 (Tool 3) that is tougher as compared to all the drills tested and yielded just a single hole, but in so doing incurred flank wear exceeding 300 μm.

Difficulties with drilling of hardened AISI D2 tool steel can be attributed to its microstructure that comprises a significant fraction of coarse M_7C_3 carbides of hardness 2400 HV, which can induce severe abrasive wear on the tool, and enhance the flow strength of the material by impeding dislocation mobility. This combined with the cutting speed approaching zero and the rake angle (α_n) assuming highly negative angles in the vicinity of the drill center, renders hard drilling of AISI D2 tool steel almost impossible.

Chipping of the cutting edges at the drill periphery is a consequence of the geometry of conventional drills. Due to the intrinsic variation of the normal rake angle (α_n) from being highly negative (typically about -20^0) near the drill center to being positive (equal to helix angle) at the drill periphery, the cutting edges at the outer edge of the drill correspond to lower wedge angles (ξ) that translate into high stresses. Finite element analysis (FEA) of the stresses in the cutting edge when machining hardened D2 tool steel indicated the highest maximum principal stress on the cutting edge to exceed 2 GPa, which is comparable to the transverse rupture strength of fine grained cemented carbides. The stress analysis pointed to the need for the use of negative rake (α_n) tools to strengthen the cutting edge. Design of drills with negative rake (α_n) along the cutting edge is infeasible due to the following reasons:

- The design of the cutting edge in conventional drilling is influenced by point an-

gle (2ρ), helix angle (δ_o) and the flute contour. The point angle (2ρ) is selected such that it provides a straight cutting edge for maximum tool life. The helix angle (δ_o) is chosen such that it imparts maximum torsional stiffness to the drill and lowers the torque and thrust forces. It was seen from numerical simulations that as the peripheral helix angle (δo) approaches zero, the normal rake angle (α_n) remains negative throughout the cutting edge length. Although advantageous from the edge strength point of view, it seriously affects the stiffness of the drill.

- The increase in cutting forces associated with the use of negative rake α_n tools necessitates higher stiffness from the drill body which is weakened as the helix angle (δ_o) is reduced towards zero. For achieving maximum stiffness, the drill peripheral helix (δ_o) should be optimized to a value between $28^0 - 32^0$

- The use of negative rake angle (α_n) tends to push the chips into the hole causing build up affecting chip evacuation which increases the cutting forces and could lead to drill breakage

The helical movement of the tool brought about by integration of the three axes in helical milling ensures gradual engagement of the tool into the workpiece and does not remove material at and near the center of the hole by extrusion as in drilling, resulting in a ten-fold reduction in thrust forces. Furthermore helical milling tools facilitate the provision of constant negative axial rake angle (α_a) which not only provides edge strength but also directs the resultant cutting force towards the body of the tool, thus controlling tool chipping. It was observed that under similar cutting parameters, the tool life in helical milling was an order of magnitude higher than conventional drilling with uniform flank wear progression. The performance of TiAlN coated helical milling inserts improved with an increase in cutting speeds in

comparison to TiCN + TiN inserts which is attributed to the superior wear resistance and higher service temperature of the former.

Thrust forces in helical milling were considerably lower in comparison to conventional drilling that precipitates work material breakout at the hole exit rendering drilling completely inapplicable. Some of the additional advantages of helical milling brought about by this simple modification of tooling and process kinematics that are significant to it success in machining of hardened D2 tool steel are listed below:

- ☞ Helical milling offers exceptional chip control on account of it being an interrupted cutting process which also provides reprieve to the cutting edges from the imposed thermal and mechanical loads.

- ☞ Unlike conventional drilling where tool design in which is essentially a compromise between the flute space necessary for chip evacuation and tool stiffness, tooling used in helical milling can entail a higher core diameter since chips are easily evacuated across the radial clearance between the hole and tool. These tools can hence counter tool deflections stemming from the high forces related to the use of negative rake (α_n) tools.

- ☞ Due to enhanced chip evacuation, helical milling can be accomplished without the use of cutting fluids as opposed to conventional drilling wherein the primary requirement for the use of cutting fluid is to flush the chips off the cutting zone.

- ☞ In helical milling, a single tool can be employed to machine a range of hole sizes. This soft tooling aspect also offers incentives to machine varies forms of holes (eg. countersink, counterbore etc.) without the use of additional tools translating into tool cost savings and reduction in tooling inventory.

- ☞ The out-of-roundness of helical milled holes using indexable insert and solid

carbide tools was found to be 25 and 10 μm. respectively. Surface finish of using solid carbide tools was measured to be ~ 0.3 μm R_a with a diametral tolerance of 17 μm corresponding to a hole quality of H7. This eliminates the need for additional hole finishing process like reaming leading to a significant enhancement in productivity.

☞ It is to be noted that the hole geometrical characteristics in helical milling is governed also by the interpolation capability and quality of the machine tool and in cases where hole quality is a factor, helical milling is best accomplished using a solid carbide tooling.

5.2 Scope for Future Work

The helical trajectory of the cutting tool in helical milling corresponds to a length of tool travel that is $[1/\sin(\theta_R)]$ times that of conventional drilling, where θ_R is the ramp angle. For similar cutting parameters this would translate into higher machining time for helical milling compared to conventional drilling operations. The primary limitation in reducing the length of tool travel in helical milling arises from the restrictions imposed in ramp angles (θ_R) that refer to the design of the cutting tool. Research in the development of cutting tools that facilitate the implementation of higher ramp angles for machining of hardened D2 tool steels needs to be initiated to further enhance the benefits achieved in helical milling.

In order to a gain better understanding of the process of helical milling, mechanistic force modeling must be undertaken. The influence of increasing cutting speeds (V) and axial depth per 360^0 of circular tool travel (a_o) on chatter and vibration also needs to be investigated (stability analysis).

Application of the helical milling technique in dry machining of aluminum components with minimum quantity lubrication (MQL) with the aim to address the issues of exit burrs, hole quality and manufacturing costs associated with application of cutting fluids. Other materials typically used in the aerospace industry such as stainless steel and titanium, which present challenges with regard to their machinability would be ideal candidates for future helical milling research. Accomplishing thread milling following helical milling of holes could also be explored.

REFERENCES

[1] König W., Komanduri R., Tönshoff H. K., and Ackershott G. Machining of hard materials. *CIRP : Annals of the International Institution for Production Engineering Research*, 33(2):417 -427, (1984).

[2] Byrne G., Dornfield D., and Denkena B. Advanced cutting technology. *CIRP · Annals of the International Institution for Production Engineering Research*, 52(2):483 507, (2003).

[3] Tönshoff H. K., Spintig W., König W., and Neises A. Machining of holes Developments in drilling technology. *CIRP : Annals of the International Institution for Production Engineering Research*, 43(2):551–561, (1994).

[4] Arai M., Ohno T., Ogawa M., and Sato S. Drilling of high hardness steels with high pressure supply of coolant. *Japan Society for Precision Engineers*, 62(9):1310–1314, (1996).

[5] Coldwell H., Woods R., Paul M., Koshy P., Dewes R. C., and Aspinwall D. K. Rapid machining of AISI H13 and D2 molds, dies and press tools. *Journal of Materials Processing Technology*, 135(2-3):301–311, (2003).

[6] Dewes R. C and Aspinwall D. K. A review of ultra high speed milling of hardened steels. *Journal of Materials Processing Technology*, 69(1-3):1–17, (1997).

[7] Koshy P., Dewes R. C., and Aspinwall D. K. High speed end milling of hardened AISI D2 tool steel (58 hrc). *Journal of Materials Processing Technology*, 127(2):266 273, (2002).

[8] Tönshoff H. K., Friemuth T., Andrae P., and Groppe M. Circular milling replacing drilling and reaming. In *Proceedings of II International Seminar on Improving Machine Tool Performance*, pages 1–12, Nantes-La Baule, France, July 3-5, (2000).

[9] Tönshoff H. K., Friemuth T., and Groppe M. High efficient circular milling A solution for an economical machining of bore holes in composite (CFK, Aluminum). In *Proceedings of the III International German and French Conference on High Speed Machining*, pages 287 296, University of Metz, France, June 27-29, (2001).

[10] H. Sasahara, M. Kawasaki, and M. Tsutsumi. Helical feed milling with mql for boring of aluminum alloy. *Transactions of the Japan Society for Mechanical Engineers Part C*, 69(8):2156–2161, (2003).

[11] Stephenson D. A. and Agapiou J. S. Metal cutting theory and practice. *Marcel Dekker*, ISBN:0-8247-9579-2:First Edition, (1996).

[12] Shaw M. C. Metal cutting principles. *Oxford University Press*, ISBN:0-19-514206-3:Second Edition, (2004).

[13] Ernst H. and Haggerty W. A. The spiral point drill A new concept in drill point geometry. *Transactions of the American Society of Mechanical Engineers (ASME)*, 80:1059–1072, (1958).

[14] Armarego E. J. A. Some fundamental and practical aspects of twist drills and drilling. *Journal of Materials Processing Technology*, 44(3-4):189 198, (1994).

[15] Oxford Jr. C. J. On the drilling of metals 1 Basic mechanics of the process.

Transactions of the American Society of Mechanical Engineers (ASME), 77:103–114, (1955).

[16] Galloway D. F. Some experiments on the influence of various factors on drill performance. *Transactions of the American Society of Mechanical Engineers (ASME)*, 79:191–231, (1957).

[17] Narasimha K., Osman M. O. M., Chandrashekhar S., and Frazao J. An investigation into the influence of helix angle on the torque thrust coupling effect in twist drills. *International Journal of Advanced Manufacturing Technology*, 2(4):91–105, (1987).

[18] Davis J. R. ASM Handbook Desk Edition. *American Society of Metals International*, ISBN:0-87170-654-7:Second Edition, (1998).

[19] Key to Steel North America. Articles Key to steel (Knowledge Base). *http://www.key-to-steel.com/Articles.htm*, (2004).

[20] Bohler Uddeholm North America. AISI D2 Cold work tool steels (Product literature). *http://www.bucorp.com*, pages 1–7, (2004).

[21] Tönshoff H. K., Arendt C., and Ben Amor R. Cutting of hardened steel. *CIRP : Annals of the International Institution for Production Engineering Research*, 49(2):547-566, (2000).

[22] Byrne Gerald Barry John. The mechanism of chip formation in machining of hardened steels. *Journal of Manufacturing Science and Engineering (ASME)*, 124(3):528–535, (2002).

[23] Hodgson T. and Trendler P. H. H. Turning hardened tool steels with Cubic Boron

Nitride inserts. *CIRP : Annals of the International Institution for Production Engineering Research*, 30(1):63–66, (1981).

[24] Boehner J., Dumitrescu M., Elbestawi M. A., El-Wardany T. I., and Chen L. Influence of material microstructure on tool performance in high speed machining. *Technical Paper - Society of Manufacturing Engineers, MR*, MR99-166:1–4, (1999).

[25] George F. Vander Voort. ASM Handbook Volume 9 (Metallography and Microstructures). *American Society of Metals International*, ISBN:0-87170-706-3, (2004).

[26] Boehner J., Dumitrescu M., Elbestawi M. A., El-Wardany T. I., and Chen L. Effect of carbide tool grades and cutting edge geometry on tool life during high speed machining of hardened steel. In *Proceedings of the II International German and French Conference on High Speed Machining*, pages 37–46, University of Darmstadt, Germany, March 10-11, (1999).

[27] El-Wardany T. I., Kishawy H. A., and Elbestawi M. A. Surface integrity of die material in high speed hard machining, Part 1: Micrographical analysis. *Journal of Manufacturing Science and Engineering (ASME)*, 122(4):417–427 (2000).

[28] Becze C. E., Clayton P., Chen L., El-Wardany T. I., and Elbestawi M. A. High speed five axis milling of hardened tool steel. *International Journal of Machine Tools and Manufacture*, 40(6):869–885, (2000).

[29] Kishawy H. A. An experimental evaluation of cutting temperatures during high speed machining of hardened D2 tool steel. *Machining Science and Technology*, 6(1):67–79, (2002).

[30] Poulachon G., Bandyopadhyay B. P., Jawahir I. S., Pheulpin S., and Seguin E. The influence of the microstructure of hardened tool steel workpiece on the wear of PCBN cutting tools. *International Journal of Machine Tools and Manufacture*, 43(2):139–144, (2003).

[31] Poulachon G., Bandyopadhyay B. P., Jawahir I. S., Pheulpin S., and Seguin E. Wear behavior of CBN tools while turning hardened steels. *Wear: An international journal on the science and technology of friction, lubrication and wear.*, 256(3-4):302–310, (2004).

[32] Aslan E. Experimental investigation of cutting tool performance in high speed cutting of hardened X210Cr12 cold work tool steel (62rc). *Materials and Design*, 26(1):21-27, (2005).

[33] König W., Klinger M., and Link R. Machining hard materials with geometrically defined cutting edges Field of applications and limitations. *CIRP : Annals of the International Institution for Production Engineering Research*, 39(1):61-64, (1990).

[34] Sandvik Coromant. Product Literature Rotating Tools Catalogue. *http://www.coromant.sandvik.com*, (2004).

[35] Kennametal Limited. Product Literature Hole Making Catalogue 3070. *http://www.kennametal.com*, (2004).

[36] Guhring Corporation. Product Literature Drilling Product Catalogue. *http://www.guhring.com*, (2003).

[37] Iscar Tools Inc. Product Literature Drilling Product Catalogue. *http://www.iscar.com*, (2004).

[38] Balzers Inc. Product Catalogue Wear Resistant Coating on Cutting Tools. *http://www.bus.balzers.com*, (2004).

[39] Dumitrescu M. Critical assessment of carbide tools performance in high speed milling of hardened tool steel. M.A.Sc. Thesis, McMaster University, (1998).

[40] Kishawy H.E.A. *Chip formation and surface integrity in high speed machining of hardened steel.* PhD. Thesis, McMaster University, (1998).

[41] Becze C. E. *A thermo-mechanical force model for machining hardened steel.* PhD. Thesis, McMaster University, (2002).

[42] Dumitrescu P. High power diode laser assisted hard turning of AISI-D2 tool steel. M.A.Sc. Thesis, McMaster University, (2004).

[43] König W., Iding M., and Link R. Fine turning and drilling of hardened steels 2. *Industrial Diamond Review*, 50(3):139–142, (1990).

[44] Wells Jason. To the Point. *Cutting Tool Engineering*, 57(8):1- 3, (2005).

[45] Nakayama K. and Ogawa M. Basic rules on the form of chip in metal cutting. *CIRP : Annals of the International Institution for Production Engineering Research*, 27(1):17 21, (1978).

[46] Armarego E. J. A. and Cheng C. Y. Drilling with flat rake face and conventional twist drillsI. Theoretical investigation. *International Journal of Machine Tool Design and Research*, 12(1):17–35, (1972).

[47] Armarego E. J. A. and Cheng C Y Drilling with flat rake face and conventional twist drillsII. Experimental investigation. *International Journal of Machine Tool Design and Research*, 12(1):36–54, (1972).

[48] Armarego E. J. A. and Brown F H. The machining of metals. *Prentice-Hall, Englewood Cliffs, New Jersey*, (1969).

[49] Chyan H. C. and Ehmann K. F Curved helical drill points for micro hole drilling. *Proceedings of the Institution of Mechanical Engineers, Part B: Journal of Engineering Manufacture*. 216(1):61–75. (2002).

[50] Becze C. E., Worswick M. J., and Elbestawi M. A. High strain rate shear evaluation and characterization of AISI D2 tool steel in its hardened state. *Machining Science and Technology*. 5(1):131–149. (2001).

[51] Dr. Eugene Ng. Study of tool stress field when machining AISI-D2 and AISI-H13 using FEA. *McMaster Manufacturing Research Institute, McMaster University, Hamilton, ON, Canada*, Technical Report:1 2. (2005).

[52] Childs T. H. C., Maekawa K., Obikawa T., and Yamani Y. Metal Machining Theory and Applications. *Arnold Publishers, London*. ISBN:0-470-39245-2. (2000).

[53] Spur G. and Masuha J. R. Drilling with twist drills of different cross section profiles. *CIRP : Annals of the International Institution for Production Engineering Research*. 30(1):31–35. (1981).

[54] Jindal P. C., Santhanam A. T., Schleinkofer U., and Shuster A. F. Performance of PVD TiN, TiCN, and TiAlN coated cemented carbide tools in turning. *International Journal of Refractory Metals and Hard Materials*. 17(1-3):163–170. (1999).

[55] Klocke F. and Krieg T. Coating tools for metal cutting Features and Applica-

tions. *CIRP : Annals of the International Institution for Production Engineering Research*. 48(2):515–525. (1999).

[56] Sandvik Coromant. Modern Metal Cutting A practical handbook. *Sandvik Coromant, Technical Editorial Department*. ISBN:91-972290-0-3. (1994).

[57] Trent E. M. and Wright P. K. Metal cutting. *Butterworth-Heinemann Publication Inc.*,, ISBN:0-7506-7069-X:Fourth Edition. (2000).

[58] Elbestawi M. A., Chen L., Becze C. E., and El-Wardany T. I. High speed milling of dies and molds in their hardened state. *CIRP : Annals of the International Institution for Production Engineering Research*. 46(1):57 62. (1997).

[59] Komanduri R. Some aspects of machining with negative rake tools simulating grinding. *International Journal of Machine Tool Design and Research*. 12(3):223 233, (1971).

[60] Kim Yong-Hyun. and Ko Sung-Lim. Development of design and manufacturing technology for end mills in machining of hardened steel. *Journal of Materials Processing Technology*. 130-131:653–661. (2002).